BIOSOURCED POLYMER ELECTROLYTES BASED ON CELLULOSE DERIVATIVE FOR APPLICATION IN ELECTROCHEMICAL CELL

MOHD SAIFUL ASMAL BIN ABDUL RANI

INSTITUTE OF GRADUATE STUDIES
UNIVERSITY OF MALAYA
KUALA LUMPUR

2018

BIOSOURCED POLYMER ELECTROLYTES BASED ON CELLULOSE DERIVATIVE FOR APPLICATION IN ELECTROCHEMICAL CELL

MOHD SAIFUL ASMAL BIN ABDUL RANI

THESIS SUBMITTED IN FULFILMENT OF THE REQUIREMENTS FOR THE DEGREE OF DOCTOR OF PHILOSOPHY

INSTITUTE OF GRADUATE STUDIES
UNIVERSITY OF MALAYA
KUALA LUMPUR

2018

BIOSOURCED POLYMER ELECTROLYTES BASED ON CELLULOSE DERIVATIVE FOR APPLICATION IN ELECTROCHEMICAL CELL

ABSTRACT

The aim of this study was to investigate the characteristics of a new type environmental friendly biopolymer electrolyte as potential applications in electrochemical cell. A cellulose derivative, carboxymethyl cellulose, CMC was synthesized by the reaction of cellulose from kenaf bast fiber with monochloroacetic acid. A series of solid biopolymer electrolytes comprised of the synthesized CMC as the host for acetate based salts; (ammonium, sodium, magnesium, zinc) and ionic liquid 1-butyl-3-methylimidazolium chloride which played role as ionic dopants and plasticizer, respectively. All biopolymer electrolyte films were successfully prepared via solution casting technique. The biopolymer electrolyte films obtained were transparent and flexible. The properties of the synthesized CMC depend on the degree of substitution of the hydroxyl group, which took part in the substitution reaction in the cellulose, respectively, as well as the purity, molecular weight and crystallinity was determined using acid-wash method. The degree of substitution value obtained was higher than that of commercial CMCs available in market. This means that the CMC had a higher number of oxygens, thus providing more active sites for coordination with the cations of the doping salt, resulting in a higher conductivity value. The prepared films were characterized using various characterization techniques such as Fourier transform infrared spectroscopy, dynamic mechanical analysis, thermogravimetric analysis, impedance spectroscopy, linear sweep voltammetry and transference number measurement in order to investigate the structural, thermal, electrical and electrochemical properties. The interactions between the biopolymer host with the ionic dopant and plasticizer were indicated by Fourier transform infrared spectroscopy. Impedance spectroscopy was conducted to obtain their ionic conductivities. The

influence of sodium acetate into the biopolymer system showed the highest ionic conductivity compared to other acetate based salts, which increased up to optimum value of 2.83×10^{-3} S cm^{-1} at room temperature for sample containing 30 wt% of sodium acetate. The conductivity was higher compared to that obtained for polymer electrolytes developed using commercial CMC. This was due to high DS value which provided more ion coordinate sites. The best conductivity achieved was 4.54×10^{-3} S cm^{-1} for the sample integrated with 30 wt% ionic liquid. The conductivity was enhanced upon addition of ionic liquid. All biopolymer electrolyte films were amorphous and have low glass transition temperature which facilitated segmental motion of the host polymer. The temperature dependence of the ionic conductivity of the biopolymer electrolyte systems obeyed the Arrhenius relation. Furthermore, all conducting biopolymer electrolytes showed an electrochemical stability more than 2 V, whereas the transference number measurement revealed that ions predominated the conduction of electrolytes. Electrochemical cell was prepared using configuration Na/ CMC-NaCH$_3$COO-30 wt% [Bmim]Cl/ I$_2$+ C+ electrolyte and the discharge characteristics was studied. The results revealed that the biopolymer electrolytes from kenaf fiber have potential for application in electrochemical devices.

Keywords: carboxymethyl cellulose, biopolymer electrolytes, ionic liquid, electrochemical cell

ELEKTROLIT POLIMER BIO-SUMBER BERASASKAN TERBITAN SELULOSA UNTUK APPLIKASI DALAM SEL ELEKTROKIMIA

ABSTRAK

Tujuan kajian ini adalah untuk menyiasat ciri-ciri elektrolit biopolimer mesra alam baru yang berpotensi sebagai aplikasi dalam sel elektrokimia. Terbitan selulosa, karboksimetil selulosa, CMC telah disintesis dengan cara tindak balas selulosa daripada gentian kulit kenaf dengan asid monokloroasetik. Satu siri elektrolit biopolimer pepejal terdiri daripada CMC disintesis sebagai perumah untuk garam asetat; (ammonia, natrium, magnesium, zink) dan cecair ionik 1-butil-3-metilimidazolium klorida yang memainkan peranan masing-masing sebagai pendopan dan pemplastik. Semua filem biopolimer elektrolit telah berjaya disediakan melalui teknik penuangan larutan. Semua filem biopolimer elektrolit diperolehi lutsinar dan fleksibel. Sifat CMC yang disintesis bergantung kepada darjah penukarganti kumpulan hidroksil, yang mengambil bahagian dalam tindak balas penggantian dalam selulosa, serta ketulenan, berat molekul dan kehabluran telah ditentukan dengan menggunakan kaedah pembasuhan asid. Nilai darjah penukarganti yang diperoleh adalah lebih tinggi berbanding dengan CMC komersil yang terdapat di pasaran. Ini bermakna CMC mempunyai jumlah oksigen yang lebih tinggi, dengan itu menyediakan lebih banyak tapak aktif untuk koordinasi dengan kation garam yang didop, menyebabkan nilai kekonduksian yang lebih tinggi. Filem yang disediakan dicirikan dengan menggunakan pelbagai teknik pencirian seperti inframerah transformasi Fourier, analisis mekanikal dinamik, analisis termogravimetri, spektroskopi impedans, voltammetri sapuan linear dan pengukuran nombor pemindahan untuk menyiasat sifat-sifat struktur, haba, elektrik dan elektrokimia. Interaksi antara biopolimer utama dengan ionik pendopan dan pemplastik telah ditunjukkan oleh spektroskopi inframerah transformasi Fourier. Spektroskopi impedans telah dijalankan

untuk keberaliran ionik mereka. Pengaruh natrium asetat dalam sistem elektrolit biopolimer ini menunjukkan bahawa kekonduksian ionik adalah yang tertinggi berbanding dengan garam asetat yang lain, yang mana telah meningkat sehingga nilai optimum 2.83×10^{-3} S cm^{-1} pada suhu bilik untuk sampel yang mengandungi 30% berat natrium asetat. Kekonduksian juga lebih tinggi berbanding dengan yang diperolehi bagi elektrolit polimer dibangunkan menggunakan CMC komersial. Ini disebabkan oleh nilai DS yang tinggi. Kekonduksian terbaik yang dicapai adalah 4.54×10^{-3} S cm^{-1} untuk sampel bersepadu dengan 30% berat cecair ionik. Kekonduksian telah ditingkatkan dengan penambahan cecair ionik. Semua filem elektrolit biopolimer ialah amorfus dan mempunyai suhu peralihan kaca yang rendah memudahkan gerakan segmen polimer perumah. Pergantungan suhu kekonduksian ionik sistem biopolimer elektrolit mematuhi hukum Arrhenius. Tambahan pula, semua biopolimer elektrolit berkonduksi menunjukkan kestabilan elektrokimia lebih daripada 2 V, manakala nilai nombor pemindahan ion mencadangkan bahawa ionik adalah pembawa cas dalam elektrolit. Peranti elektrokimia telah disediakan dengan menggunakan konfigurasi Na/ CMC-NaCH$_3$COO-30 wt% [Bmim]Cl/ I$_2$+ C+ elektrolit dan ciri-ciri nyahcas telah dikaji. Semua keputusan ini menunjukkan bahawa elektrolit biopolymer dari fiber kenaf berpotensi untuk diaplikasi dalam peranti elektrokimia.

Kata kunci: karboksimetil selulosa, elektrolit biopolimer, cecair ionik, sel elektrokimia

ACKNOWLEDGEMENTS

Alhamdulillah and blessing to the beloved Prophet Muhammad who gave me the strength, health and patience to successfully implement my PhD project and complete this thesis. I would like to express my gratitude to my supervisor, Professor Dr. Nor Sabirin Mohamed for her constant encouragement, invaluable advices, guidance and continuous support throughout the course of this research has inspired me to work harder for success. This research would not have been able to come this far without her. I also would like to extend my sincere appreciation to my co-supervisor Professor Dr. Azizan Ahmad for his assistance and advice in every possible way in completing the work in this study.

Furthermore, I would like to thank everyone in the Electrochemical Materials and Devices (EMD) research team, who had involved directly or indirectly in giving cooperation to me to learn and gain experience in this research. Not forgetting the science officer and laboratory staff of Physics Division, Centre of Foundation Studies for their dedication in providing technical support and ensuring that the students are able to carry out the project with minimal problems. Besides that, I would like to thank my parents, Abdul Rani Japar and Noor Adiatuladha Sharif for always believing in me and sacrificed their time and money to support me through my education. This dissertation is my show of gratitude and thanks to my family for supporting me throughout the journey. Lastly, I would like to express my deepest thanks to my beloved wife, Nor Shakira Bt Haji Isa and my daughter, Alisya Umaira for their prayers, patience and moral support.

TABLE OF CONTENTS

LIST OF FIGURES

LIST OF TABLES

LIST OF SYMBOL AND ABBREVIATIONS

AC	:	Alternating current
[Bmim]Cl	:	1-butyl-3-methylimidazolium chloride
CE	:	Counter electrode
CMC	:	Carboxymethyl cellulose
DMA	:	Dynamic Mechanical Analysis
EC	:	Ethylene Carbonate
EIS	:	Electrochemical Impedance Spectroscopy
FTIR	:	Fourier Transform Infrared Spectroscopy
I_2	:	Iodine
IL	:	Ionic Liquid
PEG	:	Poly(ethylene glycol)
PEMA	:	Poly(ethyl methacrylate)
PEO	:	Poly(ethylene oxide)
PEs	:	Polymer Electrolyte system
PVDF	:	Poly(vinylidene fluoride)
RS	:	Rice starch
SEM	:	Scanning Electron Microscopy
SiO_2	:	Silicon dioxide
SPE	:	Solid Polymer Electrolyte
SPEs	:	Solid Polymer Electrolyte system
SS	:	Stainless steel
TGA	:	Thermogravimetric analysis
TiO_2	:	Titanium oxide
TNM	:	Transference Number Measurment

VTF	:	Vogel-Tamman-Fulcher
WE	:	Working electrode
A	:	Area of sample holder
C	:	Capasitor
D	:	Diffusion coefficient
d.c	:	Direct current
E_a	:	Activation energy
I_{ion}	:	Current normalised ionic transference number
k	:	Boltzmann constant
K	:	Kelvin
ℓ	:	Mean free path / distance from one complexes site to another
n	:	Density of mobile ions
q	:	Charge of ion
R^2	:	Regression value
R_b	:	Bulk resistance
S cm^{-1}	:	Siemen per centimeter
T	:	Absolute temperature
t	:	Thickness
t_{ion}	:	Ionic transference number
V	:	Velocity of charge carrying species
wt %	:	Weight percentage

CHAPTER 1: INTRODUCTION

1.1 Research Background

There was a plethora of study on polymer electrolytes which has encouraged enormous research and development of polymer electrolytes worldwide after the earliest breakthrough of polymer-salt complexes by Wright in 1975 and continued by Armand and co-workers in 1978 (Armand et al., 1979; Wright, 1975). Polymer electrolytes have attracted many researchers' attention all over the world as polymer electrolytes play an important role in solid state ionic due to their unique properties such as ease of fabrication into thin film with large surface area to give high energy density, ability to accommodate a wide range of ionic salts doping compositions, good electrode-electrolyte contact and high ionic conductivity (Chandra & Chandra, 1994). Among these polymer electrolyte materials, proton conducting polymer electrolytes have been investigated due to the possibility of their application in a variety of electrochemical devices such as low energy density primary and secondary battery, fuel cells and electrochromic displays (Agrawal et al., 2007; Pratap et al., 2006; Selvasekarapandian et al., 2005).

Since a few decades ago, liquid electrolytes were applied in electrochemical power sources due to their high conductivity. However, these types of electrolytes face drawbacks such as poor electrochemical stability, corrosion reactions with electrode and leakage, thus making them unsuitable for use in electrochemical devices (Idris et al., 2009). Therefore, research on solid polymer electrolytes is extensively done to look for potential materials to replace the liquid based electrolytes as they possessed desirable characteristics including good compatibility with electrodes; easy to process, low-self discharge in batteries, good elasticity and no leakage (Yahya et al., 2006). To date,

many types of polymers have been employed as hosts to produce electrolytes. However, synthetic or petrochemical-based polymers which are commonly utilized as hosts faced disadvantages such as high cost and not 'green' to the environment. Alternatively, the use of natural polymers as polymer hosts which offer more environmental friendly, good chemical and physical properties besides lower cost of the materials is hoped to be a solution to reduce the environmental issues.

1.2   Problem Statements

Nowadays, electrochemical storage devices found an exclusive demand for low cost materials, rechargeable and environmental friendly materials. Besides that, electrochemical power sources which were fabricated using liquid electrolyte unfortunately give problems such as leakage, reaction with electrode and poor electrochemical stability which make them unsuitable for use in electrochemical devices (Mobarak et al., 2013). Corrosion during packaging also can occur by using liquid electrolytes. Due to these drawbacks, solid polymer electrolyte is the best candidate to replace liquid electrolyte.

Most of the materials that have been studied on polymer electrolytes focused synthetic polymers which are quite expensive and not too green to the environment. As alternatives, polymers from natural based have been studied due to their superior properties as polymer hosts besides cheap and biodegradable. Nowadays due to lot of peril to our environment impacts of many petrochemical-based and synthetic polymers, biodegradable-based polymers are receiving great attention due to its natural resources, abundantly available, biodegradability and low cost (Ma et al., 2007; Mohamed et al., 1995; Velazquez-Morales et al., 1998). Among the variety types of biomaterials, the potential and capability of cellulose and its derivatives to be used as polymer matrix has

been recognized due to its attractive chemical and physical properties (Barbucci et al., 2000; Marcì et al., 2006).

With the current demand for sustainable energy supplies, the development and optimization of energy storage systems is of increasing relevance. Today, Li^+ ion batteries are the most promising concept and attracted researchers' attention for vehicular application; due to the small ionic radii of Li^+ ion which could be intercalated into the layers of the layered materials in electrode (Ali et al., 2013). With the likelihood of enormous demands on available global lithium resources, concerns over lithium supply, but mostly expensive have arisen. Many global lithium reserves are located in remote or in politically sensitive areas (Risacher & Fritz, 2009; Yaksic & Tilton, 2009). Even if extensive battery recycling programs were established, it is possible that recycling could not prevent this resource depletion in time (Ellis & Nazar, 2012). Moreover, increasing lithium utilization in medium-scale automotive batteries will ultimately push up the price of lithium compounds, thereby making large-scale storage prohibitively expensive (Polu & Rhee, 2015). Therefore, study to investigate alternative sources of charge carriers in order to replace Li^+ needs to be done. Ammonium, sodium, magnesium and zinc salts seem to be best candidates due to their properties compared to lithium salts.

Ionic liquids have been widely promoted as "green solvents" due to their interesting properties such as good chemical and electrochemical stability, non-flammability, negligible vapor pressure and high ionic conductivity. However, their liquid nature limits their use in devices due to problems of leakage, non-portability and the impossibility of miniaturization. Therefore, the combination of suitable polymers, and

ionic liquids to form biopolymer electrolytes should be considered to overcome this issue.

1.3   Research Objectives

The objectives of this work are:

i.   To produce carboxymethyl cellulose from kenaf bast fiber with high degree of substitution as host polymer.

ii.   To determine the effects on composition of acetate salts to the physicochemical properties of carboxymethyl cellulose films.

iii. To optimize the electrical and electrochemical properties of biosourced polymer electrolytes by adding ionic liquid as plasticizer.

iv.   To analyze the performance of solid-state sodium battery using the enhanced electrolyte.

1.4   Scope of Study

In the present study, the potential of carboxymethyl cellulose, CMC which was isolated from kenaf fiber, as host in biopolymer electrolytes was investigated. It is believed that CMC would be a good polymer host since CMC is amorphous and contains carbonyl group in its structure. For salted systems, the prepared CMC was doped with different acetate based salts such as NH_4CH_3COO, $Mg(CH_3COO)_2$, $NaCH_3COO$ and $Zn(CH_3COO)_2$. Then, selected sample with the highest conductivity was plasticized with ionic liquid in order to enhance its conductivity. The optimum conducting electrolyte of the plasticized systems was measured in electrochemical cells. To account for the conductivity behavior of the electrolyte systems, various characterization techniques including Fourier transform infrared spectroscopy (FTIR), scanning electron microscopy (SEM), electrochemical impedance spectroscopy (EIS),

thermogravimetric analysis (TGA), dynamic mechanical analysis (DMA), linear sweep voltammetry (LSV) and transference number measurement (TNM) were carried out.

1.5   Thesis Organization

This thesis is presented into 6 chapters. Chapter 1 gives the background of this research. This chapter also states the problems with current electrolytes which has galvanized the search for new environmentally friendly electrolytes, the objectives of this research and the outline of the research as well as the layout of the thesis. In Chapter 2, an overview of previous studies on polymer electrolytes, solid polymer electrolytes, and cellulose namely on the preparations and the characterizations of the solid polymer electrolytes are presented. The basic properties of cellulose and CMC are given at the end of this chapter.

Methodology of this research is described in Chapter 3. The methodology is divided into two stages. The first stage is the synthesis and modification of CMC from kenaf bast fiber followed by sample preparation of CMC solid polymer electrolytes. Stage two comprises of the characterization of the biopolymer electrolytes in order to study their structural, electrical, thermal and electrochemical properties.

Chapter 4 gives the results and in-depth analyses for the samples of CMC containing different amounts of acetate based salts (ammonium acetate, sodium acetate, magnesium acetate and zinc acetate). The effect of different concentrations of acetate based salts on thermal and viscoelasticity properties of CMC from kenaf bast fiber were studied by using TGA and DMA, respectively while the interaction between the host biosourced polymer and salts were investigated using FTIR. The ionic conductivity, electrochemical stability window and ionic transport were determined by using EIS,

LSV and TNM, respectively. Based on these results, the best electrolytes in terms of conductivity for CMC- ammonium/sodium/magnesium/zinc acetate systems were identified and then integrated with ionic liquid, [Bmim]Cl.

Chapter 5 reveals thermal, viscoelasticity and electrical properties of the [Bmim]Cl added biosourced polymer electrolytes investigated by TGA, DMA and EIS respectively. Interaction and entrapment of ionic liquid was examined by FTIR and SEM analysis and are discussed to explain the conductivity results. The ionic transport was identified by TNM and electrochemical stability window was determined using LSV. The highest conducting film in this study was selected for application in electrochemical cells and the characteristics of the cell are discussed in Chapter 5. Chapter 6 gives conclusions and some suggestions for future works.

CHAPTER 2: LITERATURE REVIEW

2.1 Introduction

Our world now shifted towards modern technology which is focusing on development of green energy resources. The demand on energy is increasing from time to time due to the increase of economic activities. Energy sources are becoming governmental issue, with cost and stable supply as the main concern. Therefore, a lot of work should be done in order to explore the potential practical application of natural sources in electrochemical energy devices. This chapter reviews the research works reported in scientific journals related to the present research work. General properties, background studies, the principles of operation and behavior of polymer electrolytes are outlined. Some properties carboxymethyl cellulose based electrolytes are also included.

2.2 Polymer

The word polymer originated from the classical Greek word which *poly* means "many" and *meres* meaning "parts". Polymer is a large molecule that are very long and chain like, composed of many repeating subunits. Polymers can be divided into two groups; natural and synthetic. Natural polymers like natural rubber, chitosan, starch, agar, carrageenan and cellulose are also known as biopolymers. These polymers are abundantly available and can be found in living things like bacteria, animals and plants. One of the promising advantages of biopolymers is the biodegradable characteristic which is green to our environment, thus would minimize pollutions besides reducing the energy sources dependence to the petroleum based products (Mobarak et al., 2013). Synthetic polymers are man–made polymers which are produced in factories or laboratories. There are variety types of synthetic polymers available in the market such as synthetic rubbers, plastics, synthetic fibers and adhesives. Basically, most of pure

polymers exhibit very small electrical conductivity; in fact some of them are used for insulation purposes. The incorporation of ionic dopant may significantly boost up their electrical conductivity.

2.2.1 Synthetic Polymer

In the 20th century, most synthetic or artificial polymers have been used as electric insulators or as structural materials. However, in the past 40 years since the earliest breakthrough of polymer-salt complexes, there has been a plethora of research focusing on polymer electrolytes. Synthetic polymers have been tailored as ion or electron conductors when combined with appropriate dopants, their conductivity can be put to use as electrolytes. Although synthetic polymers possess advantages like easily tailored, predictable properties and batch-to-batch uniformity, the widespread use of non-biodegradable polymers is a contributor to environmental issues (Lu et al., 2009). This is because solid wastes from these materials take up a thousand years to degrade (Azahari et al., 2011). Besides, the non-biodegradable polymers are quite expensive, not suitable for temporary use and insoluble in most solvents (Lu et al., 2009; Ma et al., 2007).

Most synthetic polymers are derived from petrochemicals; chemically manufactured from separate materials through the polymerization which categorized them as non-biodegradable (Lu et al., 2009). Examples of synthetic polymers are teflon, polyethylene, epoxy, polyester and nylon. As alternatives, researchers have been working on the development of natural biopolymers to overcome problems encountered by synthetic polymers.

2.2.2 Natural Polymer

Biopolymers or natural polymers offer a degree of functionality not available in most synthetic polymers. They are known as organic strain of polymers produced naturally by living things with great frequency in nature; includes many types of plants and even some bacteria. Over the past decades, the studies of electrolytes based on biopolymers have progressed actively due to the desirable properties of biopolymers and concern on environmental issues. Biopolymers offer great choices as they are usually biocompatible, biodegradable, abundant and non-hazardous compared to synthetic polymers (Ghanbarzadeh & Almasi, 2013; Klemm et al., 2005; Kucińska-Lipka et al., 2014). The term biodegradable refers to the "biodegradability" function of the polymers that degrade under the action of microorganisms such as mold, fungi and bacteria within a specific period of time and environment (Niaounakis, 2013). There are three major classifications of biopolymer such as polynucleotides, polypeptides and polysaccharides (Aravamudhan et al., 2014). Polysaccharides are the best candidates to replace synthetic polymers as they are most plentiful and easily accessible polymers. Chitin, carrageenan, chitosan, starch, cellulose and pectin are some of the most abundant natural polymers on the earth.

2.3 Kenaf

Kenaf or its scientific name *Hibiscus Cannabinus L.*, a bast fiber, is allied to cotton or jute fiber and shows comparable characteristics. Historically, kenaf fiber is produced mainly in India and China followed by Bangladesh. Malaysia is in the process of developing kenaf cultivation and processing. In Malaysia, the development of kenaf was managed by Malaysian Agricultural Research and Development Institute (MARDI) and Tobacco Board of Malaysia. Kenaf has a single, straight and branchless stalk. Kenaf stalk is made up of an inner woody core and an outer fibrous bark surrounding the core.

The fiber derived from the outer fibrous bark is also known as bast fiber. Kenaf bast fiber has superior flexural strength combined with its excellent tensile strength that makes it the material of choice for a wide range of extruded, molded and non-woven products (Edeerozey et al., 2007; Karnani et al., 1997).

2.3.1   Kenaf Component Partitioning and Composition

A research has been done with five kenaf cultivars over a two year period produced plants at harvest which averaged 26% leaves and 74% stalks by weight (Webber III & Bledsoe, 1993; Webber III & Bledsoe, 2002). The average composition of kenaf stalks was 65% woody core and 35% bark by weight as revealed in Figure 2.1 (a). Figure 2.1 (b) shows the outer of the kenaf stalk consists of long fiber strands which composed of many individual smaller fibers called bast fibers. These individual bast fibers held together by lignin (Mohamed et al., 1995). The woody core material of the stalk as illustrated in Figure 2.1(c), the portion remaining when the bast is removed, contains core fiber. The individual bast fibers are longer and thinner than the individual shorter, thicker core fibers. Whole stalk kenaf which include bast and core fibers has been identified as a promising fiber source for paper pulp (Nieschlag, 1960; White, 1970).
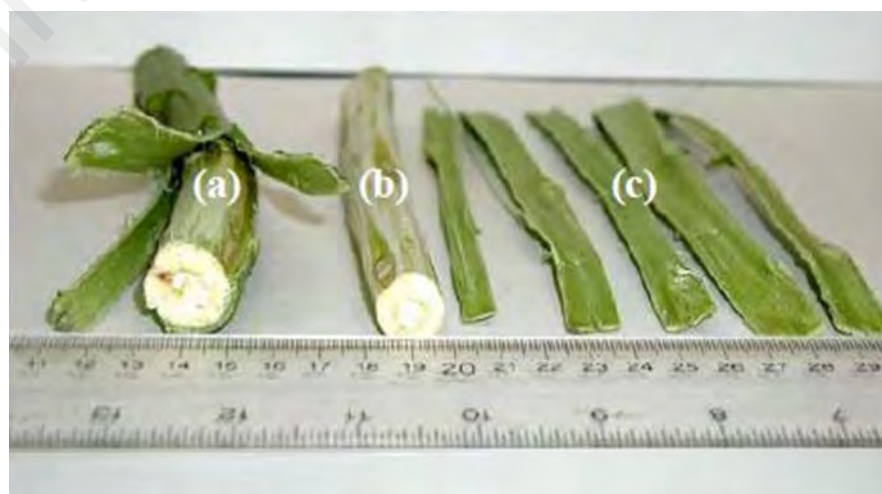
Figure 2.1: Kenaf stalk with bark and core material

2.3.2 Uses and Application of Kenaf Fiber

Actually the research work to utilize kenaf for forage, paper, animal bedding and other products began in the 1960's and continues today. Kenaf has become a potential natural fiber source for both apparel and industrial applications. Besides that, it has been used as a cordage crop to produce rope, twine and sackcloth (Dempsey, 1975). There are various new applications for kenaf including animal feeds, absorbents, building materials and paper products.

Recently, kenaf has caught many researchers' attention in order to explore its potential in electrochemical devices. Jafirin and co-workers have explored the possibility of using cellulose from kenaf as reinforcing fibres in lithium-conducting composite polymer electrolytes based on 49% poly(methyl methacrylate)-grafted natural rubber and $LiCF_3SO_3$ (Jafirin et al., 2013). The presence of cellulose fibers induced a weak decrease in the conductivity of polymer electrolytes besides leads to high mechanical strength for polymer electrolyte system at a small percentage of cellulose fibers. In another investigation, the potential of a blend system prepared from the combination of k-carrageenan and cellulose derivatives from kenaf fiber for the application in dye sensitized solar cells (DSSCs) has been reported. The highest conductivity obtained at ambient temperature was 2.41×10^{-3} S cm^{-1} for addition of 30 wt% ammonium iodide (NH_4I) salt. The fabricated FTO/TiO_2- dye/CMKC/CMC-NH_4I + I_2/Pt cell showed response under light intensity of 100 mW/cm^{-2} with efficiency of 0.13%. The efficiency of the cell, despite being quite low, showed potential to be further explored and improved.

2.4 Cellulose

On the surface of the earth, cellulose is the most abundant renewable organic material. Cellulose is extracted from natural materials such as wood and plants, and is grouped as biopolymer materials. In its native form, cellulose is not a water-soluble material. Since it is not soluble in water, the solvent can be rendered by chemical reaction of its hydroxyl groups with hydrophilic substituent (Huang et al., 2003). According to (Edeerozey et al., 2007), there are many organic substances that are derived from cellulose, that is hydroxyethyl cellulose (HEC), methyl cellulose (MC) and carboxymethyl cellulose (CMC).

2.5 Carboxymethyl cellulose

CMC is one of the water-soluble cellulose derivatives. CMC contains a hydrophobic polysaccharide backbone and many hydrophilic carboxyl groups, and hence shows amphiphilic characteristic. Due to its desirable properties such as non-toxicity, biocompatibility, biodegradability, high hydrophilicity, and good film forming ability, CMC has been used in various practical fields (Huang et al., 2003). CMC has no harmful effects on human health, and is used as highly effective additive to improve the product quality and processing properties in various fields of application, from foodstuffs, cosmetics and pharmaceuticals, to products for the paper and textile industries (Ghanbarzadeh & Almasi, 2013; Ghanbarzadeh et al., 2011). CMC is an anionic polymer. In general, cellulose is made up of glucose rings connected by –C(1)–O–C(4) ether bonds known as β-1,4 glycosidic linkages with extensive intramolecular hydrogen bonding (Cuba-Chiem et al., 2008). The molecular structure of carboxymethyl cellulose is shown in Figure 2.2 (Biswal & Singh, 2004). The carboxyl methyl groups (-CH_2-COOH) bound to some of the hydroxyl groups of the glucopyranose monomers that make up the cellulose backbone. CMC is derived from cellulose by treatment with

alkali and monochloroacetic acid or its sodium salt. Some experiments have shown that CMC is a viscous and not fermented compound, but it is associated with enhanced fermentation due to accumulation of undigested material (Juśkiewicz & Zduńczyk, 2004).
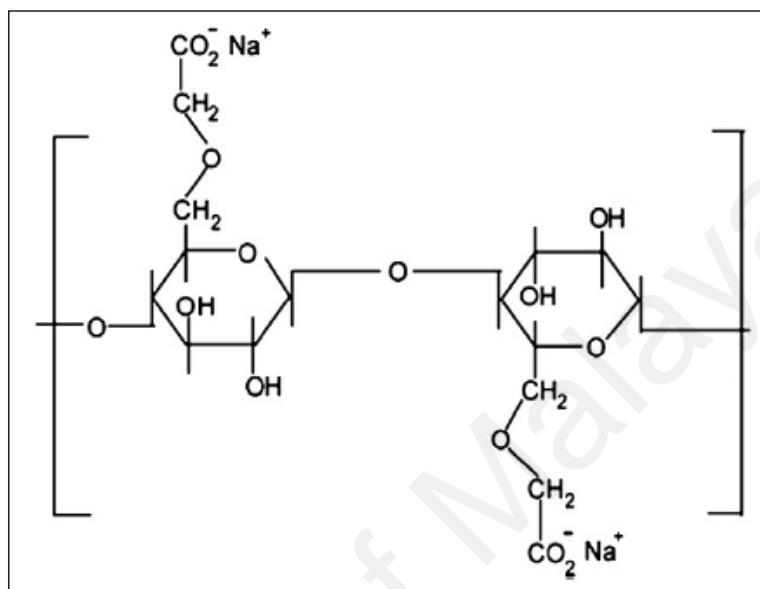
Figure 2.2: The molecular structure of CMC

2.6 Polymer Electrolytes

In the past few decades, polymer electrolytes have generated much interest as potential components in devices such as batteries and smart windows due to their low cost of production (Qiao et al., 2010; Yahya et al., 2006). Polymer electrolytes have good mechanical stability in thin film, have a wide range of composition allowing control of their properties and are able to form effective electrode-electrolyte contacts. Polymer electrolytes possess the advantage of flexibility over inorganic solids. The use of solid polymer electrolytes would also overcome the limitations of liquid electrolytes, negate the need of separator and easier handling for device fabrication (Thakur et al., 2012; Zhou & Fang, 2007). Polymer electrolytes have undergone 3 stages of development, (i) dry solid polymer electrolyte, (ii) gel polymer electrolytes and (iii)

composite polymer electrolytes (Kumar & Deka, 2010; Long et al., 2016; Stephan et al., 2002).

2.6.1   Dry Solid Polymer Electrolytes

Ionic conducting polymer was first suggested by Fenton and Wright in 1973 (Fenton et al., 1973). Since the pioneering work by Wright on ions conductivity in the poly (ethylene oxide)/alkali metal salt complexes, the studies on solid polymer electrolytes SPEs have attracted and receiving a great deal of attention due to its proposed large scale use in high energy density secondary lithium ion batteries, sensors, solar cell, fuel cell as well as electro- chromic smart windows (Duraikkan et al., 2018). SPEs based on optical materials have received great interests for applications in electrochemical devices now in a spot of interest among most of researchers and academicians in the field of electrochemical devices as an excellent substitute for aqueous/liquid electrolytes due to its properties such as thermally and mechanically stable (Li et al., 2016; Xia et al., 2017).

In the past four decades, the development of the new SPE systems has been an important part in research due to the need to search for new type of electrolytes for applications in various electrochemical devices. SPE possess interesting properties such as good compatibility with electrodes, no leakage, low self-discharge in batteries, flexibility and easy to fabricate (Chai & Isa, 2011; Yang & Hou, 2012). The SPEs have many advantageous properties for such applications, including good dimensional and thermal stability, a wide electrochemical stability window, and flame resistance (Geiculescu et al., 2002). SPEs are found to be advantageous compared to the conventional solid electrolytes in view of their flexibility, ease of preparation into required geometries and better electrode electrolyte contacts (Tripathi et al., 2013). The

limitation associated with the use of aqueous electrolytes is that water's narrow electrochemical stability window renders high-voltage cells poorly or non-rechargeable. Besides that, there are safety concerns due to dendrite formation in the aqueous electrolyte during charge/discharge cycles for rechargeable cells, which may induce internal short circuit of the batteries (Bender et al., 2002; Deng, 2015; Porcarelli et al., 2016).

Table 2.1: Some dry polymer electrolyte system and their conductivities

System	Ionic conductivity (S cm^{-1})	References
PEO-KI	1.96×10^{-5}	Reddy & Chu, 2002
PEO-NaI	5.21×10^{-5}	Mohamed et al., 1997
PVA-NHBr	5.7×10^{-4}	Hema et al., 2008
PVA-NH$_4$I	2.5×10^{-3}	Selvasekerapandian, et al., 2009
PVA-NHCl	1.0×10^{-5}	Hema et al., 2009
PVA/PVDF-LiCF$_3$SO$_3$	2.7×10^{-3}	Tamilselvi & Hema, 2014
Chitosan-NH$_4$NO$_3$	2.53×10^{-5}	Majid & Arof, 2005
Starch-NH$_4$NO$_3$	2.83×10^{-5}	Khiar & Arof, 2010
Methylcellulose-NH$_4$F	6.4×10^{-7}	Aziz et al., 2010
PVA-PEG-Mg(NO$_3$)$_2$	9.63×10^{-5}	Polu & Kumar, 2011
PVA-LiBOB	2.85×10^{-4}	Noor et al., 2013
PAN-LiNO$_3$	1.5×10^{-3}	Genova et al., 2015
2-hydroxyethyl cellulose-NH$_4$NO$_3$	4.51×10^{-4}	Hafiza & Isa, 2017

2.6.2 Gel/Plasticized Polymer Electrolytes

GPEs or plasticized polymers are single phase and contain organic additives/plasticizers which have the effect of softening the host polymers. Since ionic conductivity comes about through molecular motion in the structure, GPEs have higher ionic conductivity than the dry SPEs because of greater freedom for molecular motion.

GPE essentially has evolved since 1975 in order to obtain ionic conductivity ranging between 10^{-5} to 10^{-3} S cm^{-1}. The ionic conductivity of GPEs depends on the viscosity and the dielectric constant of the plasticizers. Plasticizers such as polyethylene carbonate (PC) and ethylene carbonate (EC) have been much used because of low vapour pressure and high dielectric constant, ε = 64.92 and 89.78, respectively. However, EC and PC are corrosive and flammable. In attempts to overcome concerns with energy and pollution while maintaining the properties of good plasticizers, room temperature ionic liquids (RTILs) have been found to be most potential candidates as plasticizers due their thermally stable at high temperature, can improve electrode-electrolyte interfacial contact and as well as wide electrochemical stability window (Ye et al., 2013). In particular, PEMA-based gel polymer electrolytes incorporated with ionic liquid have been found to exhibit high ionic conductivity with high transparency (Anuar et al., 2012). Table 2.2 lists the conductivities of some gel polymer electrolytes reported in the literature.

Table 2.2: Some gel polymer electrolyte system and their conductivities

System	Ionic conductivity (S cm^{-1})	References
PMMA-LiClO$_4$-EC-PC	2.3×10^{-3}	Bohnke et al., 1993
PVDF-EC/PC-LiN(CF$_3$SO$_2$)$_2$	2.2×10^{-3}	Jiang et al., 1997
CMC-OA-glycerol	1.3×10^{-3}	Chai & Isa, 2016
PVDF-(PC+DEC)-LiClO$_4$	1.3×10^{-3}	Saikia & Kumar, 2004
PAN-LiI-Pr$_4$Ni-BMII	3.93×10^{-3}	Bandara et al., 2015
PEMA-NH$_4$CF$_3$SO$_3$-BMATFSI	8.35×10^{-4}	Anuar et al., 2012
PVA-Chitosan-NH$_4$NO$_3$-EC	1.6×10^{-3}	Kadir et al., 2010
PMMA-PVC-BmimTFSI	8.08×10^{-4}	Ramesh et al., 2011
PVDF-HFP-NaI-EC/PC	1.53×10^{-4}	Noor et al., 2014
PVA-CH$_3$COONH$_4$-BmimTf	1.74×10^{-3}	Liew et al., 2014
PEO-LiDFOB-EmimTFSI	1.85×10^{-4}	Polu & Rhee, 2017

2.6.3   Composite Polymer Electrolytes

Composite polymer electrolytes (CPEs) are prepared by adding inert particulate fillers into polymer electrolytes either dry polymer electrolytes or gel polymer electrolytes. In a pioneering research work by Weston and Steel (1982), the influence of doping inert filler (α-alumina) in PEO system was investigated. The mechanical strength and the ionic conductivity were significantly enhanced upon the incorporation of inert particles into the composite polymer systems. Since then, numerous polymer composites have been studied using filler such as ZrO_2, TiO_2, SiO_2, $BaTiO_2$ and hydrophobic fumed silica (Jayathilaka et al., 2002; B. Kumar et al., 2001; Q Li et al., 2001). The benefits of doping fillers can enhance ionic conductivity at low temperature and improvement in stability at the interface with electrodes (Ahn et al., 2003; Bhattacharya et al., 2017; Ji et al., 2003; X. Jiang et al., 2005; K. J. Kim & Shahinpoor, 2003).

Fillers can trap any remaining traces of organic solvent impurities and this may account for the enhanced interfacial stability of the composite polymer electrolytes. The composite polymer electrolytes with nano-sized filler show better electrode/electrolyte compatibility than those containing filler of micron size. It has also been suggested that the surface group of the ceramic filler play an active role in promoting local structural modifications in polymer electrolytes. (Wieczorek et al., 1996) applied the Lewis acid-base theory to explain the structure and the ionic conductivity of a number of polymer complexed with alkali metal salts such as PEO-LiClO$_4$ system incorporated with filler particles of three different characters, namely Lewis acid centres (AlCl$_3$), Lewis base centers poly(N,N dimethylacrylamide) and amphoteric Lewis acid-base (α-Al$_2$O$_3$). Since PEO has a Lewis base and Li$^+$ cation has Lewis acid character, the phenomena occurring in the composite electrolytes could be explained in terms of equilibrium

between various Lewis acid-base reactions. Table 2.3 lists a few of composite polymer electrolyte that have been reported in the literature.

Table 2.3: Some composite polymer electrolyte system and their conductivities

System	Ionic conductivity (S cm^{-1})	References
PMMA-LiBF$_4$-DBP-ZrO$_2$	4.6×10^{-5}	Rajendran & Uma, 2000a
PVDF-HFP-Al$_2$O$_3$	2.11×10^{-3}	Li et al., 2005
PVC–PMMA–LiBF$_4$–DBP–ZrO$_2$	2.391×10^{-3}	Rajendran & Uma, 2000b
PVDF-PAN-ESFM-LiClO$_4$-PC	7.8×10^{-3}	Gopalan et al., 2008
PVDF-HFP-NH$_4$CF$_3$SO$_3$-SiO$_2$	1.07×10^{-3}	Muda et al., 2011
PVA-LiClO$_4$-TiO$_2$	1.3×10^{-4}	Lim et al., 2017
PEO-EMIHSO$_4$-SiO$_2$	2.15×10^{-3}	Ketabi et al., 2014
PEO-AgNO$_3$-FE$_2$O$_3$	2.2×10^{-6}	Verma & Sahu, 2015
Starch/PVA- SiO$_2$	$\sim 10^{-3}$	Holkar et al., 2016

2.7   Modification of Polymer Electrolyte

Conventional polymer-salt electrolytes generally show low conductivities. Various methods have been proposed and developed in order to optimize the properties of the polymer electrolytes such as polymer blending, copolymerization, plasticization as well as impregnation of additives such as inorganic fillers and ionic liquids.

2.7.1   Polymer Blend

Polymer blends have received great interest in recent years as it is an economical technique to develop new polymeric materials with superior properties. It is the cheapest and easiest way to obtain new polymeric materials compared to developing new polymers. However, the properties of materials produced by this technique depend on the degree of miscibility of the polymers (da Silva Neiro et al., 2000). It has been

reported that the polymer blend electrolytes exhibited high conductivity (Baskaran et al., 2006; Sivakumar et al., 2007) and good mechanical strength (Fan et al., 2002; Ramesh et al., 2007; Sivakumar et al., 2007). The conductivity enhancement can also be attributed to increase in amorphous regions responsible for ionic conduction (Rudziah et al., 2011).

Buraidah and Arof reported that the highest conductivity value obtained at ambient temperature was 1.77×10^{-6} S cm^{-1} for the chitosan-PVA-NH$_4$I system. As comparison, the ionic conductivity achieved for unblended system, chitosan-NH$_4$I was 3.73×10^{-6} S cm^{-1} of two natural polymers; chitosan and starch. The highest ionic conductivity achieved by them was 3.89×10^{-5} S cm^{-1} at ambient temperature at the doping concentration of 35 wt% NH$_4$I. These results proved that the blending of polysaccharides is a promising technique that can be used to improve the ionic conductivity of polymer system. The improvement in the ionic conductivity is due to the availability of more complexation sites which raise the ion migration and exchange to take place (Buraidah & Arof, 2011).

2.7.2 Copolymerization

Copolymerization is a technique of combining two or more types of different monomers to produce a new polymer with tailor made properties. Modified copolymers with more functional monomers have been proposed as a solution to impede leakage problem of liquid electrolyte besides improve mechanical strength of polymer electrolytes (Zentner et al., 2001). This technique also increases the ionic conductivity by providing more amorphous region for ion transport (Dzulkurnain et al., 2015; Imperiyka et al., 2013).

2.7.3 Addition of Filler

Another alternative to improve the properties of the polymer electrolytes is to add inorganic fillers; micro or nano sized filler particles. The idea of incorporating fillers into polymer matrices as a means to increase mechanical stability of the polymer electrolytes has been demonstrated by (Weston & Steele, 1982). Besides that, addition of fillers also enhanced the properties of the polymer electrolytes (Gang et al., 1992) and improved anode-polymer interfacial stability (Cheung et al., 2003). Nanosized materials such as TiO_2 (Ambika et al., 2015; Rudhziah et al., 2011), SiO_2 (Agrawal et al., 2009), ZrO_2 (Ibrahim et al., 2010) and Al_2O_3 (Köster & van Wüllen, 2010) have been used to enhance conductivity of polymer electrolytes.

2.7.4 Addition of Plasticizers

Addition of plasticizers to polymer electrolytes is another useful technique to improve their conductivity. Plasticizers are substances incorporated into materials to increase flexibility and workability of a material (Rahman & Brazel, 2006). The essence of plasticization is to boost the conductivity of polymer electrolytes using low molecular weight and high dielectric constant additives (Osman, 2011). Kuila and co-workers reported that the conductivity of PEO-NaClO$_4$ increased by two orders of magnitude with the addition of 30 wt% PEG (Kuila et al., 2007).

The plasticization is also an alternative way to lower T_g, reduce crystallinity and improve the amorphous phase content of polymer electrolytes because of their high polarity and low vapour pressure (Johan & Fen, 2010; Pitawala et al., 2008). According to (Frech & Chintapalli, 1996) and (Koksbang et al., 1994), the plasticizers help in dissolution and dissociation of doping salts, thereby increasing the mobility of the cations while (Cowie & Martin, 1987) suggested that the addition of plasticizers

increases the amorphous phase in a polymer system. Generally, incorporation of plasticizer enhances the conductivity of polymer electrolytes. However in some cases, plasticization leads to low performances due high vapor pressure, narrow electrochemical window, small working voltage range, and poor interfacial stability with lithium electrodes (Kim et al., 2004; Pandey & Hashmi, 2009).

2.7.5   Incorporation of Ionic Liquid

Ionic liquids are room-temperature molten salts that possess unique properties, such as negligible vapour pressure, good thermal stability and non-flammability, together with high ionic conductivity and a wide window of electrochemical stability. Ionic liquids have been widely promoted as "green solvents", have recently attracted considerable attention due to their interesting and potentially useful physicochemical properties, including their good chemical and electrochemical stability, non-flammability, negligible vapour pressure and high ionic conductivity.

Ionic liquids meet the requirements of plasticizing salts and offer improved thermal and mechanical properties to flexible polymers. Polymer electrolytes containing ionic liquids have been reported to possess high conductivity. Besides that, the incorporation of ionic liquids into polymer electrolytes distinctively improves their electrochemical stability and increases their ionic conductivity (Noda & Watanabe, 2000). Ionic liquids have attracted the most attention as green chemistry substitutes for volatile organic solvents (Welton, 1999). Due to their unique properties, ionic liquids have been investigated as potential electrolytes for application in electrochemical devices including lithium ion batteries (Park et al., 2011), fuel cells (De Souza et al., 2003) and solar cells (Wang et al., 2002). However, their liquid nature limits their use in actual

devices due to problems of leakage, non-portability, and the impossibility of miniaturization.

2.8   Ionic Conductivity and Transport Mechanisms of Polymer Electrolyte

Ionic conductivity is a measure of a material's ability to conduct current. It is one of the important properties of polymer electrolytes. The ionic conductivity depends on various factors, such as cation and anion types, doping salt concentration and temperature (Hirankumar et al., 2005). The dependence of ionic conductivity on the salt concentration provides information on the specific interaction among the salt and the polymer matrix. The initial increase of ionic conductivity can be explained by association of ions of doping salt which leads to the enhancement of number of charge carriers. The decrement of conductivity at high salt content is commonly associated to the formation of ion pairs or aggregates that reduces the number of mobile charge carriers and gives limitation of the mobility of ions (Selvasekarapandian et al., 2005).

Conductivity of an electrolyte is contributed by the charge carrier density and ionic mobility. The general expression of ionic conductivity of a homogenous PE is as follows:

$$\sigma = nq\mu \tag{2.1}$$

The ionic mobility, μ is related to the diffusion coefficient D given by the Nerst-Einstein equation:

$$\sigma = \frac{qD}{kT} \tag{2.2}$$

when combine with Equation (2.1), the conductivity can be written as:

$$\sigma = \frac{nq^2 D}{kT} \qquad (2.3)$$

Several models have been proposed to interpret the ion conduction process in polymer electrolytes. The mechanism can be inferred from temperature dependent conductivity studies. For most PEs, their temperature dependent conductivity exhibits one of the following behaviour (Chandra & Chandra, 1994; Harris et al., 1987; Ratner, 1987):

(a) Vogel Tamman-Fulcher (VTF) behaviour

(b) Arrhenius behaviour for low temperature and VTF behaviour at a higher temperature

(c) Arrhenius behaviour throughout but with different activation energies in different temperature ranges

(d) VTF behaviour for temperatures slightly greater than T_g but Arrhenius behaviour at high temperatures

(e) Behaviour which is neither follows Arrhenius nor VTF behaviour in any temperature range

However, most experimental results show behaviours like (a), (b) and (c). Behaviour (d) can be explained in terms of the free volume theory, whereas behaviour (e) is the most complicated and difficult to understand. Arrhenius theory was developed in 1889, by Swedish chemist Svante Arrhenius (Crawford, 1996). It was found to be applicable for liquids and solids electrolytes later. The Arrhenius type relation is expressed as follows:

$$\sigma = \sigma_0 \exp(-E_a/kT) \qquad (2.4)$$

where, σ_0 is the pre-exponential factor, E_a is the activation energy, k_b is the Boltzmann constant and T is the absolute temperature. E_a can be calculated from the linear-least-square fit of the data from log σ versus $1000/T$ curve. In solids, the ions hop from one vacant site to another by overcoming the energy barrier (Kumar et al., 2006).

On the other hand, some polymer electrolytes obey VTF behaviour which was first developed to describe the viscosity of supercooled liquids (Baril et al., 1997; Pas et al., 2005; Vogel, 1921). From a macroscopic point of view, it is well accepted that the variation of ionic conductivity, σ with temperature for a fully amorphous polymer electrolyte can be more accurately represented by the Vogel-Tamman-Fulcher (VTF) (Fulcher, 1925; Tamman & Hesse, 1926; Vogel, 1921) equation:

$$\sigma = A/T^{\frac{1}{2}} \exp(-B/R(T - T_o) \tag{2.5}$$

In the above VTF equation, A is the pre-exponential factor, which is related to the number of charge carriers, R is gas constant, T is the temperature of measurement, B is the pseudo-activation energy of ion transport and hence relates to the segmental motion of polymer chains (Harris et al., 1987), k is the Boltzmann constant, and T_o is the equilibrium glass transition temperature or the thermodynamic limiting glass transition temperature (T_g) at which the configurational entropy is zero that corresponds to the T_g of the samples. The ionic conductivity σ is usually obtained from AC impedance measurements (Jacobs et al., 1989). The VTF equation can adequately describe the diffusion of uncharged molecules through disordered media such as fluids or polymers. In the case of polymer electrolyte systems, the ions are assumed to be transported by the semi-random motion of short polymer segments.

The correlation between ion transport and segmental mobility can be understood by recognizing the free volume model (Uma et al., 2005). As the temperature increases, polymers can expand easily and produces free volume. Therefore, ions solvated molecules or polymer segments can move into the free volume which enhances and segmental mobility that assists ion transport.

2.9   Application of Polymer Electrolytes

Polymer electrolytes have been numerously reported as successful candidates for application in various electrochemical devices. Described in the following sub-sections are a few of recent research on application of polymer electrolytes in electrochemical devices including Dye Sensitized Solar Cells (DSSCs), Solid State Batteries and Electric Double Layer Capacitor (EDLC).

2.9.1   PEs for Dye Sensitized Solar Cells Application

Bella and co-workers reported the high efficiency of 2.06% in a system based on carboxymethyl ƙ-carrageenan for DSSC application. The highest ever measured conductivity of 5.53×10^{-2} S cm^{-1} was reached for biopolymer based solid electrolyte system. NaI and EC were introduced into the biopolymer system. An innovative sublimation process was developed in order to make the material suitable for DSSC application. This finding is one of interesting ones related to research on green material (Bella et al., 2015).

On the other hand, high efficiency of 4.74% was achieved by a quasi-solid state DSSCs system composed of agarose, lithium iodide (LiI)/ iodine (I$_2$) as redox couple and titania nanoparticles (TiO$_2$) as fillers. It was found that increasing agarose and TiO$_2$

concentrations have led to a decrease in T_g, thus results in high σ of the electrolytes (Yang et al., 2011).

Recently, the potential of a blend system prepared from the combination of ƙ-carrageenan and cellulose derivatives for the application in dye sensitized solar cells (DSSCs) has been reported. Highest σ at ambient temperature published was 2.41 x 10^{-3} S cm^{-1} at 30 wt % of ammonium iodide (NH_4I) salt. The fabricated FTO/TiO_2-35 dye/CMKC/CMC-NH_4I + I_2/Pt cell showed response under light intensity of 100 mW/cm^{-2} with efficiency of 0.13%. The efficiency of the cell, despite being quite low, showed potential to be further explored and improved (Rudhziah et al., 2015).

Khanmirzaei and co-workers have also investigated the potential of rice starch based SPEs to be applied in DSSC. The highest ionic conductivity of 1.2×10^{-3} S cm^{-1} was achieved upon incorporation of 20 wt% of MPII ionic liquid while the highest energy conversion efficiency of 2.09 % is attained for that system (Khanmirzaei et al., 2015). In another article, the same authors described the potential of hydroxypropyl cellulose in DSSC application. Hydroxypropyl cellulose (HPC), sodium iodide (NaI), 1-methyl-3-propylimidazolium iodide (MPII) as ionic liquid (IL), ethylene carbonate (EC) and propylene carbonate (PC) were used for preparation of non-volatile gel polymer electrolyte for DSSC. The highest ionic conductivity of 7.37×10^{-3} S cm^{-1} was achieved after introducing 100 % of MPII with respect to the weight of HPC. The gel polymer electrolyte with 100 wt% of MPII ionic liquid showed the best performance and energy conversion efficiency of 5.79%, with short-circuit current density, open-circuit voltage and fill factor of 13.73 mA cm^{-2}, 610 mV and 69.1%, respectively.

2.9.2 PEs for Electric Double Layer Capacitor Application

The application of corn starch as an electrolyte in EDLC has been investigated by Shukur and co-workers using lithium acetate (LiOAc) and glycerol as ionic dopant and plasticizer, respectively. The maximum conductivity was $(1.04 \pm 0.10) \times 10^{-3}$ S cm^{-1}. The electrochemical stability achieved by the highest conducting electrolyte was up to 2.1 V. Cyclic voltammetry and discharge-charge measurement gave the calculated C_s of 33.00 F g^{-1} at scan rate of 0.5 mV s^{-1} and was found to increases as the scan rate decreases. From the charge-discharge measurement, the value of C_s is almost constant for 1000 cycles. This revealed that the biopolymer electrolyte system has potential to be utilized for EDLC application (Shukur et al., 2014).

Meanwhile, a blend system composed of two biopolymers, chitosan and iota carrageenan doped with orthophosphoric acid (H_3PO_4) and polyethylene glycol (PEG) as the plasticizer were developed by Arof and co-workers (2010). Ionic conductivity of 6.29×10^{-4} S cm^{-1} was obtained. The biopolymer electrolytes prepared were found to be efficiently function as a separator in an electrical double layer capacitor (EDLC) with a specific charge capacitance (C_s) of 35 F g^{-1} at 0.11 mA cm^{-2} current drain and was constant for 30 cycles.

Liew and co-workers (2014) reported a study on corn starch based electrolyte for EDLC application. Two types of ionic liquids, [Bmim][OTf] and [Bmim][PF6] were utilized and attained optimum conductivity of 3.21×10^{-4} and 1.47×10^{-4} S cm^{-1} respectively, at ambient temperature. They claimed that the EDLC based on triflate anion showed better potential window range and capacitance due to the higher value of σ. Besides that, good adhesion between the biopolymer electrolyte with the electrodes has improved the interfacial contact and result in the higher capacitance value of 42.44

F g^{-1}. The EDLC was reported to possess excellent electrochemical stability upon charging and discharging for 500 cycles.

2.9.3 PEs for Battery Application

The potential of polymer electrolyte to be applied in battery was successfully shown by Polu & Kumar (2013). They reported a magnesium battery based on polyvinyl alcohol (PVA) complexed with magnesium acetate ($Mg(CH_3COO)_2$). The highest conductivity measured at ambient temperature was 1.34×10^{-7} S cm^{-1} for 80 PVA: 20 $Mg(CH_3COO)_2$ at 303 K. The fabricated polymer electrolyte battery produced a maximum open circuit voltage of 1.84 V.

Recently, Shukur & Kadir (2015) reported the application of starch-chitosan blend in proton battery. LSV measurement revealed that the electrolyte composed of starch-chitosan-NH_4Cl-glycerol decomposed at 1.65 V, confirming the suitability of the electrolyte in the application. The open circuit potential (OCP) of the primary proton battery was (1.54 ± 0.01) V while that of secondary proton battery was (1.58 ± 0.01) V lasted for 48h. The secondary proton batteries has been charged and discharged for 40 cycles.

In other investigation, the influence of adding the room-temperature ionic liquid *N*-methyl-*N*-propylpyrrolidinium bis(trifluoromethanesulfonyl)imide ($PYR_{13}TFSI$) to $P(EO)20LiTFSI$ polymer electrolytes and the use of these electrolytes in solid-state Li/V_2O_5 batteries were investigated (Shin et al., 2006). The addition of the ionic liquid into $P(EO)20LiTFSI$ electrolytes resulted in freestanding and highly conductive electrolyte films reaching 10^{-3} S cm^{-1} at 40° C. The electrochemical stability of the ionic liquid was found to significantly improved by the addition of LiTFSI. Excellent

reversible cyclability with a capacity fading of 0.04% per cycle over several hundred cycles at 60 °C was achieved by the Li/V_2O_5 cells. The authors proved that the incorporation of the ionic liquid into lithium metal-polymer electrolyte batteries has resulted in a promising improvement in performance at moderate to low temperatures.

Table 2.4: Comparison of present cell parameters with the data of other cells reported earlier

Solid-state electrochemical cells configuration	Open Circuit Voltage (V)	Discharged time for plateau region (h)	References
$Ag/(PVP+AgNO_3)/(I_2+C+electrolyte)$	0.46	48	Reddy et al., 1995
$Na/(PEO+NaYF_4)/(I_2+C+electrolyte)$	2.45	96	Rao et al., 1995
$Mg/(PEO+Mg(NO_3)_2)/(I_2+C+electrolyte)$	1.85	142	Ramalingaiah et al., 1996
$K/(PVP+PVA+KBrO_3)/(I_2+C+electrolyte)$	2.3	72	Reddy et al., 2006
$Zn+ZnSO_4.7H_2O/(PVA+Chitosan+NH_4NO_3+EC)/MnO_2$	1.7	17	Kadir et al., 2010
$Mg/(PVP+MgCl_26H_2O)/(I_2+C+electrolyte)$	2.1	115	Basha et al., 2016
$Na/(PEO+NaF)/(I_2+C+electrolyte)$	2.52	101	Sasikala et al., 2012
$V_2O_5 + PbO_2 + C / TSP + NH_4Br / Zn + ZnSO_4. 7 H_2O + C + polymer electrolyte$	1.54	167	Premalatha et al., 2017
$Na/(PVA+CH_3COONa_3H_2O)/(I_2+C+electrolyte)$	1.9	75	Basha et al., 2015
$Mg/(PVP + MgCl_2 \cdot 6H_2O + Al_2O_3)/(I_2 + C + electrolyte)$	1.75	118	Basha et al., 2017
$Mg/(PVA+PAN+MgCl_2)/(MnO_2 + C + electrolyte)$	2.17	500	Selvin, et al., 2017

The potential of biopolymer electrolyte to be applied in battery was successfully fabricated by Samsudin and co-workers (2014). They reported a rechargeable proton battery based on carboxymethyl cellulose by incorporating ammonium bromide (NH_4Br) as the proton conductor. The highest σ measured at ambient temperature was

1.12 x 10^{-4} S cm^{-1}. The fabricated biopolymer electrolyte battery produced a maximum OCP of 1.36 V and showed good rechargeability. This result has contributed to the new invention of biopolymer electrolytes application in electrochemical devices (Samsudin et al., 2014).

2.10   Summary

In this chapter, review and background of kenaf fiber, cellulose and polymer electrolytes have been reviewed. Brief discussions about the application of polymer electrolytes in electrochemical devices have also been presented. From the information and knowledge gained in this literature review, it is expected that the biopolymer electrolytes obtained from this work can be applied in electrochemical devices. The following chapter presents the methods of preparation and characterization of the studied CMC based electrolytes.

CHAPTER 3: EXPERIMENTAL & METHODOLOGY

3.1 Overview

This chapter describes the chemicals, instruments and methods used in preparing and characterizing the samples. The method employed in preparation of biopolymer electrolytes is solution casting technique. Sample characterizations comprise of Fourier transform infrared spectroscopy (FTIR), scanning electron microscopy (SEM), electrochemical impedance spectroscopy (EIS), thermogravimetric analysis (TGA), dynamic mechanical analysis (DMA), linear sweep voltammetry (LSV), and transference number measurement (TNM) were employed in order to investigate the structural, optical, thermal, and electrical properties of the samples. The highest conducting electrolyte was used in electrochemical cell.

3.2 Samples Preparation

Raw kenaf bast (*Hibiscus cannabinus L*) fiber was obtained from KFI Sdn. Bhd., Malaysia. The sodium hydroxide, sulphuric acid, sodium chlorite, isopropanol, glacial acetic acid and monochloroacetic acid were purchased from Sigma-Aldrich, Germany and SYSTERM-chemAR, Malaysia. Meanwhile, ammonium acetate, NH_4CH_3COO (98%), $Mg(CH_3COO)_2$, $NaCH_3COO$, $Zn(CH_3COO)_2$ and 1-butyl-3-methylimidazolium chloride ([Bmim]Cl) were procured from Sigma-Aldrich, Germany. All materials were used as received without further purification.

3.2.1 Synthesis of Cellulose from Kenaf Bast Fiber

Cellulose was prepared from raw kenaf bast fiber. Firstly, kenaf fiber was blended into small pieces and then treated with a 4% NaOH solution at 90 °C for 3 h under mechanical stirring as illustrated in Figure 3.1. This treatment was repeated three times,

and the fiber was filtered and washed with distilled water. The fiber was later bleached in a solution consisting of equal parts of acetate buffer (solution of NaOH and acetic acid in distilled water), aqueous sodium chlorite and distilled water. Treatment was repeated three times and was performed at 90 °C for 4 h under mechanical stirring. Then, the bleached fiber was cleaned by using distilled water and dried at room temperature. The significance of the alkali treatment was to eliminate the alkali-soluble components, while the bleaching treatment was conducted to remove residual lignin. Figure 3.2 shows photographs of the kenaf fiber, the fiber after alkali treatment and lignin-free cellulose, respectively.

Figure 3.1: Alkali treatment and bleaching process

Figure 3.2: Photographs of (a) kenaf fiber, (b) fiber after alkali treatment and (c) lignin-free cellulose

3.2.2 Modification of Carboxymethyl cellulose from Lignin-free Cellulose

5 g of lignin-free cellulose was mixed with 100 mL of isopropanol in 500 mL conical flask. The conical flask was placed in a flask filled with water at the temperature around 40 $^{\circ}$C. Then, 20% NaOH was added into the conical flask drop by drop and stirred for 15 minutes. Next, solution of 20 g monochloroacetic acid and 15 mL isopropanol were added into the conical flask. The mixture was heated, stirred and etherified for another 4 hours. The reaction was then terminated by addition of ethanol. 7% of ethanol was added into the mixture and further heating was done for another one hour. Lastly, CMC obtained was washed with 7%, 8% and 9% of ethanol until a clean powder was obtained. The remaining powder was dried in a desiccator for several days until the powder was completely dried for further characterization. Figure 3.3 shows the carboxymethyl cellulose obtained after etherification.
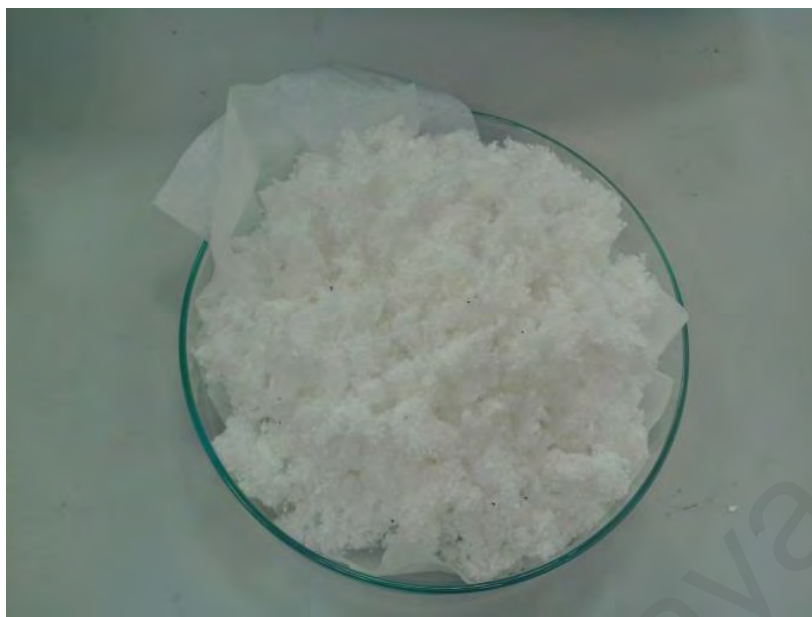
Figure 3.3: Carboxymethyl cellulose after etherification

3.2.3   Preparation of CMC-acetate Salts Biopolymer Films

Solution casting technique was employed to obtain films with various amounts of ammonium acetate (0-40 wt%), magnesium acetate (0-40 wt%), sodium acetate (0-40 wt%) and zinc acetate (0-40 wt%). Pure CMC film was also prepared as a control. For preparing the salted systems, weighed amounts of CMC powder and acetate based salts were dissolved in 40 mL of 1% acetic acid at room temperature. Complete dissolution of CMC and salt was achieved after several hours of stirring at room temperature using a magnetic stirrer. The composition and designation of electrolytes in salted systems are tabulated in Table 3.1. The final clear solution was then poured into separate Petri dishes and left to dry at room temperature to form highly translucent thin films (Figure 3.4). Biopolymer electrolyte films were transferred to a desiccator for further drying prior to characterization.
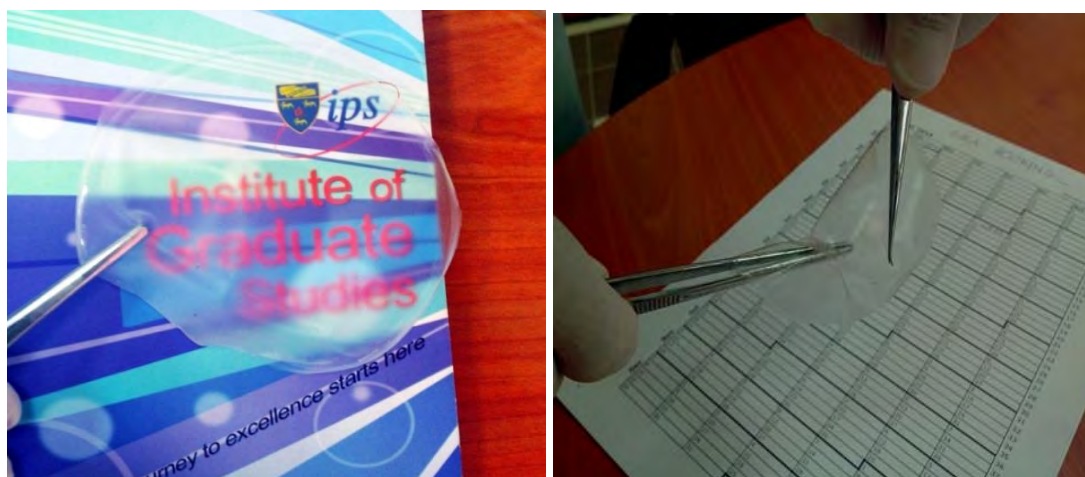
Figure 3.4: Biopolymer electrolyte film

Table 3.1: Composition and designation of biopolymer electrolytes containing ammonium acetate

Composition (wt%) CMC: NH_4CH_3COO	Designation
100:0	A0
90:10	A1
80:20	A2
70:30	A3
60:40	A4

Table 3.2: Composition and designation of biopolymer electrolytes containing magnesium acetate

Composition (wt%) CMC: $Mg(CH_3COO)_2$	Designation
100:0	B0
90:10	B1
80:20	B2
70:30	B3
60:40	B4

Table 3.3: Composition and designation of biopolymer electrolytes containing sodium acetate

Composition (wt%) CMC: NaCH₃COO	Designation
100:0	C0
90:10	C1
80:20	C2
70:30	C3
60:40	C4

Table 3.4: Composition and designation of biopolymer electrolytes containing zinc acetate

Composition (wt%) CMC: Zn(CH₃COO)₂	Designation
100:0	D0
90:10	D1
80:20	D2
70:30	D3
60:40	D4

3.2.4 CMC-NaCH₃COO-[Bmim]Cl Plasticized System

In order to prepare IL-biopolymer system, another set of solutions containing fixed amount of CMC and salt (the highest conducting salted electrolyte composition) incorporated with different amounts of ionic liquid (0-40 wt%), [Bmim]Cl were prepared. All homogeneous solutions were cast onto glass Petri dishes and left dry at ambient temperature for film formation. The dry films were then kept in desiccators for further drying before being characterized. The compositions and designations of electrolytes in the plasticized systems are listed in Table 3.2.

Table 3.5: Composition and designation of electrolytes in plasticized system

Composition (wt%) C3: ionic liquid, [Bmim]Cl	Designation
100:0	S0
90:10	S1
80:20	S2
70:30	S3
60:40	S4
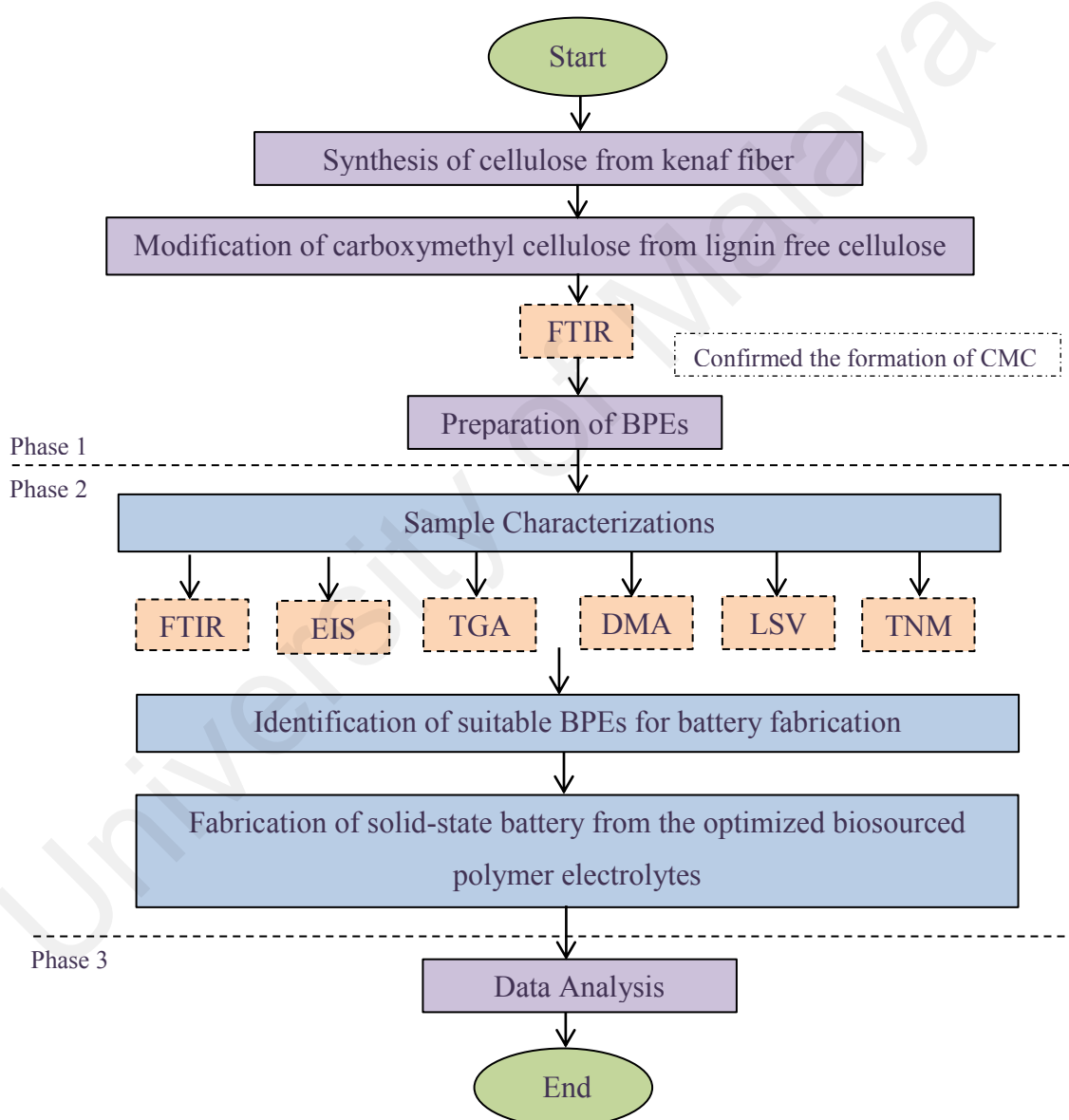
Figure 3.5: Experimental flow chart

3.3 Characterization of Biopolymer Films

The properties of CMC depend on the degree of substitution (DS) of the hydroxyl group which takes part in the substitution reaction in the cellulose. Therefore, DS of CMC from kenaf fiber was determined. The biopolymer electrolyte films obtained were then characterized. This phase also focused on determining the complexation, structural, thermal, morphology, electrical and ionic transport study of biopolymer electrolytes produced by using FTIR, TGA, DMA, EIS, LSV and also TNM.

3.3.1 Degree of Substitution

The titration method was used to determine the DS of the synthesized CMC. The first step was to change the substituent COONa to COOH. 3 g of Na–CMC was suspended in 80% of ethanol, and 20 mL hydrochloric acid (37% concentration) were added to the mixture. The mixture was stirred for 30 min, and after that, the solid was then filtered and rinsed with 70%–90% ethanol. CMC–H was then obtained. Next, about 0.5 g of CMC–H was immersed in 100 mL of distilled water in a conical flask and stirred. 25 mL of 0.3 M NaOH was later poured into the flask and heated for 15 min. Then, the mixture was titrated with 0.3 M hydrochloric acid, with phenolphthalein as an indicator. In this work, the DS was determined by using acid-wash method and calculated using equation (3.1).

$$DS_{abs} = \frac{162 \times \%CM}{[5900 - (58 \times \%CM)}$$

(3.1)

where carboxymethyl content, (% CM) is given by Equation (3.2):

$$(\% \, CM) = \frac{[(V_0 - V_n)M \times 0.059 \times 100]}{m}$$

(3.2)

In Equation (3.2), V_0 is the amount of hydrochloric acid used to titrate the blank solution, V_n is the amount of hydrochloric acid used to titrate samples, M is the molar concentration of hydrochloric acid used and m is the sample amount. The value of 162 g·mol^{-1} is the molar mass of the anhydroglucopyranose unit (AGU), and 58 g·mol^{-1} is the molar mass of –CH$_2$COOH (El Seoud et al., 2013).

3.3.2 FTIR Spectroscopy

FTIR is one of efficient tools to investigate the interactions among various constituents in the biopolymer electrolyte systems. In this study, FTIR measurement was performed by using a Perkin Elmer Frontier FTIR spectrometer (Waltham, MA, USA) equipped with attenuated total reflection as shown in Figure 3.6. The sample was placed on top of a diamond surface with a pressure arm applying force onto the sample, and infrared light passed through the sample. FTIR spectra were recorded in the spectral range from 4000 to 500 cm^{-1} at a resolution of 2 cm^{-1} with a scan rate of 4 at room temperature. The FTIR data were recorded in the transmittance mode. The FTIR spectroscopy was carried out to study interactions between CMC, NH$_4$CH$_3$COO, Mg(CH$_3$COO)$_2$, NaCH$_3$COO, Zn(CH$_3$COO)$_2$ and [Bmim]Cl.

Figure 3.6: Perkin Elmer Frontier FTIR spectrometer

3.3.3 Electrochemical Impedance Spectroscopy

The impedance study was performed by using a Solartron 1260 impedance/gain phase analyser with frequency ranging from 10 to 4 MHz. Each biopolymer electrolyte sample was sandwiched between two stainless steel electrodes of diameter 2.0 cm (area = 3.142 cm^2) under spring pressure. The impedance of the samples was measured at temperatures in the range from 0 to   C . The dc conductivity, σ (S cm^{-1}) was calculated using the equation,

$$\sigma = \frac{t}{R_b A} \tag{3.3}$$

where, t (cm) is the thickness of polymer electrolytes measured using Mitutoyo digital micrometer, R_b is the bulk resistance obtained from the intercept of high frequency semicircle or the low frequency spike on the Z_r-axis of Cole-cole plots, and A (cm^2) is the area of electrolyte-electrode contact.

3.3.4 Thermogravimetric Analysis

TGA is an analytical technique used to determine the thermal stability of a material and its freaction of volatile components by monitoring the weight change that occurs as a specimen is heated. The measurement is normally carried out in air or in an inert atmosphere (such as Helium or Argon) and the weight is recorded as a function of increasing temperature. In this work, thermal analysis of biosourced polymer films was carried out from ambient temperature up to 600 C at a heating rate of 10 C min^{-1} by using a Setaram EVO Labsys thermal analyser in nitrogen atmosphere. The first run was up to 100 C to remove absorbed water and the second and third runs were performed up to 600 C The data were then analysed using Calisto software.

3.3.5 Dynamic Mechanical Analysis

Glass transition temperatures of CMC films were determined by using a Perkin Elmer dynamic mechanical analysis (DMA) 8000 instrument. The analysis was done in tension mode. The samples used were of 2 cm length and 1 cm width. The thickness of the samples was around 0.01 cm to 0.0 cm. The temperature range was from -100 C to 100 C at heating rate of 1 C min^{-1} while the frequency was fixed at 1 Hz. Liquid nitrogen was supplied to the instrument in order to start the analysis at low temperature. Glass transition temperatures of samples were determined from the peak of the tan δ-T curves.

3.3.6 Transference Number Measurement

Ionic transference number is another important parameter for polymer electrolyte materials. Transference number of moving charges is defined as the ratio of the conductivity due to themselves to the total conductivity given by equation (3.4):

$$\sigma_T = \sigma_i + \sigma_e \tag{3.4}$$

where σ_i and σ_e are the conductivities contributed by ions (cations/anions) and electrons/holes respectively. The transference number of an ion (t_i) and electron (t_e) in solid electrolytes is the ratio of the conductivity due to the ionic species to the total conductivity of the electrolytes, that is

$$t_i = \frac{\sigma_i}{\sigma_T} \tag{3.5}$$

and

$$t_e = \frac{\sigma_e}{\sigma_T} \tag{3.6}$$

If a solid electrolyte is purely ionic, then $t_i = 1$ while for an electronic conductor, $t_e = 1$. For mixed conductors, t_i varies between 0 and 1.

Various techniques have been proposed by many researchers to measure ionic transference number. The techniques are as follows:

     i.   Wagner's polarization method (Chandra, 1981)

    ii.   Direct current (DC) polarization method (Chandra, 1981)

   iii.   Electrochemical potential measurements (Chandra, 1981)

   iv.   Turbandt's DC electrolytes method (Chandra, 1981)

    v.   Complex impedance spectroscopy method or combine AC and DC technique (Bruce et al., 1988; Watanabe et al., 1988)

   vi.   Potentiostatic polarization method (Blonsky et al., 1986)

  vii.   Deducing t_i from diffusion coefficient with

        a.   Radiotracer method (Chadwick et al., 1983)

        b.   Pulsed field gradient NMR (PFG-NMR) method (Bhattacarja et al., 1986)

 viii.   Hittorf method (Kontturi et al., 1994; Yang et al., 2005)

   ix.   Moving boundary method (Glasstone, 2008)

In this work, ionic transference number was carried out using a direct current polarization technique by monitoring the polarization current as a function of time. The biopolymer electrolyte films were sandwiched between two stainless steel blocking electrodes connected to a 1.5 V voltage source.

3.3.7 Electrochemical Stability Window Determination

LSV is a voltammetric method where the current at a working electrode is measured while the potential between the working electrode and a reference electrode is swept linearly in time (Peerce & Bard, 1980). Oxidation or reduction of species is registered as a peak or trough in the current signal at the potential at which the species begins to be oxidized or reduced (Wang et al., 2006).

The electrochemical stability window of selected electrolyte films was measured on a Wonatech ZIVE MP2 multichannel electrochemical workstation. The LSV was carried out using stainless steel electrodes at a scanning rate of 1 mVs^{-1} from 0 to 4 V. Measurement was done at room temperature.

3.4 Fabrication and Characterization of Electrochemical Cells

Solid-state electrochemical cells were fabricated by sandwiching the highest conducting biopolymer electrolyte between anode and cathode pellets, with the configuration, Na|CMC/NaCH$_3$COO/[Bmim]Cl|(I$_2$+C+electrolyte). The entire assembly was finally enclosed as a coin cell. Sodium metal obtained from Sigma Aldrich was used as the anode. A proper mixture of iodine (I$_2$), graphite (C) and the electrolyte material in weight ratio of 5:5:1 respectively was obtained by physical grinding. This was then pressed to form of thin pallet as the cathode at a pressure of 440 MPa after proper mixing of constituents. While iodine is an active cathodic material, graphite provides an adequate electronic conductivity and electrolyte material to favour electrode/electrolyte interfacial contact and helps in reducing electrode polarization (Agrawal et al., 2007). The fabricated coin cell was then tested using NEWARE BTS 3000 battery tester interfaced with a computer.
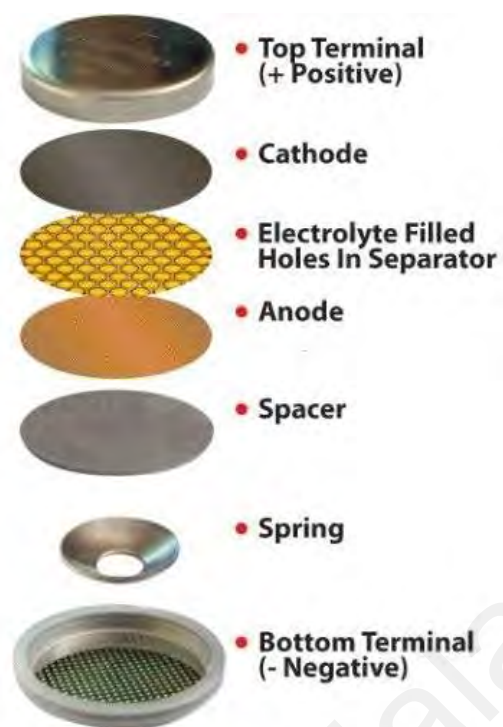
Figure 3.7: Coin-cell battery configurations

3.5 Summary

This chapter has explained the preparation method of CMC and biopolymer electrolytes based on carboxymethyl cellulose in detail as well as the characterization techniques employed in this study. Fabrication of electrochemical devices has been clearly described. Results from the conducted experiments using various techniques will be discussed in chapters 4 and 5.

CHAPTER 4: PREPARATION AND CHARACTERIZATION OF BIOPOLYMER ELECTROLYTES BASED ON CMC-ACETATE SALTS

4.1 Introduction

In this chapter, the results of the carboxymethyl cellulose from renewable resources, kenaf bast fiber which was synthesized for application as host materials in polymer electrolytes are presented. The results from various characterizations of synthesized CMC and the results of CMC doped with acetate salts (NH_4CH_3COO, $Mg(CH_3COO)_2$, $NaCH_3COO$, $Zn(CH_3COO)_2$) biopolymer electrolytes are also presented and discussed. The idea of incorporating with different acetate salts is to determine the effect of cation size on the physicochemical and electrical properties of biopolymer films. Besides that, we are looking an alternative for lithium ion batteries which suffer from safety limitations due to explosive nature and expensive. Therefore these ionic dopants could be an excellent substitute for lithium ion batteries which offer cost effectiveness, low toxicity, ease of handling and safer than lithium. The biopolymer electrolytes were characterized using different methods consisting of FTIR, TGA, DMA, IS, TNM and LSV.

4.2 Carboxymethyl cellulose

4.2.1 Degree of Substitution

The DS was determined to identify the quality and properties of CMC, as well as the purity, molecular weight and crystallinity (Kurita, 2001). Methods, like the acid-wash, the conductometric and the coulometric methods (Eyler et al., 1947), can be applied in order to determine the degree of substitution of CMC. CMC was obtained at a DS range of 0.5 to 2.9 (El Seoud et al., 2013). The DS value obtained for CMC from kenaf fiber synthesized in this study was 1.49. The DS value obtained in this work is higher

compared to those of the commercial CMCs available in the market, which are around 0.7 to 1.2. The higher DS value means that the CMC has a higher number of oxygens, thus providing more active sites for coordination with the cations of doping salts, which is hoped to give higher conductivity values.

4.2.2 Confirmation of Carboxymethyl cellulose Formation
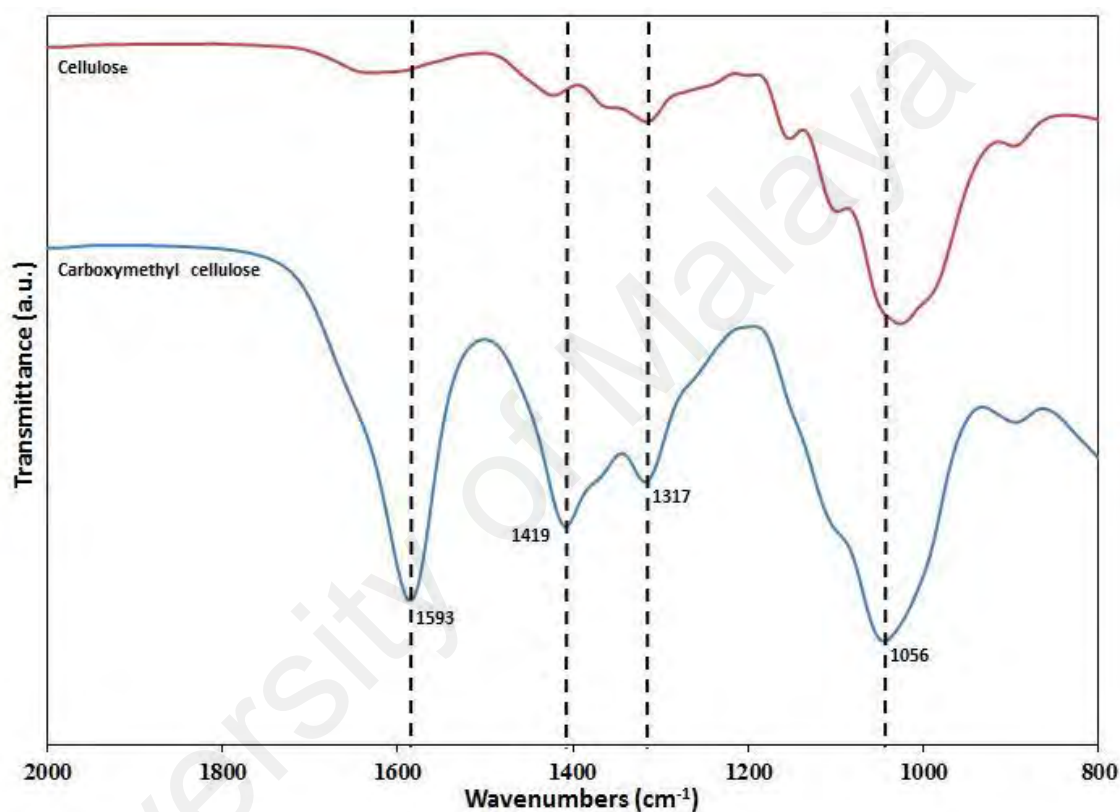
Figure 4.1: IR spectra of cellulose and CMC in the region between 2000 and 800 cm^{-1}

Figure 4.1 illustrates the IR-spectra of white cellulose and modified cellulose, CMC in the spectral range from 800 to 2000 cm^{-1}. The absorption bands at 1593 cm^{-1} is assigned to asymmetrical COO$^-$ stretching, 1419 cm^{-1} (CH$_2$ symmetrical bending) and 1056 cm^{-1} (CHO-CH$_2$ stretching). The appearance of these bands confirms the formation of CMC (Biswal & Singh, 2004; Dos Santos et al., 2015; Pushpamalar et al., 2006).

4.2.3 Decomposition Analysis of Carboxymethyl cellulose

The result of TGA carried out on the synthesized CMC is presented in Figure 4.2. Two distinct weight losses are observed. The first weight loss is about 24.51% in the temperature range from 30 to 135 °C. The initial weight loss is due to the presence of moisture in the sample. A similar observation was reported by (Lam et al., 2012). This is because biopolymer tends to absorb moisture from its surroundings (Kargarzadeh et al., 2012). The second weight loss is 14.79% in the temperature range of 250 to 323 °C due to the loss of COO^- from the polysaccharide (Biswal & Singh, 2004). The final loss of 7.05% is observed in the temperature range of 373 to 511 °C, representing the degradation of the remaining material into carbon residues. This result reveals that the CMC can be used as host polymer electrolytes at ambient temperature and moderate temperatures up to 250 °C, which are suitable for applications in electrochemical devices, such as in solar cells or batteries.
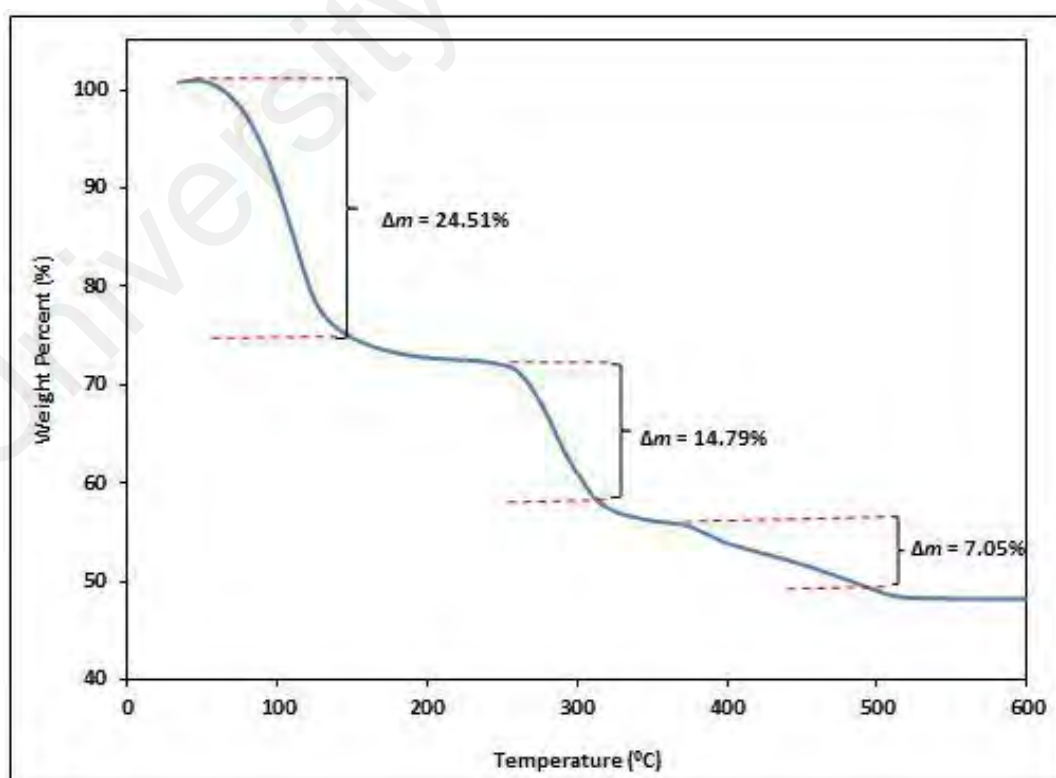
Figure 4.2: TGA curve of the pure CMC from kenaf bast fiber

4.2.4 Dynamic Mechanical Analysis

The T_g of CMC film was determined using DMA. Figure 4.3 depicts the damping curves (tan δ) for CMC film. The damping curve presented in Figure 4.3 shows the main relaxation process in the amorphous region of CMC. As the temperature increases, damping increases to a maximum before decreasing with further increase in temperature. The temperature corresponding to the peak of the curve is attributed to the T_g. The glass transition of CMC film determined from the DMA curve is −18.0 °C.
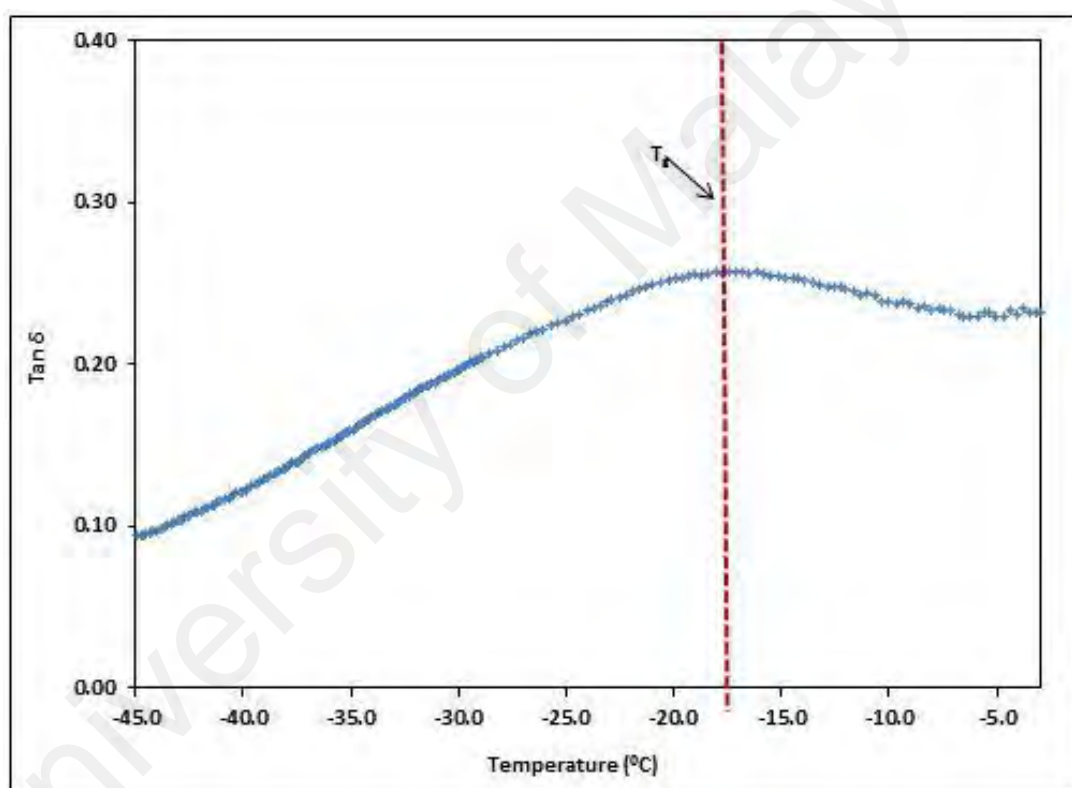
Figure 4.3: DMA curve for the pure CMC biopolymer film

4.3 CMC-acetate Salts Biosourced Polymer Electrolyte Films

This section focuses on discussion to determine the complexation, thermal, morphology, electrical and electrochemical properties as well as ionic transport study of biosourced polymer electrolytes prepared in this study.

4.3.1 CMC-NH$_4$CH$_3$COO Biosourced Polymer Electrolytes

4.3.1.1 Study on interactions between CMC with NH$_4$CH$_3$COO

In this study, FTIR was done to investigate the interactions between polymers in the CMC and NH$_4$CH$_3$COO to provide evidence of the interactions between the polymer host and ionic dopant. Depicted in Figure 4.4 are the FTIR spectra of NH$_4$CH$_3$COO, pure CMC and CMC doped with NH$_4$CH$_3$COO (10–40 wt%). The characteristic absorption band at 3315 cm^{-1} can be attributed to OH stretching. Meanwhile the small hump at 2946 cm^{-1} is ascribed to C–H stretching (Sain & Panthapulakkal, 2006). Upon addition of 20 wt% NH$_4$CH$_3$COO, it can be observed that the carboxyl group (C=O) at 1597 cm^{-1} has shifted to a lower wavenumber (1586 cm^{-1}), which suggests the interaction of the (C=O) moiety in CMC with the H$^+$ of the (NH$_4^+$) substructure in NH$_4$CH$_3$COO. This phenomenon can be related to the lone pair electrons that attracted the salt molecule of NH$_4$CH$_3$COO to the system (Selvasekarapandian et al., 2005). The concentration of H$^+$ increases when the composition of NH$_4$CH$_3$COO; implying that more electrons were withdrawn toward C=O to form hydrogen bonding which in turn resulted in the shift of the band at 1585 to 1559 cm^{-1}. The vibration band at 1420 cm^{-1} corresponds to the presence of N-H deformation in NH$_4$CH$_3$COO; however, this band overlapped with the O–H band, as reported by (Kamarudin & Isa, 2013). Lastly, the intense band around 1060 cm^{-1} was reported to be related to the C–O–C stretching, signifying the characteristics of the polysaccharide skeleton.
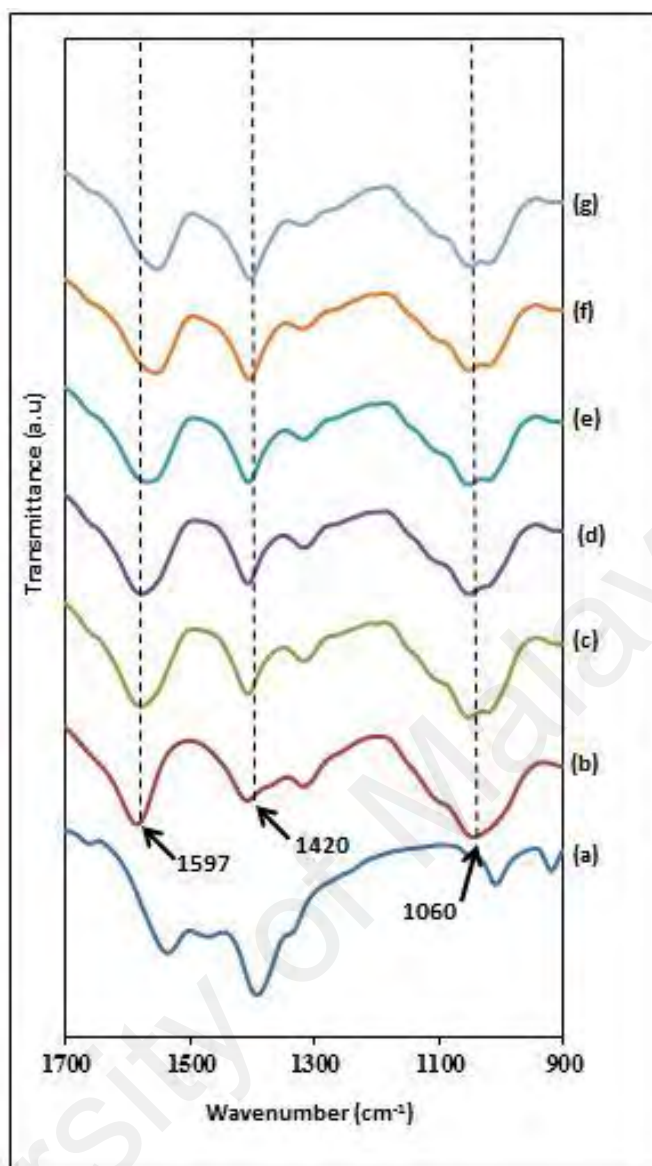
Figure 4.4: IR-spectra of (a) NH₄CH₃COO, (b) CMC powder, and CMC added with (c) 10, (d) 20, (e) 30 and (f) 40wt% NH₄CH₃COO in the spectral region between 1700 and 900 cm⁻¹

4.3.1.2   Impedance study on CMC-NH₄CH₃COO biosourced polymer electrolytes

Figure 4.5 represents Nyquist plot of CMC with 20 wt% NH₄CH₃COO at room temperature. Normally, the spectra of polymer electrolytes show two different regions; incomplete semicircle at the high frequency and a spur at the low frequency. However in this study, the plot depicts a titled spike indicates that the conductivity is mainly due to ion conductions (Ramya et al., 2007).
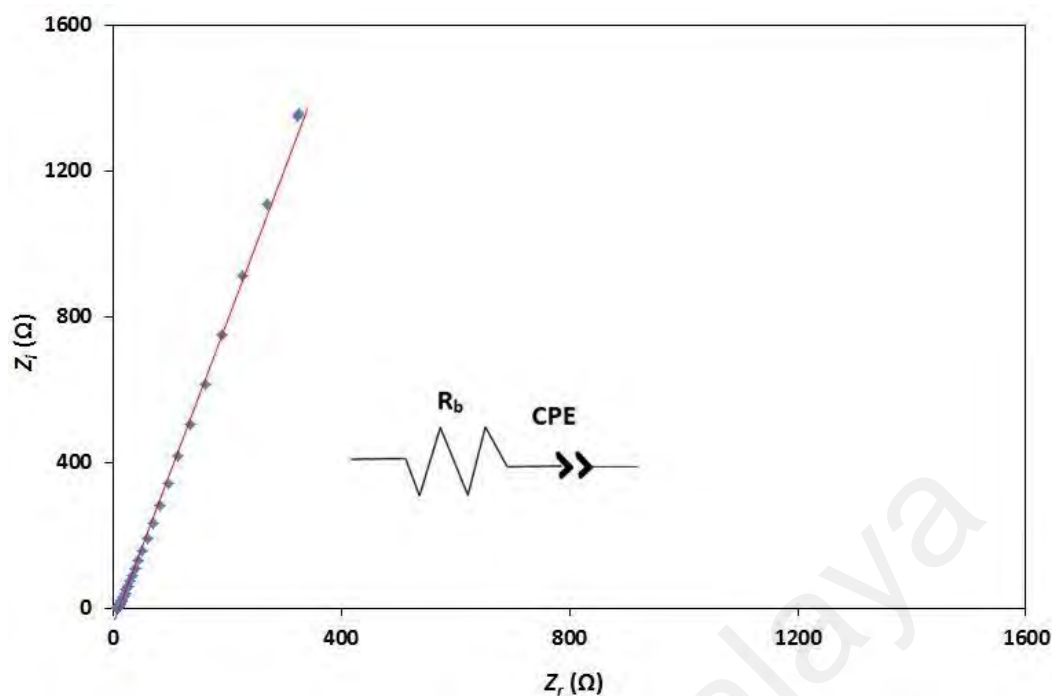
Figure 4.5: Typical Nyquist plot of CMC- 20 wt % NH₄CH₃COO at room temperature. The inset figure illustrates the corresponding equivalent circuit.

The electrical equivalent circuit representation is commonly used in impedance analysis as it is fast, simple and provides complete picture of the system (Han & Choi, 1998). The fitting of impedance plots can further confirm the values of R_b. In the present work, the data can be well fitted with the equivalent circuit consist of R_b (bulk electrolyte resistance) and CPE (constant phase element) as presented in the inset figure of Figure 4.5. The existence of CPE could be due to capacitive behaviour changes with the frequency and arises if there is air presence in between the electrode-electrolyte surface (Noor et al., 2010; Ali et al., 2008). The R_b of the film was calculated from the intercept of the tilted spike at real impedance axis. With increasing salt concentration, the value of R_b decreases.

Figure 4.6 reveals the graph for conductivity against concentration of NH₄CH₃COO at ambient temperature. The conductivity was calculated using equation (3.3). The R_b is the bulk resistance obtained from the intercept of high frequency semicircle or the low

51

frequency spike on the Z_r-axis of Nyquist plots, and A (cm^2) is the area of electrolyte-electrode contact.
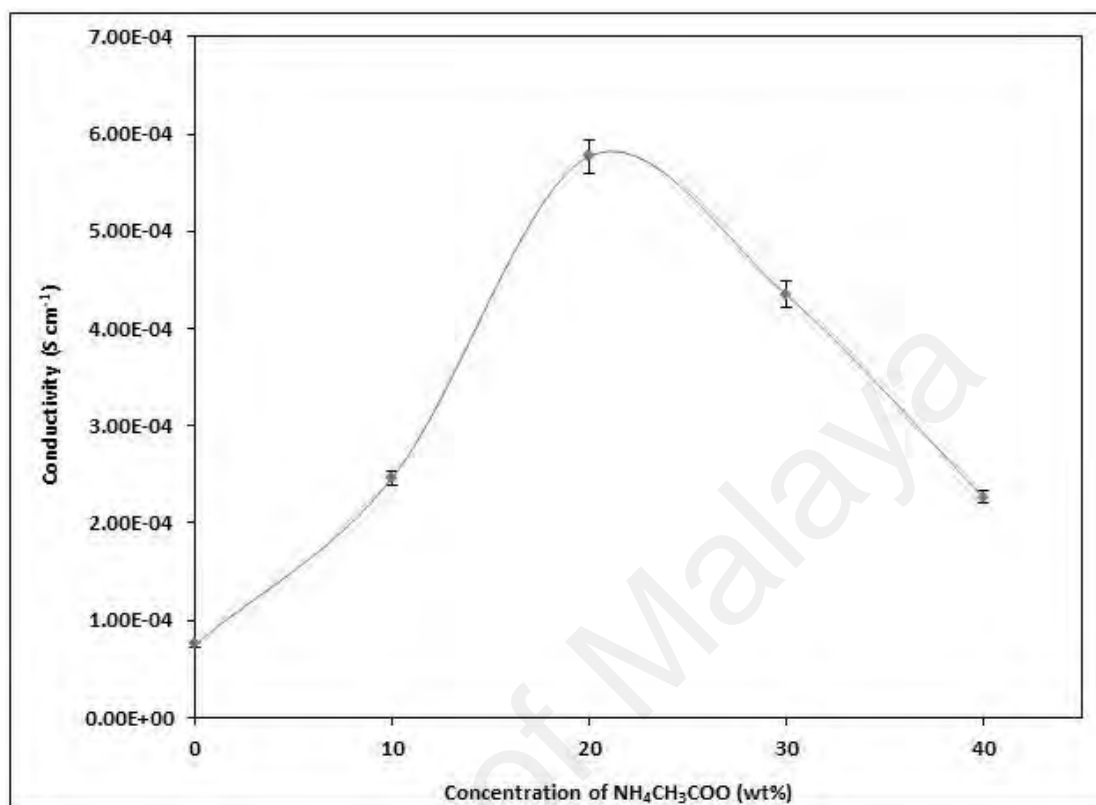
Figure 4.6: Ambient temperature ionic conductivity of CMC-NH$_4$CH$_3$COO

As expected, the addition of the NH$_4$CH$_3$COO ionic dopant gave a significant effect on the conductivity of the CMC–NH$_4$CH$_3$COO biopolymer system. From Figure 4.6, it is noted that the conductivity starts to increase from 10 wt% to 20 wt% of NH$_4$CH$_3$COO. The increase in ionic conductivity for this natural biopolymer electrolyte system with increasing salt concentration can be associated with an increase in the number of mobile ions (Ramya et al., 2007). In the CMC–NH$_4$CH$_3$COO biopolymer system, the NH$_4$CH$_3$COO interacted with the carboxyl anion groups of the CMC host. Therefore, ion hopping and exchange took place at more sites; see Figure 4.6. As the salt composition increases, more protons (H$^+$) are supplied, due to the dissociation of the ionic dopant. Meanwhile, the conductivity of CMC obtained was found to be higher

compared to those prepared by using commercial CMC. According to (Chai & Isa, 2011), the highest conductivity achieved for polymer electrolyte prepared using commercial CMC was 2.11×10^{-5} S cm^{-1}. This can be explained by the higher DS value of CMC obtained in this work. This means that the CMC synthesized in this study possessed a higher number of oxygens, thus providing greater number of active sites for coordination with the cations of the doping salt. Upon addition of more than 20 wt% NH$_4$CH$_3$COO, the conductivity of the biopolymer decreases. The decrement of conductivity can be ascribed to the increase of the dipole interaction between the proton (H$^+$) and the CMC–NH$_4$CH$_3$COO medium. The conductivity decrement may also be due to the aggregation of ions, which reduces the number of charge carriers and impedes the mobility of ions (Chai & Isa, 2011; Selvasekarapandian et al., 2005). The schematic diagram of CMC interaction with NH$_4$CH$_3$COO via (N–H$_4^+$) is shown in Figure 4.7.
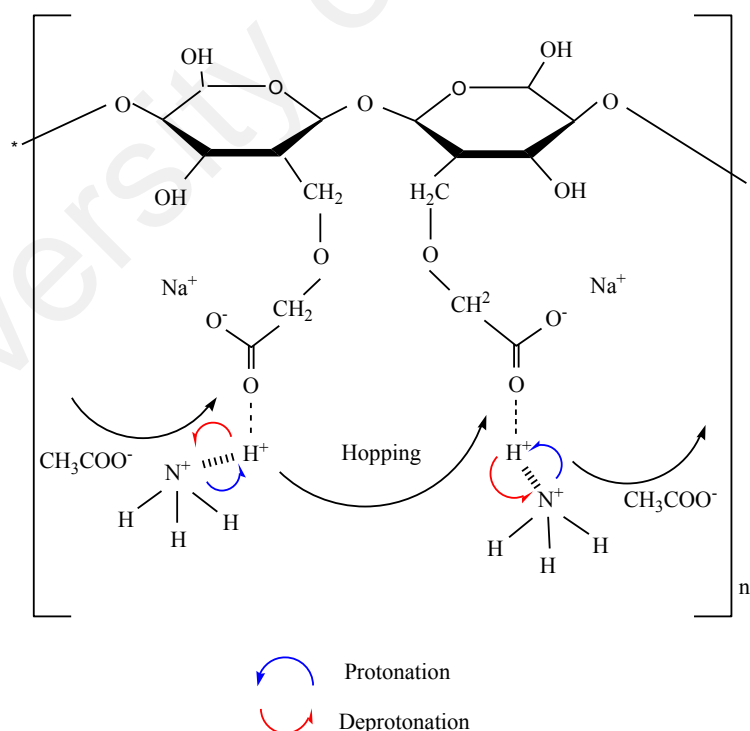
Figure 4.7: Schematic diagram of CMC interaction with NH$_4$CH$_3$COO via (N–H$_4^+$)

For further understanding of the ionic conductivity mechanism, the ionic conductivity of the biopolymer systems was measured at elevated temperatures ranging from 303 to 338 K. Figure 4.8 shows the plot of log conductivity, σ against $1000/T$, for the samples with 0 wt% to 40 wt% of NH_4CH_3COO. The regression values of the plots are approximated to one, indicating that the temperature dependence of the ionic conductivity for all samples is linear and obeys Arrhenius' rule (Khiar & Arof, 2010). This relation implies that the conductivity was thermally assisted. The activation energy, E_a, was also calculated from the slope of the plots in Figure 4.8 by using the following equation:

$$\sigma = \sigma_0 \, exp(-E_a/kT) \tag{4.1}$$

where, σ_0 is the pre-exponential factor, E_a is the activation energy, k is the Boltzmann constant and T is the absolute temperature. It can be observed that the trend of E_a, as shown in Figure 4.9, is the inverse of the conductivity trend shown in Figure 4.6. According to Selvasekarapandian et al. (2005), when the NH_4CH_3COO concentration increases, the barrier, known as the band gap for proton transport to pass through, is reduced; thus, E_a decreases. Samples with lower E_a possessed a smaller band gap, which allowed the conducting ions to move more easily as a free ion-like state, giving higher ionic conductivity and vice versa (Chandra et al., 1995).
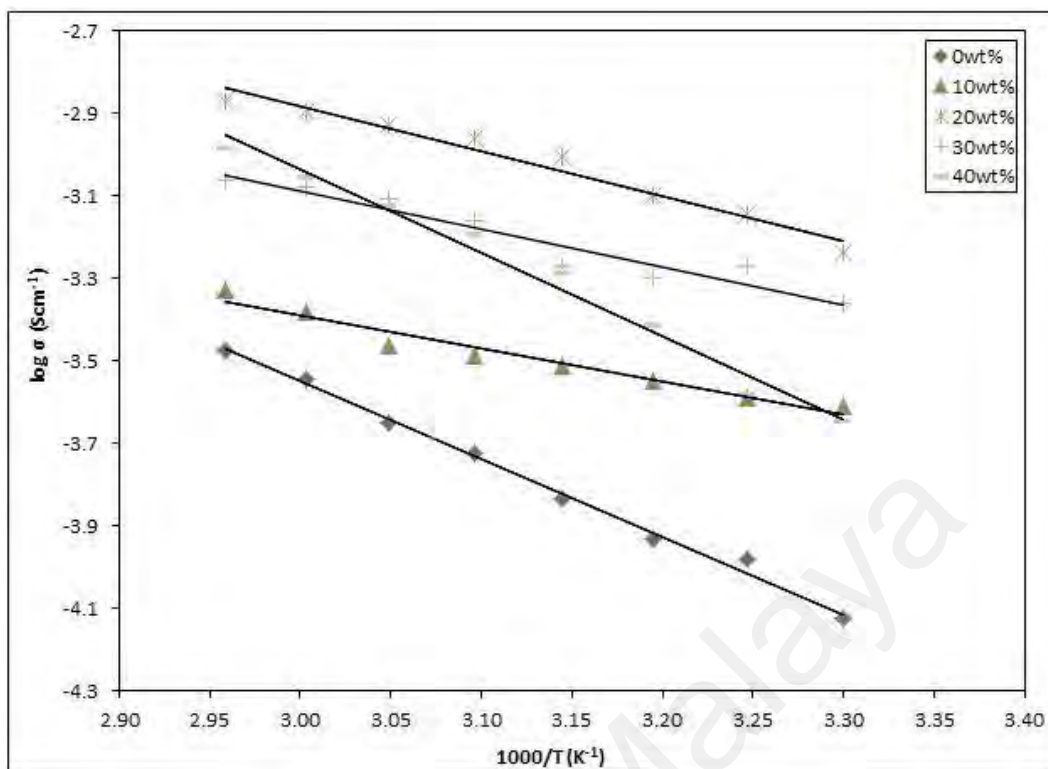
Figure 4.8: Temperature dependence of ionic conductivity of pure CMC (0 wt%) and CMC with 10-40 wt% of NH₄CH₃COO
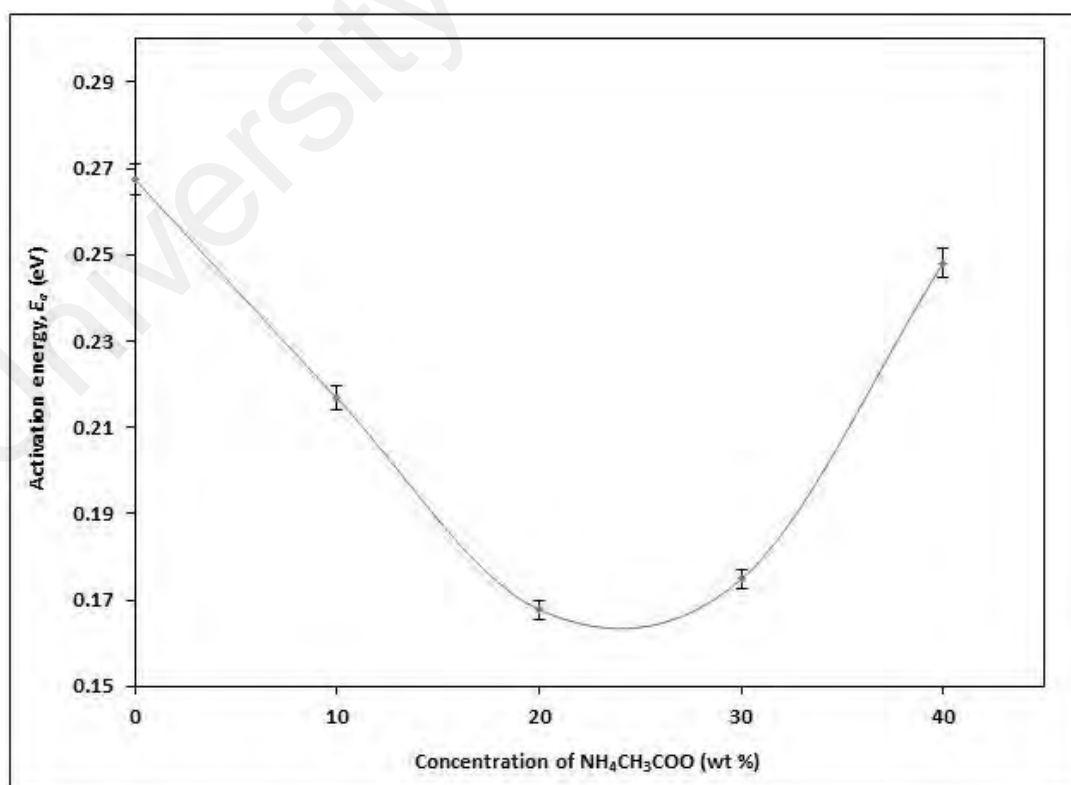
Figure 4.9: Activation energy vs concentration of NH₄CH₃COO salt

4.3.1.3 Transference number of NH₄CH₃COO biosourced polymer electrolytes

TNM was performed to correlate the diffusion phenomenon to the conductivity behaviour of biopolymer electrolytes. In polymer-ammonium salt system, proton (H^+) was identified as charge species that responsible for ionic conduction to take place which was originated from ammonium ion (Hema et al., 2008). Figure 4.10 illustrates the normalized polarization current-time plot for CMC containing 20 wt % NH₄CH₃COO biopolymer electrolytes. The ionic contribution to the conductivity in the biopolymer electrolytes was determined by monitoring the current as a function of time on application of fixed dc voltage (1.5 V) across the biopolymer disk sandwiched between two stainless steel electrodes (Majid & Arof, 2005). The transference number has been calculated from the polarisation graph using the following equation:

$$t_i = \frac{I_{initial} - I_{final}}{I_{initial}} \tag{4.2}$$

where, $I_{initial}$ is the initial current and I_{final} is the final residue current (constant current). If the charge transport in the sample is ionic, the current through an ion blocking electrode decreases rapidly with time.
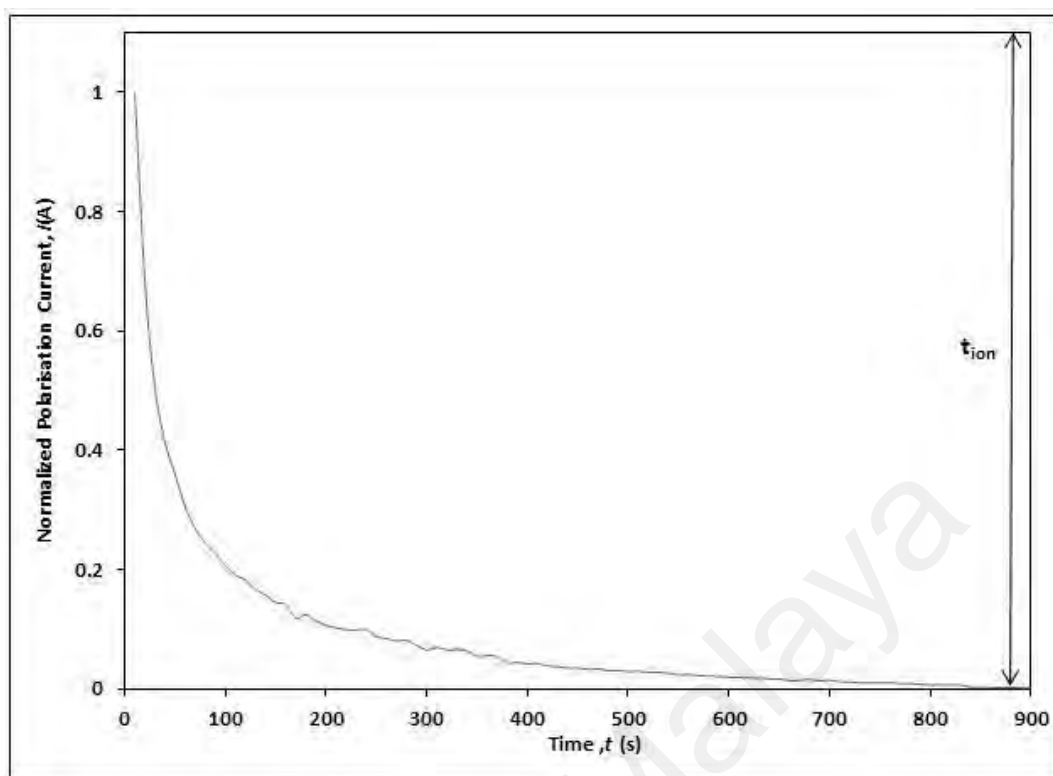
Figure 4.10: Normalized polarization current time for the biopolymer film of CMC-20 wt% NH₄CH₃COO

As observed in Figure 4.10, the initial total current decreases with time due to the depletion of the ionic species in the biopolymer electrolytes and becomes constant in the fully depleted situation. At this steady state, the cell was polarized and any residual current flows were due to electron migration across the electrolyte and interfaces. The t_{ion} of NH_4CH_3COO into CMC biopolymer electrolyte is found to be 0.99 suggesting that the conductivity in the electrolyte was mainly due to ions.

4.3.1.4 Electrochemical stability window of CMC-NH₄CH₃COO biosourced polymer electrolytes

As shown in Figure 4.6, the CMC doped with 20 wt% of NH_4CH_3COO exhibited the highest ionic conductivity of the order of 10^{-4} Scm^{-1}. This system was then subjected to

an electrochemical stability window investigation by using LSV and the voltammogram is shown in Figure 4.11.
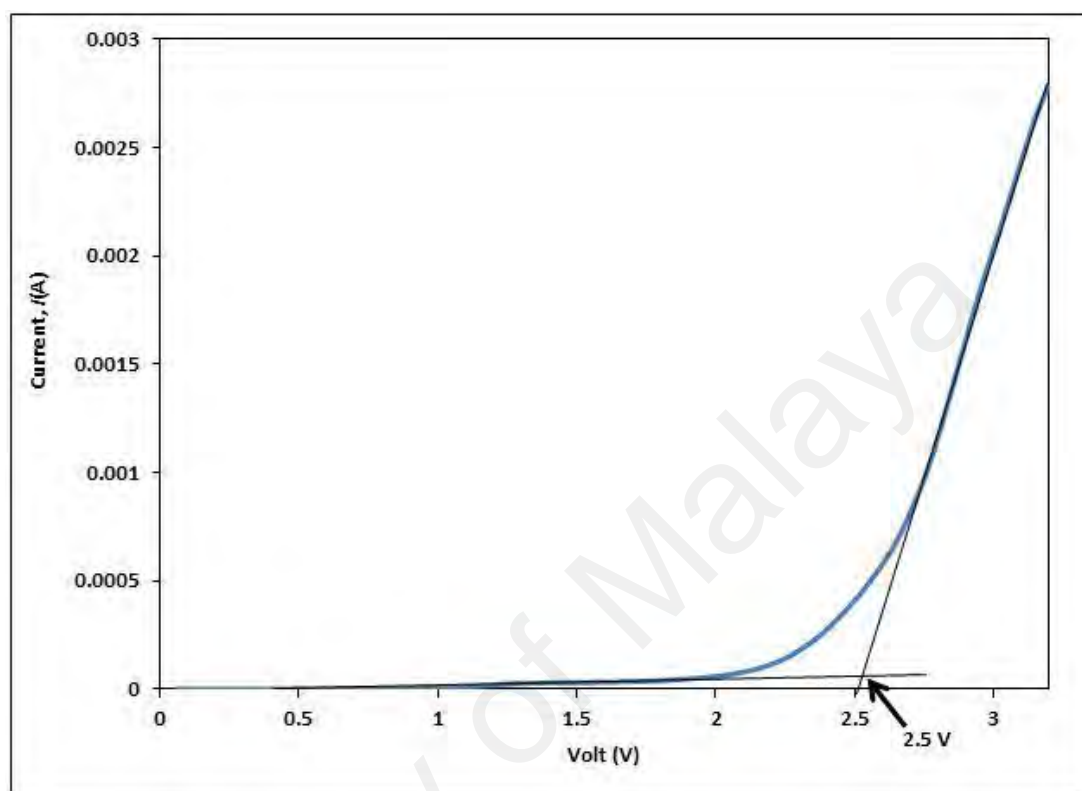
Figure 4.11: Linear sweep voltammetry curve for the biopolymer film of CMC-20 wt% NH₄CH₃COO

It can be observed that the onset current of biopolymer occurs at 2.5 V at ambient temperature. The onset current is assumed to be the biopolymer electrolytes breakdown voltage. The current increases gradually when the electrode potential is greater than 2.5 V. This amount of voltage is good enough to allow the use of this biopolymer for the fabrication of protonic batteries, since the electrochemical window standard of a protonic battery is about ~1 V (Ng & Mohamad, 2008; Pratap et al., 2006). The result obtained in the present study is better than that reported by (Ng & Mohamad, 2008), who observed that the onset current for EC plasticized chitosan–NH_4NO_3 polymer electrolyte film at 1.80 V (Ng & Mohamad, 2008). Besides that, the biopolymer electrolyte sample in this study showed a wider electrochemical stability window than

that reported by (Samsudin et al., 2014), who used synthetic CMC. They obtained electrochemical stability up to 1.38 V.

4.3.2   CMC-Mg(CH₃COO)₂ Biosourced Polymer Electrolytes

4.3.2.1 Study on interactions between CMC with Mg(CH₃COO)₂

The FTIR spectra of $Mg(CH_3COO)_2$, pure CMC as reference and CMC-$Mg(CH_3COO)_2$ (10-40 wt%) in the region from 550 cm^{-1} to 4000 cm^{-1} are shown in Figure 4.12. The hydroxyl band for pure CMC (Figure 4.12 (b)) appears at 3347 cm^{-1}. As the $Mg(CH_3COO)_2$ concentration increases, the hydroxyl band is observed to shift to a lower wavenumbers. This is ascribed to the interaction of cation $[Mg^{2+}]$ substructure of $Mg(CH_3COO)_2$ with oxygen atoms of the hydroxyl group of CMC (Tiwari et al, 2012). Although interaction between polymer host and ionic salt normally occurs at the oxygen atom, other bands can also be affected (Stygar et al., 2005). Upon addition of 20 wt% $Mg(CH_3COO)_2$, it can be observed that the carboxyl group (C=O) at 1597 cm^{-1} has shifted to a lower wavenumber (1557 cm^{-1}), giving an additional evidence of interaction between the (C=O) moiety in CMC with the Mg^{2+}. This phenomenon can be related to the lone pair electrons that attracted the salt molecule of $Mg(CH_3COO)_2$ to the system (Selvasekarapandian et al., 2005). The concentration of Mg^{2+} increased with the increase of $Mg(CH_3COO)_2$ composition; implying that more electrons were withdrawn toward C=O which led to the shift of band from 1557 to 1549 cm^{-1}.
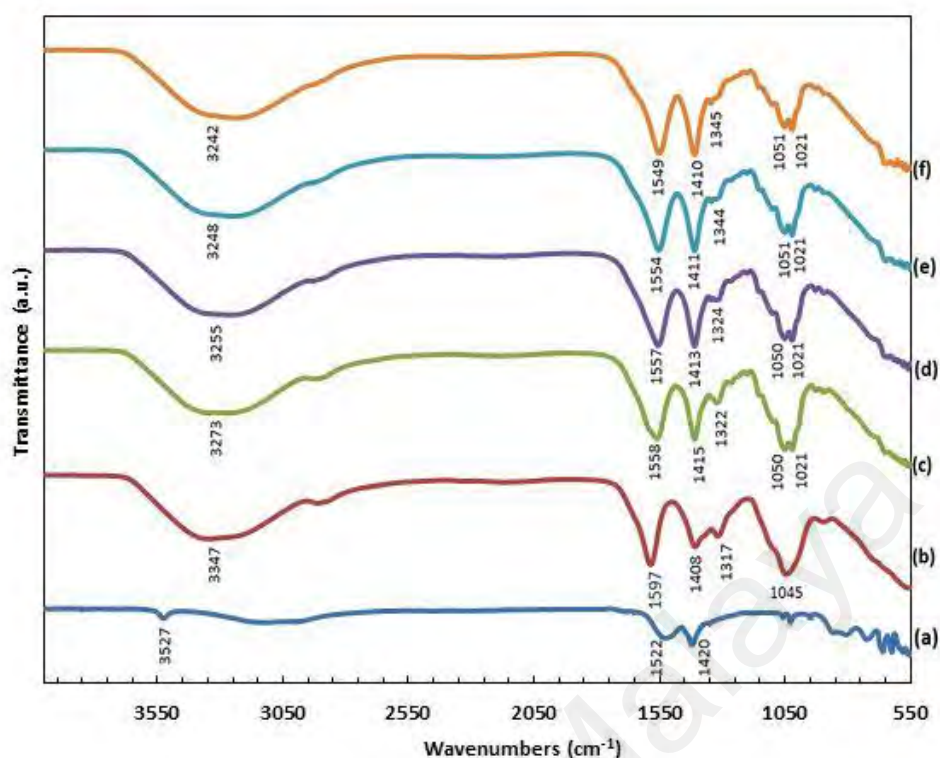
Figure 4.12: IR-spectra of (a) Mg(CH₃COO)₂, (b) CMC powder, and CMC added with (c) 10, (d) 20, (e) 30 and (f) 40 wt% Mg(CH₃COO)₂ in the spectral region between 4000 and 550 cm⁻¹

4.3.2.2 Impedance study on CMC-Mg(CH₃COO)₂ biosourced polymer electrolytes

Figure 4.13 shows typical complex impedance spectra for BPE film of CMC: 20 wt% Mg(CH₃COO)₂ system at different temperatures. There is no semicircle found in this complex impedance plot suggesting that the prevailing of the resistive component of the PEs (Ramya et al., 2007). The impedance spectra illustrate a low frequency spike indicating that the conduction was mainly due to ions. Besides that, the inclined spikes which are at an angle of less than 90° to the real impedance axis obtained in this present work can be explained by the roughness of the electrode-electrolyte interface (Jurado et al., 2003). From Figure 4.13, it can be observed that the bulk resistance decreases with temperature. This is attributed to the enhancement in the number of charge carriers and their mobility with temperature (Sheha et al., 2015).
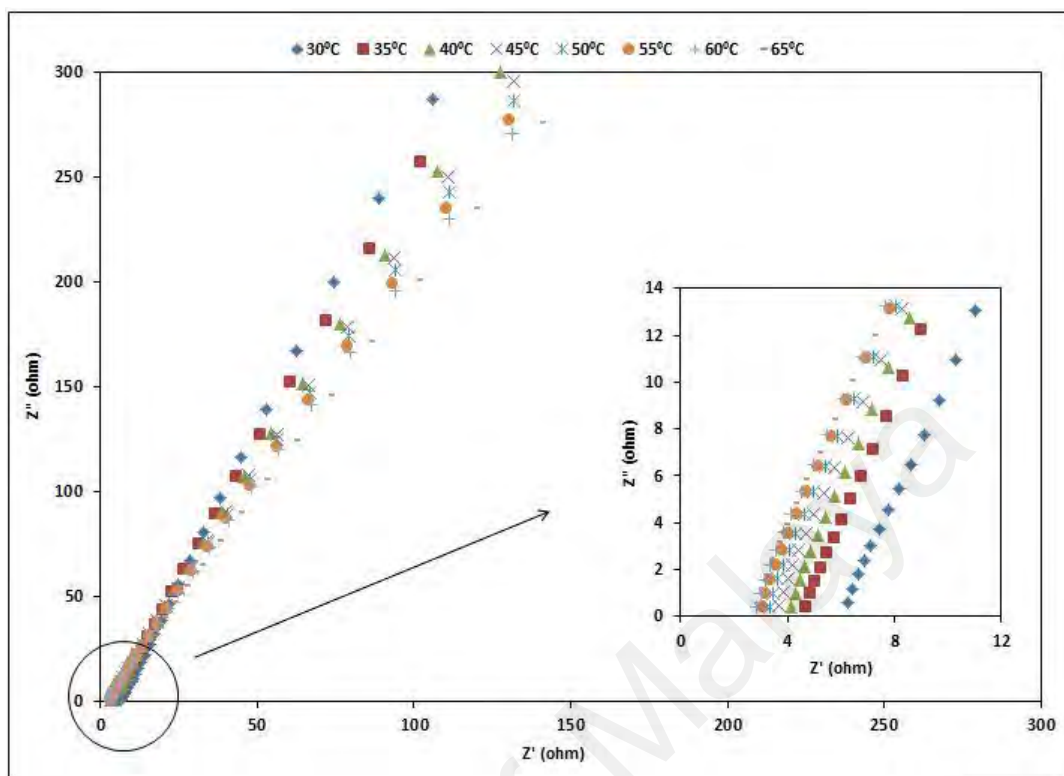
**Figure 4.13: Complex impedance spectra for CMC added with 20 wt%
Mg(CH₃COO)₂ films at different temperatures**

Figure 4.14 depicts room temperature conductivity as a function of weight percent of Mg(CH₃COO)₂. The conductivity ascends with increase in salt concentration until it reaches a maximum value of 1.83×10^{-3} S cm⁻¹ at 20 wt% Mg(CH₃COO)₂ and decreases slowly with further increase in Mg(CH₃COO)₂ content. The improved ionic conductivity could be attributed to enhancement in number of charge carrier. (Buraidah et al., 2009) reported that the aggregation of ions impedes the movement of mobile ions resulting in a decrease in ionic conductivity. A similar trend was reported by (Mobarak et al., 2015). The highest conductivity of the carboxymethyl iota carrageenan and carboxymethyl kappa carrageenan doped lithium nitrate biopolymer electrolyte achieved by these researchers were 5.85×10^{-3} S cm⁻¹ and 5.51×10^{-3} S cm⁻¹,

respectively. The high conductivity value obtained in this work reveals that the conductivity of BPE can be enhanced further by using derivatives of cellulose.
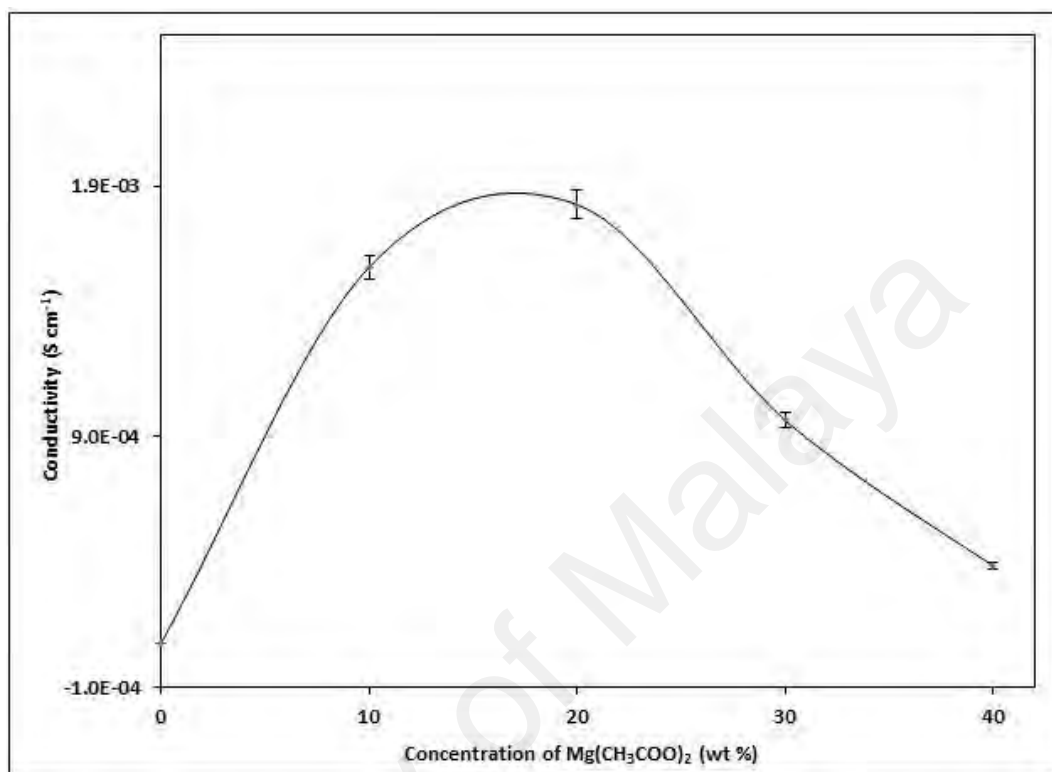
Figure 4.14: Ambient temperature ionic conductivity of CMC-Mg(CH$_3$COO)$_2$

The drop in conductivity for films containing more than 20 wt% of Mg(CH$_3$COO)$_2$ is attributed to the host matrix which become packed with ions (overcrowding) resulting in limited charge carrier mobility (Ng & Mohamad, 2008). For this study, the amount of Mg(CH$_3$COO)$_2$ was limited to 40 wt% since the biopolymer films containing more than this amount suffered from poor mechanical stability.
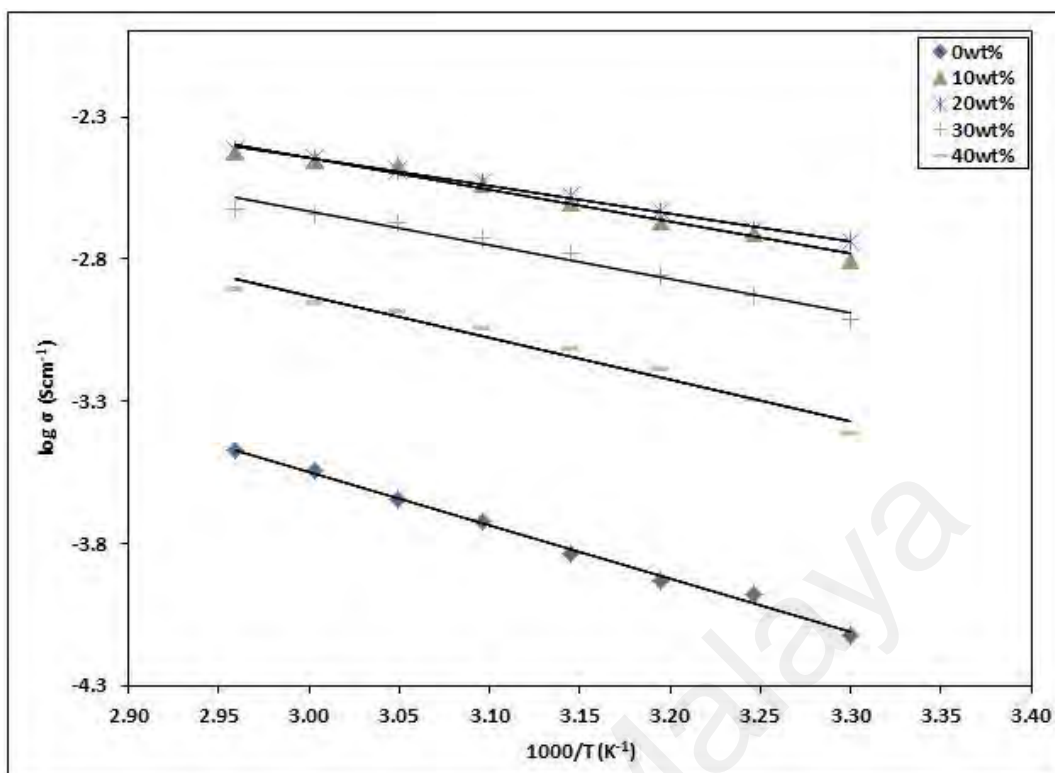
Figure 4.15: Temperature dependence of ionic conductivity of pure CMC (0 wt%) and CMC with 10-40 wt% of Mg(CH$_3$COO)$_2$

The variations of conductivity with temperature for samples of CMC-Mg(CH$_3$COO)$_2$ BPEs are presented in Figure 4.15. The conductivity of both BPEs shows an increasing trend with increase in temperature that is ascribed to the increase in number of density and mobility of ions (Rajendran et al., 2004). All the points of each plot in Figure 4.15 lie on a straight line and the regression value is approximately 1. The linear relationship confirms that the biopolymer system obeyed the Arrhenius type thermally activated process. From the plot of log σ versus 1000/T, the activation energy, E_a was calculated using equation (4.1):
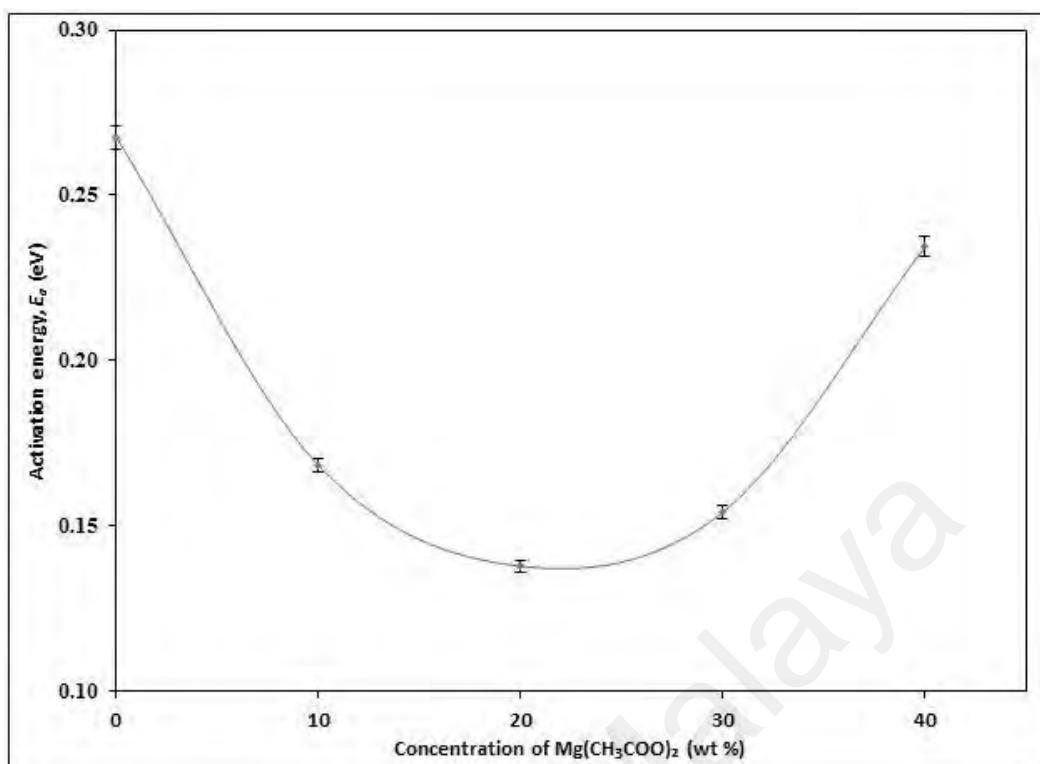
Figure 4.16: Activation energy vs. concentration of Mg(CH₃COO)₂ salt

Displayed in Figure 4.16 is the plot of activation energy versus concentration of Mg(CH$_3$COO)$_2$. E_a is the energy required for an ion to migrate from one site to another. The BPE system has a low E_a value of 0.14 eV.

4.3.2.3   Transference number of Mg(CH₃COO)₂ biosourced polymer electrolytes

The ionic transference number for the highest conducting system, CMC-20 wt% Mg(CH$_3$COO)$_2$ was determined by using Wagner's polarization method. In this technique, the direct current (DC) is monitored as a function of time on an application of a fixed DC voltage of 1.0 V across the SS/biopolymer electrolytes/SS. After polarization, the graph of normalized current versus time was plotted. Figure 4.17 depicts the plot of the normalized polarization current versus time for the CMC-20 wt% Mg(CH$_3$COO)$_2$ system. The t_i value was calculated using equation (4.3). The value of

ionic transference number for this system is 0.98. This suggests that the charge transport in the CMC-20 wt% Mg(CH$_3$COO)$_2$ was predominantly due to ions.
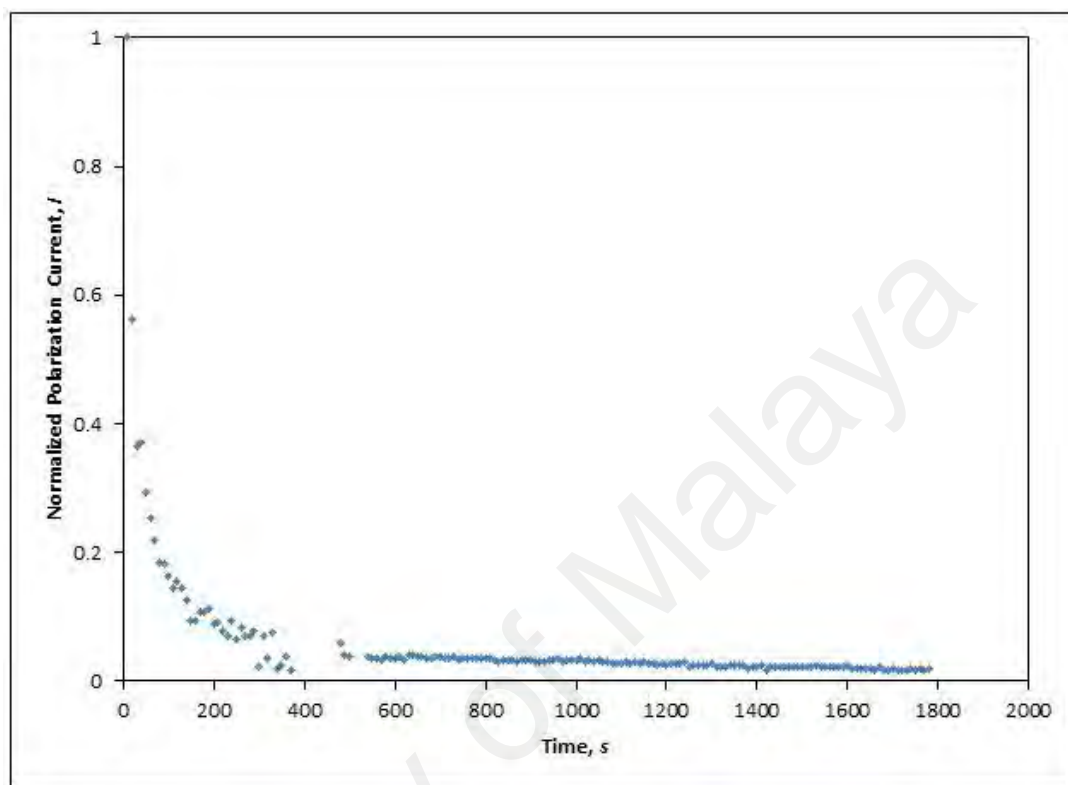
Figure 4.17: Normalized Polarization current time for the biopolymer film of CMC-20 wt% Mg(CH$_3$COO)$_2$

4.3.2.4 Electrochemical stability window CMC-Mg(CH$_3$COO)$_2$ biosourced polymer electrolytes

The electrochemical stability window of electrolytes in this system was carried out by using LSV measurement. LSV was done to determine the decomposition voltage of the electrolyte; the maximum operational voltage of an electrochemical device in which the electrolyte can be applied (Reddy & Reddy, 2003). Figure 4.18 illustrates the LSV curve of CMC-30 wt% Mg(CH$_3$COO)$_2$ biopolymer electrolyte system. The figure shows that the current increases gradually with the increment of voltage above 2.7 V. This voltage is the decomposition voltage of the studied sample and suggests that the

65

sample is stable enough to be applied as biopolymer electrolytes in electrochemical devices.
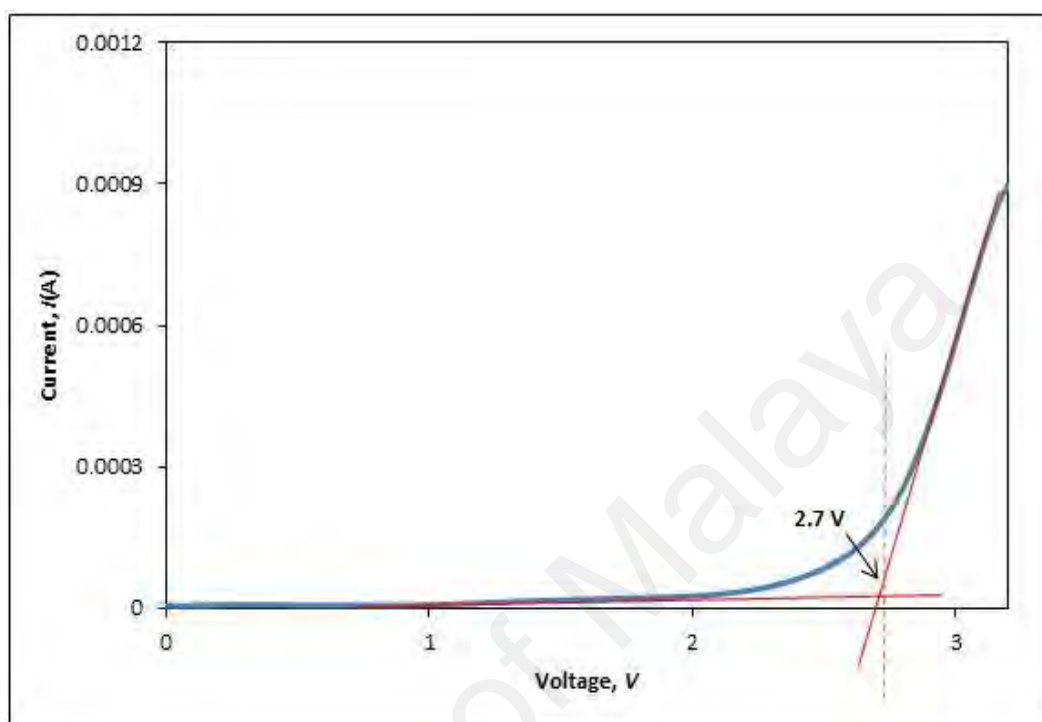
Figure 4.18: Linear sweep voltammetry curve for the biopolymer film of CMC-20 wt% Mg(CH$_3$COO)$_2$

4.3.3   CMC-NaCH$_3$COO Biosourced Polymer Electrolytes

4.3.3.1 Study on interactions between CMC with NaCH$_3$COO

Figure 4.19 illustrates the FTIR spectra in the region from 550 cm^{-1} to 4000 cm^{-1} of NaCH$_3$COO, pure CMC as reference and CMC-NaCH$_3$COO (10-40 wt%). The absorption band for O-H stretching which appears at 3347 cm^{-1} for pure CMC (Figure 4.19 (b)) shifted to a lower wavenumbers as the NaCH$_3$COO concentration increases. It indicates that there was an interaction between polymer and dopant salt. This is attributed to interaction of the cation [Na$^+$] substructure of NaCH$_3$COO with oxygen atoms of the hydroxyl group of CMC (Tiwari et al., 2012). Although interaction between polymer host and ionic salt normally occurs at the oxygen atom, however other

66

bands also can be affected (Stygar et al., 2005). In pure CMC, carboxyl group (C=O) is the band of interest to be investigated. Addition of 30 wt% NaCH$_3$COO into the polymer matrix, the band of C=O at 1597 cm^{-1} shifted to a lower wavenumber (1552 cm^{-1}), indicating occurrence of interaction between the (C=O) moiety in CMC with the Na$^+$. All these changes in the FTIR spectra are clear indications of formation of CMC-NaCH$_3$COO complexes.
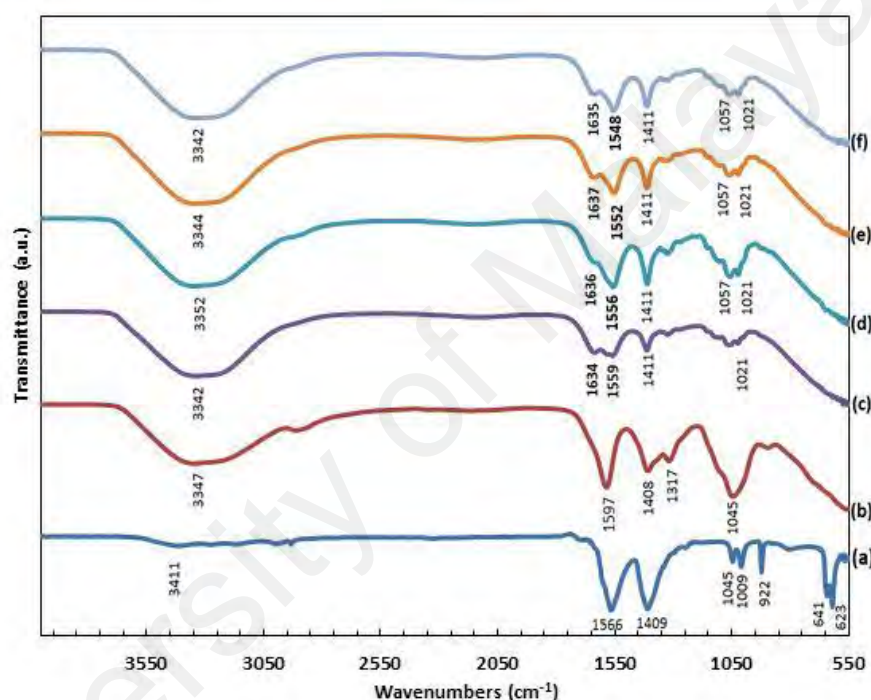
Figure 4.19: IR-spectra of (a) NaCH$_3$COO, (b) CMC powder, and added with (c) 10, (d) 20, (e) 30 and (f) 40 wt% NaCH$_3$COO in the spectral region between 4000 and 550 cm^{-1}

4.3.3.2 Impedance study on CMC-NaCH$_3$COO biosourced polymer electrolytes

The CMC doped NaCH$_3$COO BPE films were analysed using EIS. EIS is a non-destructive and powerful technique to compute the electrical properties of electrolyte materials and their interfaces with electronically conducting electrodes. Complex impedance spectra for BPE film of CMC 30 wt% NaCH$_3$COO system at different

temperatures are depicted in Figure 4.20. Normally, the spectra of polymer electrolytes show two different regions; incomplete semicircle at the high frequency region and a spur at low frequency region. However, in this study, the complex impedance plots show only spikes indicating that the conductivity was mainly due to ion conduction (Ramya et al., 2007). The R_b of the films was calculated from the intercept of the tilted spike at real impedance axis. With increasing salt concentration, the values of R_b decreases.
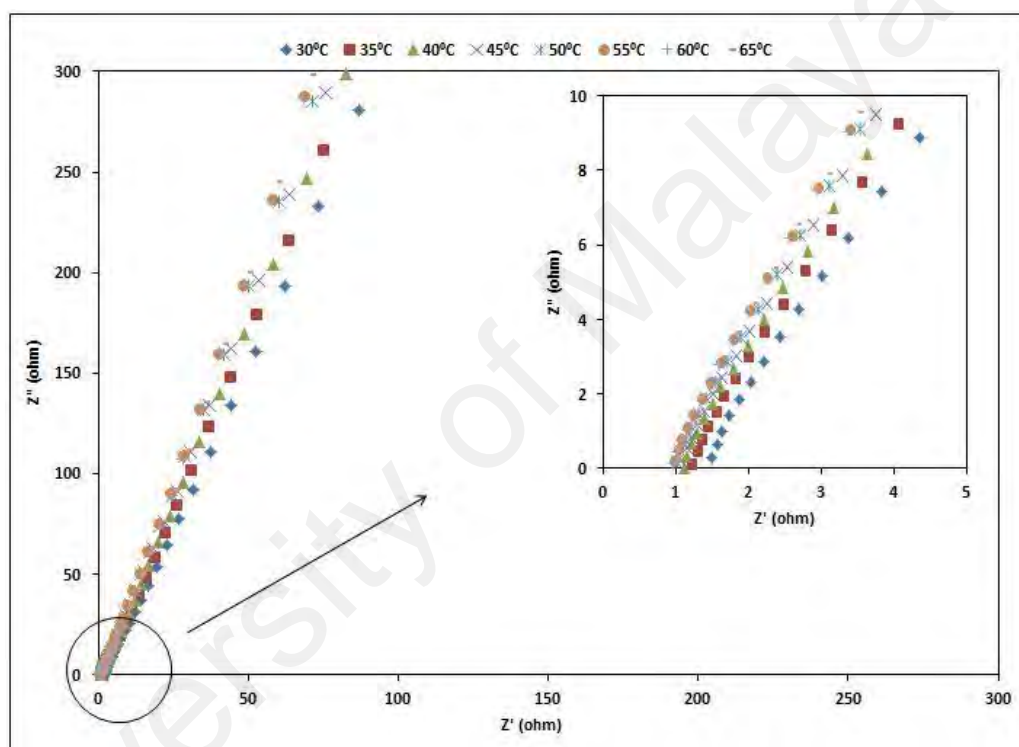
Figure 4.20: Complex impedance spectra for CMC added with 30 wt% NaCH$_3$COO films at different temperatures

Figure 4.21 depicts the variation of ionic conductivity with NaCH$_3$COO content. Based on the figure, it can be observed that the ionic conductivity enhances with the addition of NaCH$_3$COO which can be explained by the increase of free charge carrier movement in the membrane. The highest ionic conductivity of 2.83×10^{-3} S cm^{-1} was achieved for the film incorporated with 30 wt% of NaCH$_3$COO. As seen in the surface morphology analysis, the film 30 wt% of NaCH$_3$COO is found to be the most

amorphous film which supports the conductivity result. This was similar to what previously reported in the literature (Singh et al., 2014). The charge carriers became more densely packed with the addition of salt, thus the attractive interactions between these free charge carriers increased (Lewandowski et al., 2001). Beyond the system reached the maximum value; at 30 wt% of NaCH$_3$COO, the conductivity decreases. This phenomenon is attributed to the host matrix which become packed with ions (overcrowding) impeding charge carrier mobility (Ng & Mohamad, 2008).
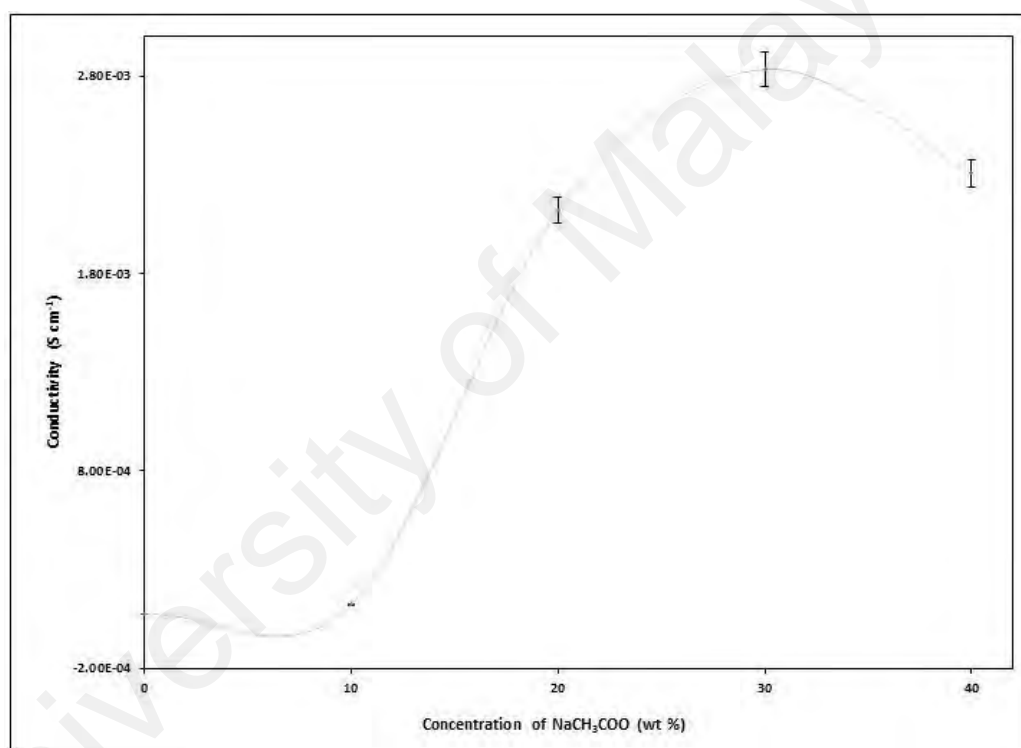
Figure 4.21: Ambient temperature ionic conductivity of CMC-NaCH$_3$COO

Figure 4.22 shows the plot of log conductivity, σ against 1000/*T*, for the samples with 0 wt% to 40 wt% of NH$_4$CH$_3$COO. The regression values of the plots are approximated to one, indicating that the temperature dependence of the ionic conductivity for all samples is linear showing that the conductivity was thermally assisted (Ahmad & Isa, 2015; Premalatha et al., 2017).

The activation energy, E_a, was also calculated from the slope of the plots in Figure 4.25 by using the equation (4.1).
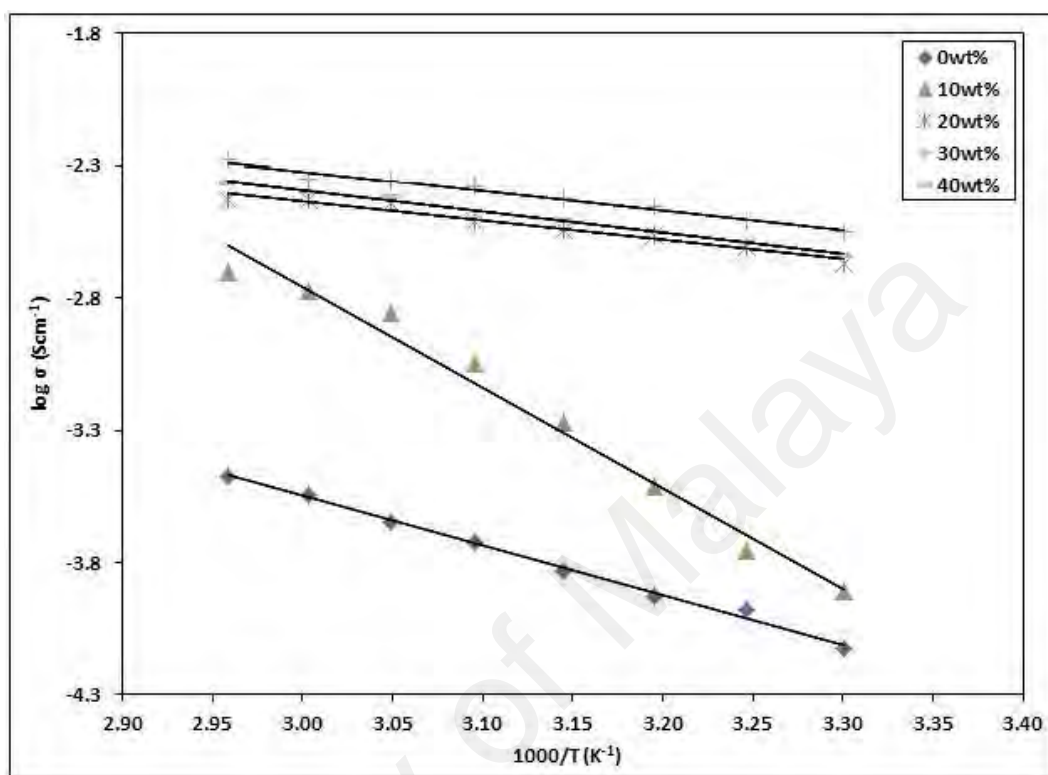
Figure 4.22: Temperature dependence of ionic conductivity of pure CMC (0 wt%) and CMC with 10-40 wt% of NaCH₃COO

The trend of E_a, shown in Figure 4.23, is the inverse of the conductivity trend shown in Figure 4.21. When the NaCH₃COO concentration increases, the barrier, known as the band gap for Na$^+$ transport to pass through, is reduced; thus, E_a decreases (Selvasekarapandian et al., 2005). The lowest E_a value was found at 0.101 eV for the highest conducting membrane (CMC-30 wt% NaCH₃COO); illustrates that the ionic conduction is the most favorable, since less energy is required for ions to hop from one coordinate site to another coordinate site (Premalatha et al., 2017). However the slight increase in the activation energy for the system incorporated with 40 wt% of

NaCH₃COO is probably due to decrease the ionic mobility in the system (Yilmaz et al., 2011).
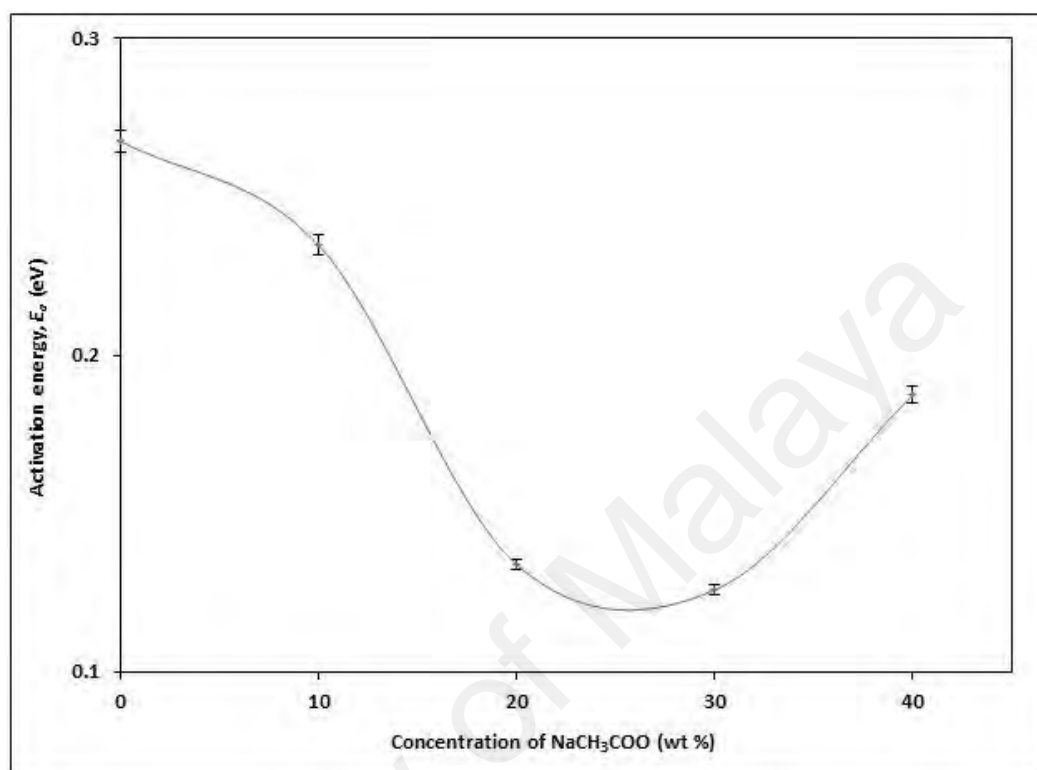
Figure 4.23: Activation energy vs concentration of NaCH₃COO salt

4.3.3.3 Transference number study of NaCH₃COO biosourced polymer electrolytes

The information about the contribution of the particular charge species, whether ions or electrons in the polymer electrolytes to the overall charge transport was determined by measuring their transference number. The plot of normalized polarization current versus time for the highest conducting film CMC-30 wt% NaCH₃COO is illustrated in Figure 4.24. The depletion of the charge carriers or ionic species in the electrolyte caused the initial total current to decrease with time. In the completely depleted condition, the current becomes constant. The ionic transference number of the film is found to be 0.98. The electron transference number in CMC-30 wt% NaCH₃COO is

only 0.02 which can be neglected (Deraman et al., 2013; Samsudin et al., 2011). This suggests that ions were predominantly responsible in the conduction of CMC-30 wt% NaCH$_3$COO electrolytes film.
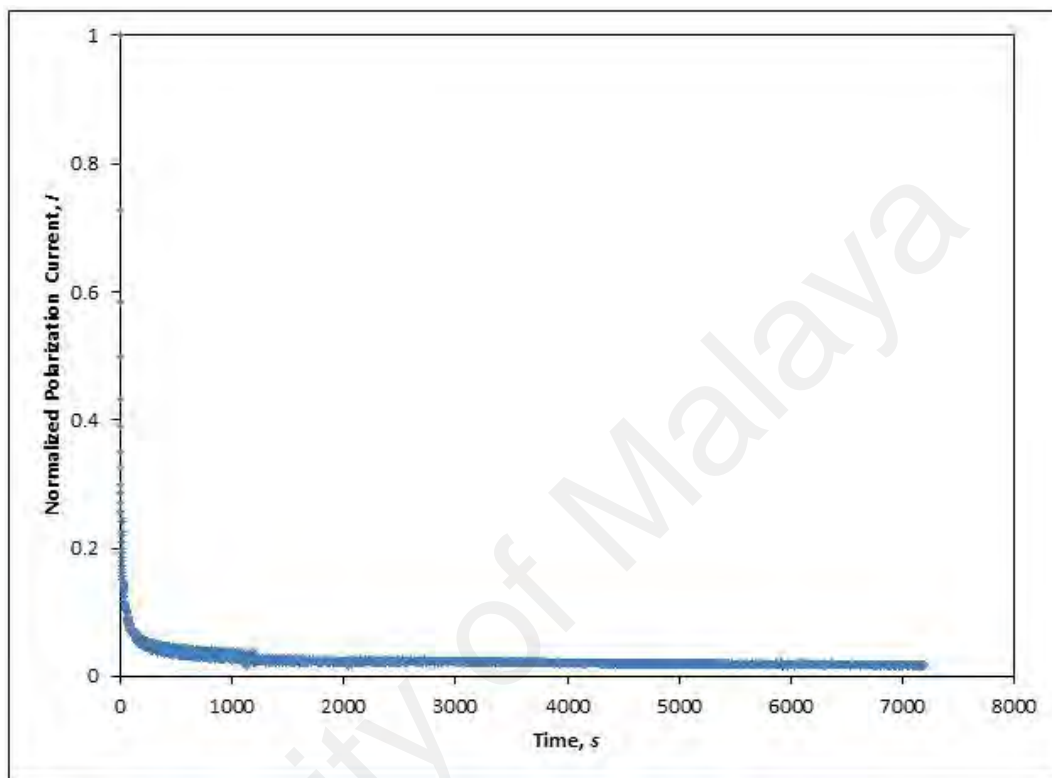
Figure 4.24: Normalized Polarization current time for the biopolymer film of CMC-30 wt% NaCH$_3$COO

4.3.3.4 Electrochemical stability window of CMC-NaCH$_3$COO biosourced polymer electrolytes

The electrochemical stability window of electrolytes in this system was investigated LSV measurement. LSV was done to determine the decomposition voltage of the electrolyte (Reddy & Reddy, 2003). Figure 4.25 illustrates the LSV curve of CMC-30 wt% NaCH$_3$COO biopolymer electrolyte system. The electrochemical stability of this film was up to 2.8 V.
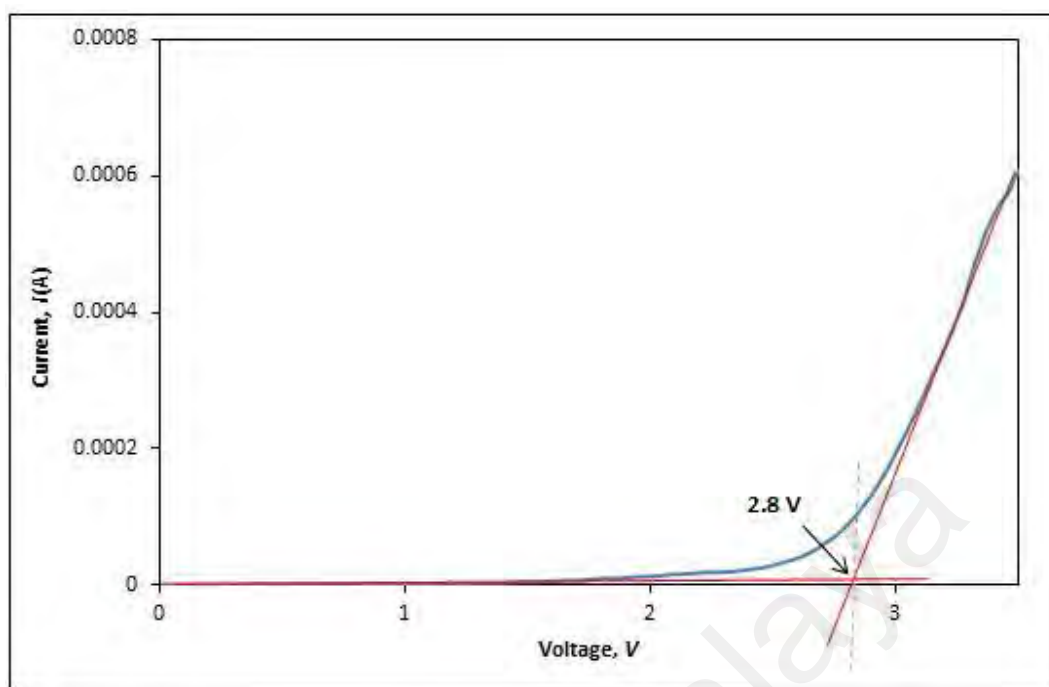
Figure 4.25: Linear sweep voltammetry curve for the biopolymer film of CMC-30 wt% NaCH₃COO

4.3.4 CMC-Zn(CH₃COO)₂ Biosourced Polymer Electrolytes

4.3.4.1 Study on interactions between CMC with Zn(CH₃COO)₂

The FTIR spectra of pure CMC as reference, $Zn(CH_3COO)_2$ and CMC-$Zn(CH_3COO)_2$ (10-40 wt%) complexes in the region from 550 cm^{-1} to 4000 cm^{-1} are depicted in Figure 4.26. The bands at 1443 and 1559 cm^{-1} are assigned to symmetric and asymmetric stretches of the carboxylate ion in $Zn(CH_3COO)_2$ (Nava et al., 2002). The band of interest to identify the complexation is at the –COO band. Upon addition of 20 wt% $Zn(CH_3COO)_2$, it can be observed that the carboxyl group (C=O) at 1597 cm^{-1} has shifted to a lower wavenumber (1557 cm^{-1}), which suggests the interaction of the (C=O) moiety in CMC with the Zn^{2+}. This phenomenon can be related to the lone pair electrons that attracted the salt molecule of $Zn(CH_3COO)_2$ to the system (Selvasekarapandian et al., 2005). The concentration of Zn^{2+} increases when the

73

composition of $Zn(CH_3COO)_2$ increases; implying that more electrons are withdrawn toward C=O which in turn results in the shift of the band from 1557 to 1549 cm^{-1}.
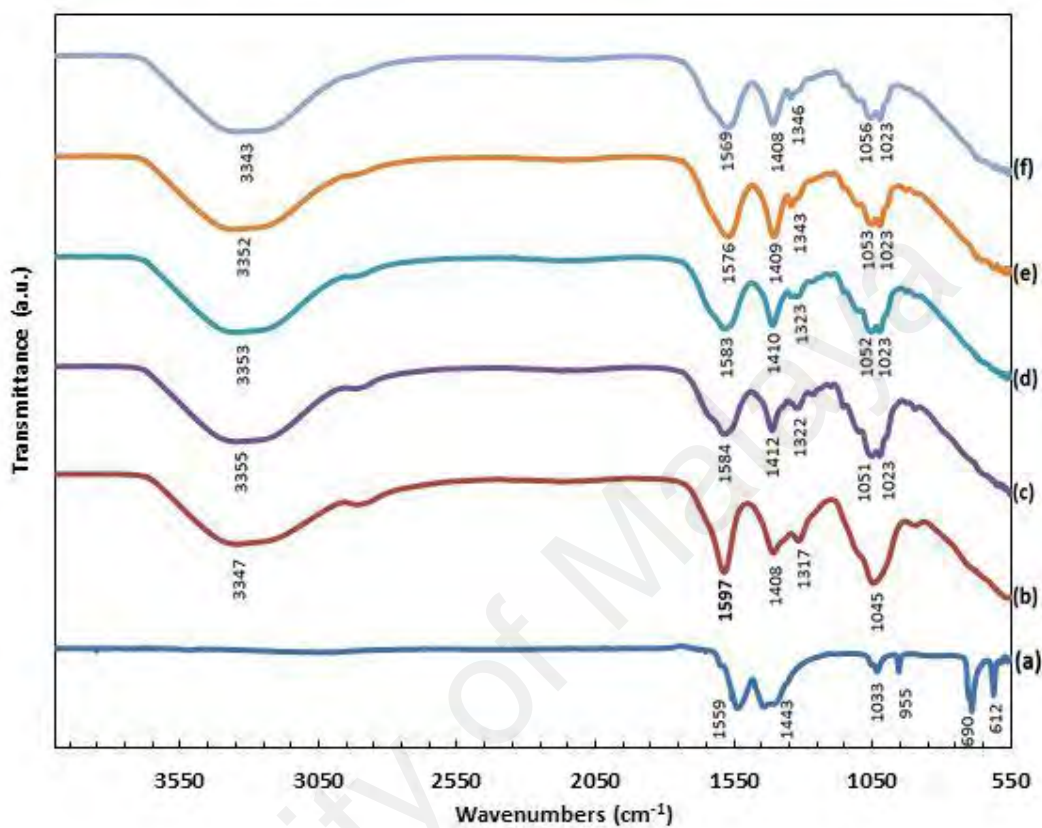

Figure 4.26: IR-spectra of (a) $Zn(CH_3COO)_2$, (b) CMC powder, and CMC added with (c) 10, (d) 20, (e) 30 and (f) 40 wt% $Zn(CH_3COO)_2$ in the spectral region between 4000 and 550 cm^{-1}

The hydroxyl band for pure CMC (Figure 4.26 (b)) appears at 3347 cm^{-1}. It can be noted here that all of the spectra of the biopolymer films have absoption characteristic of O-H stretching which located between 3340 to 3350 cm^{-1}. As the $Zn(CH_3COO)_2$ concentration increases, the hydroxyl band is observed to shift to a lower wavenumber. This is ascribed to the cation [Zn^{2+}] substructure of $Zn(CH_3COO)_2$ interaction with oxygen atoms of the hydroxyl group of CMC (Tiwari et al., 2012). The interaction

between polymer host and ionic salt normally occurs at the oxygen atom, however other bands can also be affected (Stygar et al., 2005).

4.3.4.2 Impedance study on CMC-Zn(CH₃COO)₂ biosourced polymer electrolytes

Figure 4.27 illustrates complex impedance plot of BPE film of CMC doped with 20 wt% $Zn(CH_3COO)_2$ recorded at different temperatures. Normally, there are two-well defined regions that can be observed; high frequency region semicircle arc and low frequency region inclined spike. The appearance of the semicircle can be explained by the bulk effect of BPE. This is due to the parallel combination of a resistor (the migration of the ions occur through the free volume matrix) and a capacitor (the immobile polymer chains) (Ramya et al., 2006). However in the present work, the complex impedance plots indicate that the conductivity in the BPE films was mainly due to ion conduction (Ramya et al., 2007). The R_b of the films was calculated from the intercept of the tilted spike at real impedance axis. With increasing salt concentration, the values of R_b decreases. The same behaviour was also observed in PVA/PVP-NH_4NO_3 polymer electrolytes (Rajeswari et al., 2014).

The spectra in Figure 4.27 also show that the value of R_b decreases with increasing temperature. This can be explained by the decrease in resistance of the BPE sample resulting in enhancement in the charge carriers mobility with temperature (Tamilselvi et al., 2014). The formation of inclined spikes indicates the prevailing in the resistive component of the BPE (Ramya et al., 2007). However, the spikes inclined at an angle less than 90 instead of the vertical axis observed in the high frequency region may be attributed to the roughness of the electrode/electrolyte interface (Sivadevi et al., 2015).
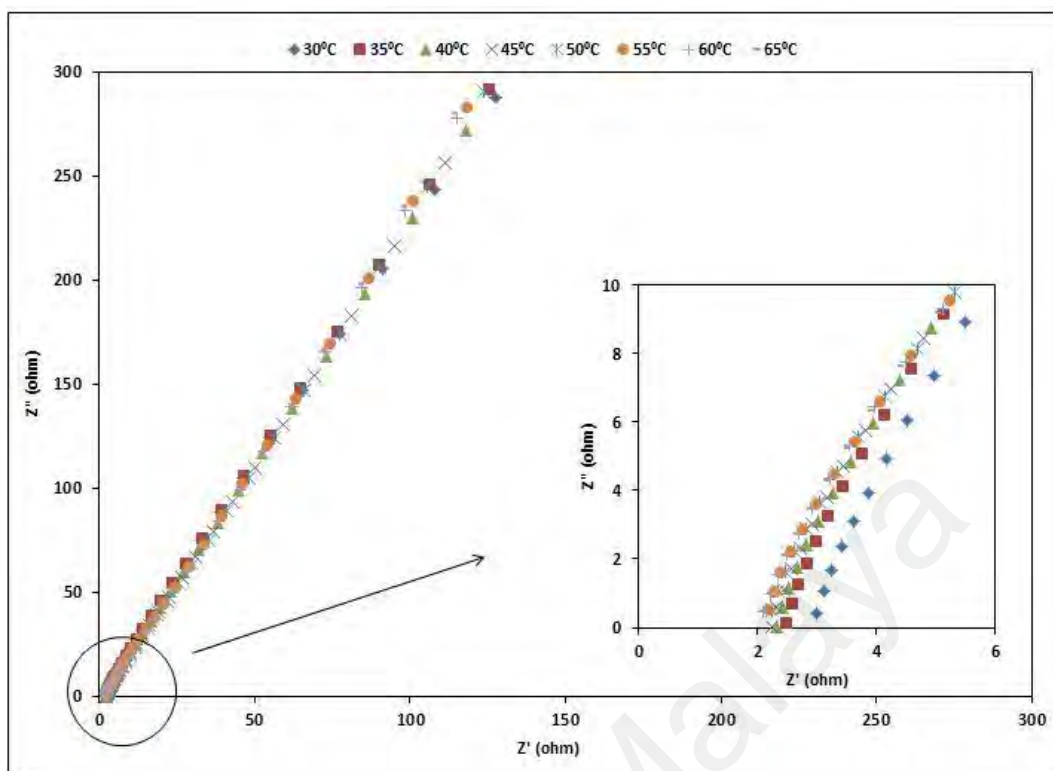
**Figure 4.1: Complex impedance spectra for CMC added with 20 wt%
Zn(CH₃COO)₂ films at different temperatures**

Displayed in Figure 4.28 is the graph of conductivity against concentration of Zn(CH₃COO)₂ at ambient temperature (303 K). As we can see from Figure 4.28, the conductivity of pure CMC (Zn(CH₃COO)₂-0 sample) is 7.51×10^{-5} S cm⁻¹. The conductivity increases upon addition of 10 until 40 wt% of Zn(CH₃COO)₂. The maximum ionic conductivity achieved is 1.75×10^{-3} S cm⁻¹. The increase of ionic conductivity with addition of Zn(CH₃COO)₂ concentration is due to the increase of the number and mobility of charge carrier (Polu et al., 2014). However, the conductivity dramatically declines after addition of 30 wt% Zn(CH₃COO)₂. Ng & Mohamad (2006) reported that as NH₄NO₃ concentration increases, the host matrix becomes crowded with the dopant ions. Hence, reduces the transportation of charge carriers due to limitation of ionic mobility (Rozali et al., 2012). For further understanding on the ionic

conductivity mechanism, the ionic conductivity of biopolymer systems were tested at elevated temperatures, 303 K to 338 K.
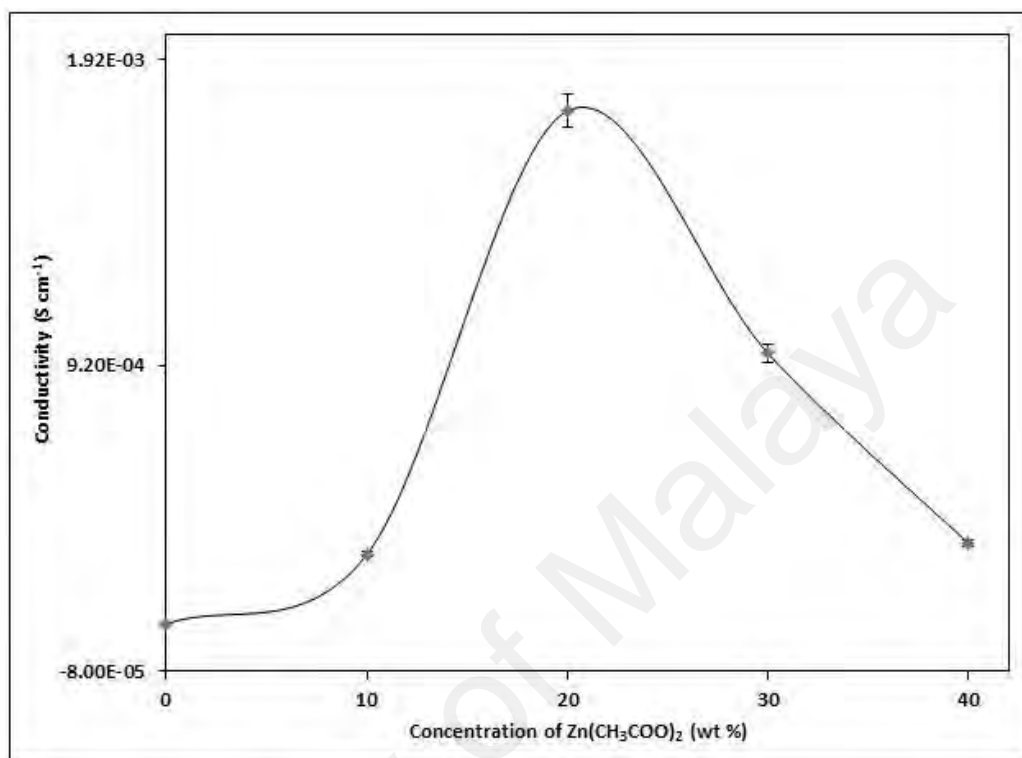
Figure 4.28: Ambient temperature ionic conductivity of CMC-Zn(CH₃COO)₂

Figure 4.29 shows the plot of log conductivity, σ against $1000/T$ for the samples with 0 to 40 wt% of $Zn(CH_3COO)_2$. Since the regression values of the plots are approximated to 1, the temperature dependence of the ionic conductivity for all samples thus can be said to obey Arrhenius' rule (Bhargav et al., 200) . These relation implies that the conductivity was thermally assisted which means that the variation of temperature affects the conductivity of the samples.
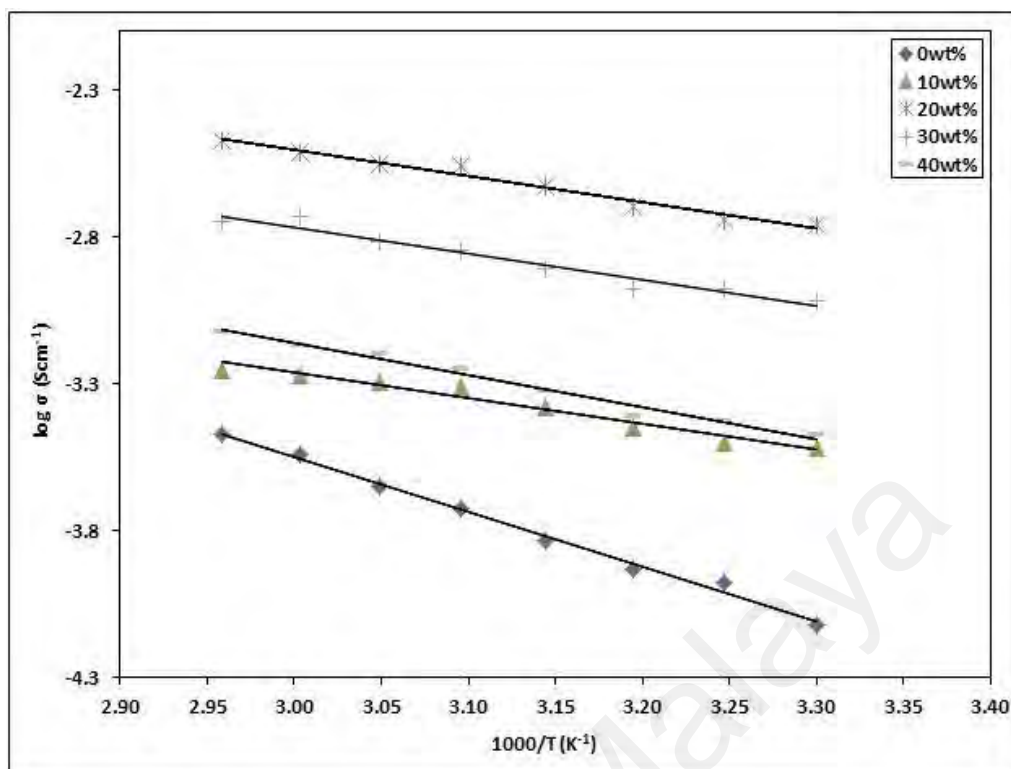
Figure 4.29: Temperature dependence of ionic conductivity of pure CMC (0 wt%) and CMC with 10-40 wt% of $Zn(CH_3COO)_2$

The variation of activation energy, E_a, calculated using equation (4.1) is showed in Figure 4.30. The trend of E_a illustrated in Figure 4.33 is the inverse to that of the conductivity trend presented in Figure 4.28. According to (Selvasekarapandian et al., 2005), when $Zn(CH_3COO)_2$ concentration increases, the barrier known as the band gap for Zn^{2+} transport to pass through is reduced, thus E_a decreases. Samples with lower E_a provided smaller band gap which allowed the conducting ions to move more easily to free ion-like state.
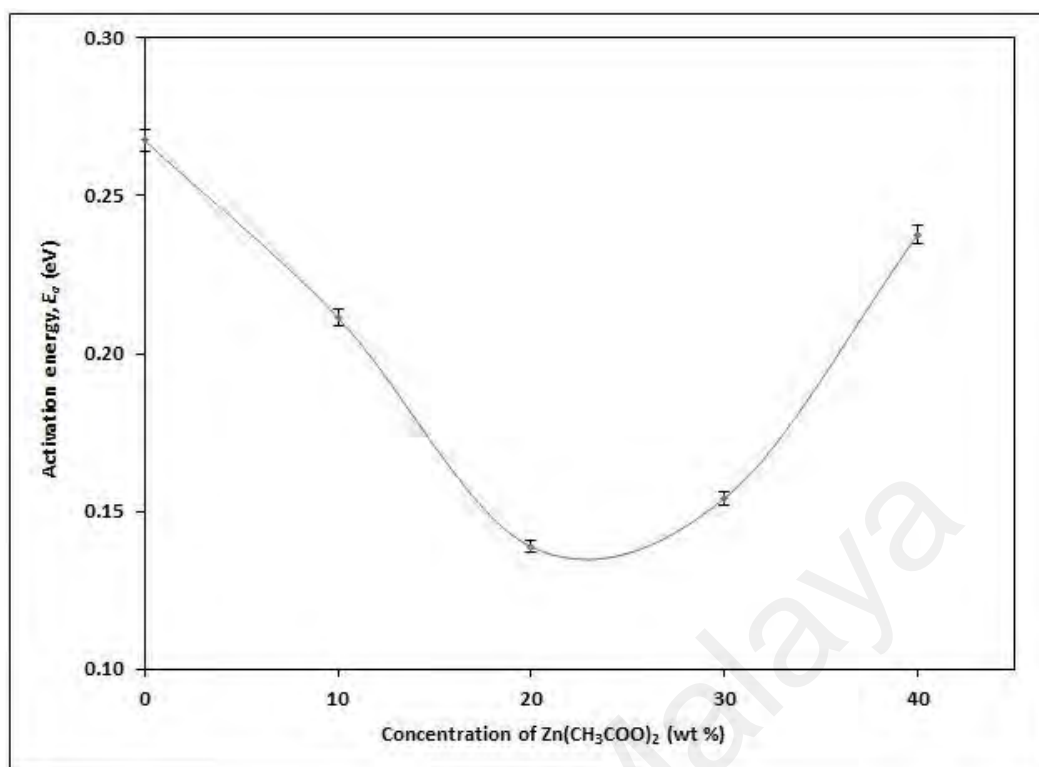
Figure 4.30: Activation energy vs. concentration of Zn(CH₃COO)₂ salt

4.3.4.3 Transference number studies of Zn(CH₃COO)₂ biosourced polymer electrolytes

Transference number measurement was performed to correlate the diffusion phenomenon to the conductivity behaviour of the studied biopolymer electrolytes. The ionic transference number in the BPE films was determined by monitoring the current as a function of time on application of a fixed dc voltage (1.5 V) across the BPE sample sandwiched between two stainless steel electrodes (Manjuladevi et al., 2017). The transference number has been calculated from the polarization graph using the equation (4.3).
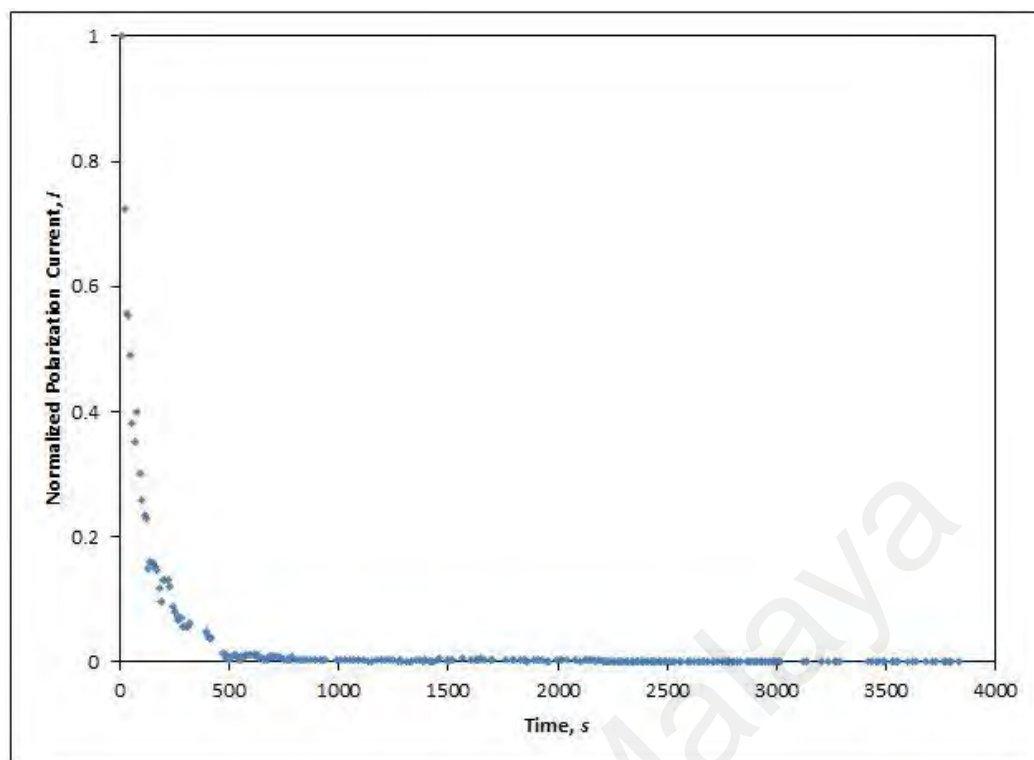
Figure 4.31: Normalized polarization current time for the biopolymer film of CMC- 20 wt% Zn(CH₃COO)₂

The plot of normalized current against time for the sample CMC-20 wt% $Zn(CH_3COO)_2$ is displayed in Figure 4.31. The calculated transference number is ~0.99 which implies that the conductivity was mainly due to ion hence it was electrolytic in nature.

4.3.4.4 Electrochemical stability window of CMC-Zn(CH₃COO)₂ biosourced polymer electrolytes

The electrochemical stability study was done on the CMC incorporated with 30 wt% of $Zn(CH_3COO)_2$ since it was the highest ionic conducting biopolymer electrolyte. The voltammogram of this biopolymer electrolyte is shown in Figure 4.32. The onset current of the biopolymer electrolyte is detected at about 2.04 V. The onset current is assumed to be the biopolymer electrolyte's breakdown voltage. As such, it can be inferred that the electrochemical stability window is good enough to allow its safe use for fabrication

of batteries, since the electrochemical window standard of battery is about ~1 V (Ng & Mohamad, 2008; Pratap et al., 2006).
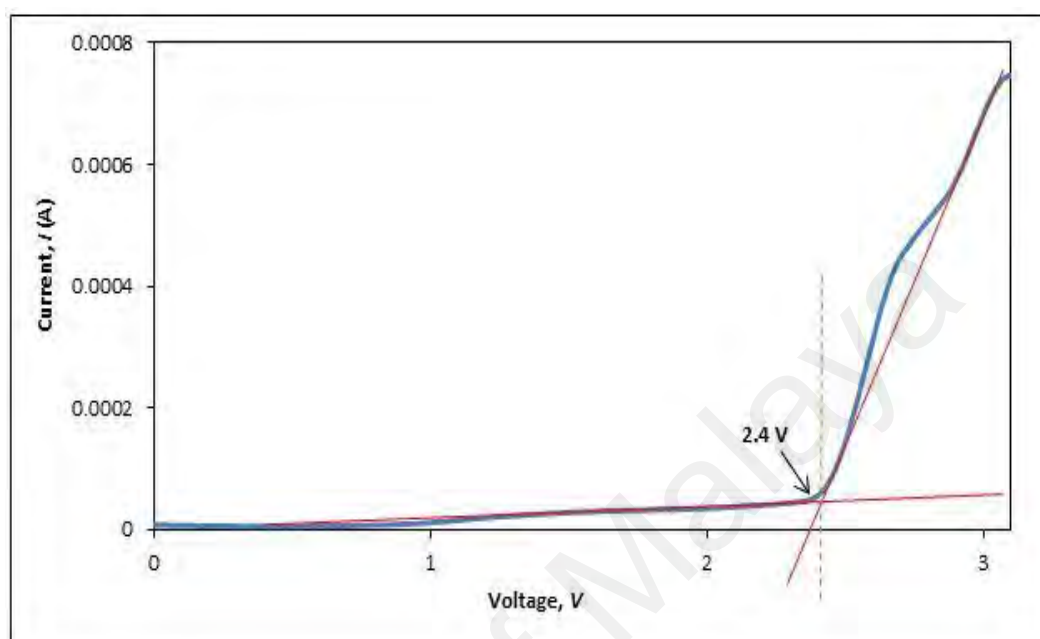
Figure 4.32: Linear sweep voltammetry curve for the biopolymer film of CMC-20 wt% Zn(CH₃COO)₂

4.4 Overall Results

This chapter describes the effect of salts containing cations of various size; NH^{4+}, Mg^{2+}, Na^+ and Zn^{2+} to the optimum CMC system. Table 4.1 compares the results of CMC added with different acetate salts. The CMC containing $NaCH_3COO$ shows the highest ionic conductivity compared to those containing NH_4CH_3COO, $Mg(CH_3COO)_2$ and $Zn(CH_3COO)_2$. This outcome can be explained to low lattice energy of $NaCH_3COO$. The lower lattice energy of the doping salt is generally expected to promote greater dissociation of salts thus provides higher concentration of ions to mobile (Su'ait et al., 2011).

The size of cation of salts increases in the order of $NaCH_3COO < Mg(CH_3COO)_2 < Zn(CH_3COO)_2 < NH_4CH_3COO$. Therefore, theoretically the ionic conductivity is expected to enhance in order of $NaCH_3COO < Mg(CH_3COO)_2 < Zn(CH_3COO)_2 < NH_4CH_3COO$. Based on the results in Table 4.1, it is shown that the size of cation plays an important role in determining the properties of the system.

Table 4.1: Comparative results between CMC-acetate salts

Parameters	CMC-NH$_4$CH$_3$COO	CMC-Mg(CH$_3$COO)$_2$	CMC-NaCH$_3$COO	CMC-Zn(CH$_3$COO)$_2$
Highest Ionic conductivity (S cm^{-1})	5.77×10^{-4}	1.83×10^{-3}	2.83×10^{-3}	1.75×10^{-3}
Highest Transference Number Measurements	0.99	0.98	0.98	0.99
Highest Linear Sweep Voltammetry	2.5V	2.7V	2.8V	2.4V

4.5 Summary

The biosourced polymer electrolytes films of kenaf fiber based carboxymethyl cellulose were prepared using four different doping salts; ammonium acetate, magnesium acetate, sodium acetate and zinc acetate via solution cast technique. The influences of different types of cations (NH_4^+, Mg^{2+}, Na^+ and Zn^{2+}) on the BPEs properties were investigated. The highest ionic conductivity was exhibited by the system containing 30 wt% of sodium acetate of 2.83×10^{-3} S cm^{-1}; and will be used to incorporate with ionic liquid in the following chapter. Temperature-dependent ionic conductivity study revealed that all polymer electrolytes follow Arrhenius thermal-activated model. FTIR analysis confirmed the interaction between polymer hosts with acetate based salts. Ionic transference number was found to be predominantly due to

ions. The addition of acetate based salts increases the film's amorphicity, besides reducing the pores in pure CMC, which could help to enhance the contact at the electrolyte-electrode interface. Linear sweep voltammetry result showed that the current that is related to the decomposition of polymer electrolytes increases gradually when the electrode potential are higher than 2.0 V thus they are suitable for electrochemical device applications.

CHAPTER 5: STUDIES ON CMC-NaCH₃COO-[Bmim]Cl BIOPOLYMER

ELECTROLYTE SYSTEM AND ITS APPLICATION IN

ELECTROCHEMICAL CELL

5.1   Introduction

This chapter presents and discusses the results of CMC-NaCH$_3$COO incorporated
with [Bmim]Cl biopolymer electrolyte. CMC-NaCH$_3$COO system was chosen to be
integrated with ionic liquid due to their good properties; the highest ionic conductivity
system from previous chapter. The idea of incorporating the ionic liquid was to improve
the properties of the electrolyte system as ionic liquids tend to have excellent
conductivity and solvent transport properties which make them ideal for electrolytes
(Singh & Sekhon, 2005a, 2005b). Besides that, addition of ionic liquid into a polymer
matrix is one of the methods to further enhance the chain flexibility which leads to ionic
conductivity enhancement. The influences of ionic liquid on the properties of polymer
electrolytes were investigated using different techniques including FTIR, TGA, IS,
TNM and LSV.

5.2   CMC-NaCH₃COO-[Bmim]Cl Biosourced Polymer Electrolyte Films

5.2.1   Studies on the Interaction of [Bmim]Cl with CMC-NaCH₃COO Electrolyte

For investigating interactions between host polymer, ionic salt and ionic liquid, FTIR
spectroscopy was performed on the CMC-NaCH$_3$COO-[Bmim]Cl biopolymer
electrolyte films. Figure 5.1 shows the IR spectra of pure CMC, CMC-30 wt%
NaCH$_3$COO and CMC-NaCH$_3$COO containing 30 wt% [Bmim]Cl in the 4000-550 cm^{-1}
spectral range. Figure 5.1(c) shows the effects of NaCH$_3$COO salt on the CMC FTIR
spectrum. The existence of significant band at 1552 cm^{-1} is assigned to the stretching

mode of COO⁻ in the carboxylic group which is the main backbone in CMC (Ramlli et al., 2013).

As explained in Section 4.3.3.1, addition of NaCH₃COO to the CMC-salt system, led to a shift of the symmetry of C=O stretching peak of CMC from 1597 cm⁻¹ to 1548 cm⁻¹ suggesting that the cation (Na⁺) substructure in NaCH₃COO interacted with the (C=O) in pure CMC. The weak band ascribed to the characteristic of C-O stretching on polysaccharide skeleton observed at 1040 cm⁻¹ (Lii et al., 2002; Taleb et al., 2009) and the small shifting of the band at 1057 cm⁻¹ to lower wavenumbers were other evidences to prove that complexation had occurred. The bands observed at 1411 cm⁻¹ and 1325 cm⁻¹ were due to the stretching mode of –CH₂ scissoring and the -OH bending vibration of CMC, respectively. The peak at 1411 cm⁻¹ was attributed to the presence of N-H deformation in NH₄CH₃COO. However, this band overlapped with the O-H band as reported by (Kamarudin & Isa, 2013).

Introduction of 30 wt% [Bmim]Cl into the biopolymer electrolyte system caused the shifting of the asymmetric stretching of COO⁻ in the CMC-NaCH₃COO at 1552 cm⁻¹ to a higher wavenumber (1565 cm⁻¹). (Shamsudin et al., 2015) reported a similar effect in their work where the asymmetric stretching peak of COO⁻ in the carboxymethyl carrageenan was shifted to a higher wave number upon the inclusion of ionic liquid. All peaks observed in Figure 5.2(d) were almost similar to those in Figure 5.1(c). The result reveals that the [Bmim]Cl has successfully integrated into the biopolymer electrolyte complexes. The incorporation of [Bmim]Cl theoretically weaked the dipole-dipole interactions in the polymer chains thus reduced the solvation of Na⁺ by polymer matrix, and enhanced the segmental motion of the biopolymer electrolytes.
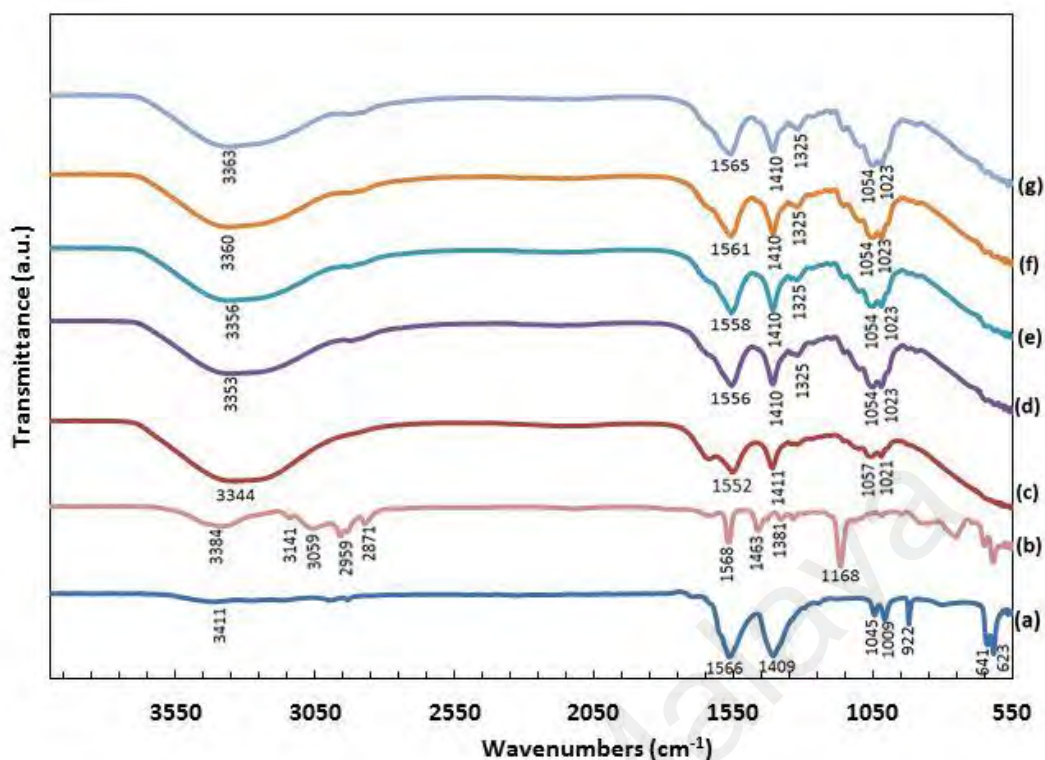
Figure 5.1: IR-spectra of (a) sodium acetate salt, (b) [Bmim]Cl, (c) CMC-NaCH₃COO,(d) CMC-NaCH₃COO-10wt% [Bmim]Cl, (e) CMC-NaCH₃COO-20wt% [Bmim]Cl, (f) CMC-NaCH₃COO-30wt% [Bmim]Cl and (g) CMC-NaCH₃COO-40wt% [Bmim]Cl

5.2.2   The Effect of [Bmim]Cl on the Thermal Properties of CMC-NaCH₃COO Biosourced Polymer Electrolyte

TGA was carried out on the CMC-NaCH₃COO-[Bmim]Cl biopolymer electrolytes, and the results are presented in Figure 5.2. Two distinct stages are observed in the TGA curves. The first weight loss is about 16.57% to 18.2% in the temperature range between 30 and 120 °C for all biopolymer electrolyte samples. The initial weight loss is credited to the presence of entrapped moisture in the samples (Ramesh et al., 2010). A similar observation was reported by (Lam et al., 2012). This can be explained by the behaviour of biopolymer which tends to absorb moisture from its surroundings during loading or evaporation of solvents in the biopolymer electrolyte samples (Stephan et al., 2002). The second weight loss is due to the decarboxylation of CMC.
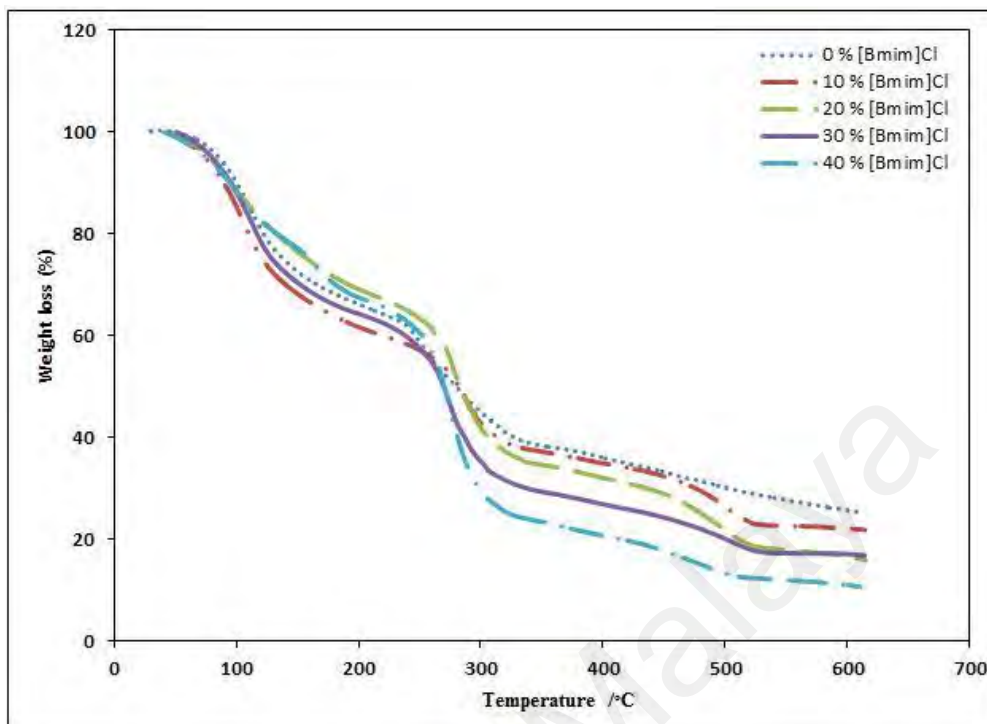
Figure 5.2: TGA curves of CMC-NaCH₃COO containing (a) 0 wt%, (b) 10 wt%, (c) 20 wt%, (d) 30 wt% and (e) 40 wt% of [Bmim]Cl

The CMC-NaCH$_3$COO complex integrated with [Bmim]Cl shows an improvement in heat-resistivity and thermal stability. This proves that the ionic liquids in polymer electrolyte played an important role in order to their thermal properties (Baranyai et al., 2004). Apparently, with the incorporation of [Bmim]Cl, the decomposition temperature, T_d increases while the total weight loss of biopolymer electrolytes film decreases. It can also be observed that from Figure 5.3 that the biopolymer electrolyte samples integrated with 30 wt% of [Bmim]Cl achieved the highest T_d at temperature 307.5 $^{\circ}$C with delineates the total weight loss of 66.8%. This phenomenon can be explained by the loss of COO$^-$ from the polysaccharide backbone (Biswal & Singh, 2004) which interacted with ammonium salt and ionic liquid as discussed in FTIR results. At this stable range, the weight of polymer complexes is drastically reduced as the main contributor for this weight loss is attributed to COO$^-$. Besides that, the presence of amorphous phase in

87

biopolymer electrolyte system results in an increase in heat sensitivity. Since it is thermally stable, less monomer is detached from the complex structure of biopolymer electrolyte, hence reducing the total weight loss (Samsudin et al., 2014).

5.2.3 The Effect of [Bmim]Cl on Conductivity of CMC-NaCH₃COO Biosourced Polymer Electrolyte Systems

Figure 5.3 shows typical complex impedance spectra for BPE film of CMC: 30 wt% NaCH$_3$COO: 30 wt% [Bmim]Cl system at different temperatures. There is no semicircle found in the complex impedance plots, suggesting the dominance of the resistive component of the PEs (Ramya et al., 2007). On the other hand, the presence of a low frequency spike, gives an indication that the conduction was mainly due to ions. A similar observation was reported by Jacob and co-workers (Jacob et al., 1997). Besides that, the inclined spikes, which are at an angle of less than $90°$ to the real axis, is also observed. The spikes are related to the roughness of the electrode-electrolyte interface (Jurado et al., 2003). The conductivity was calculated using equation (3.3):
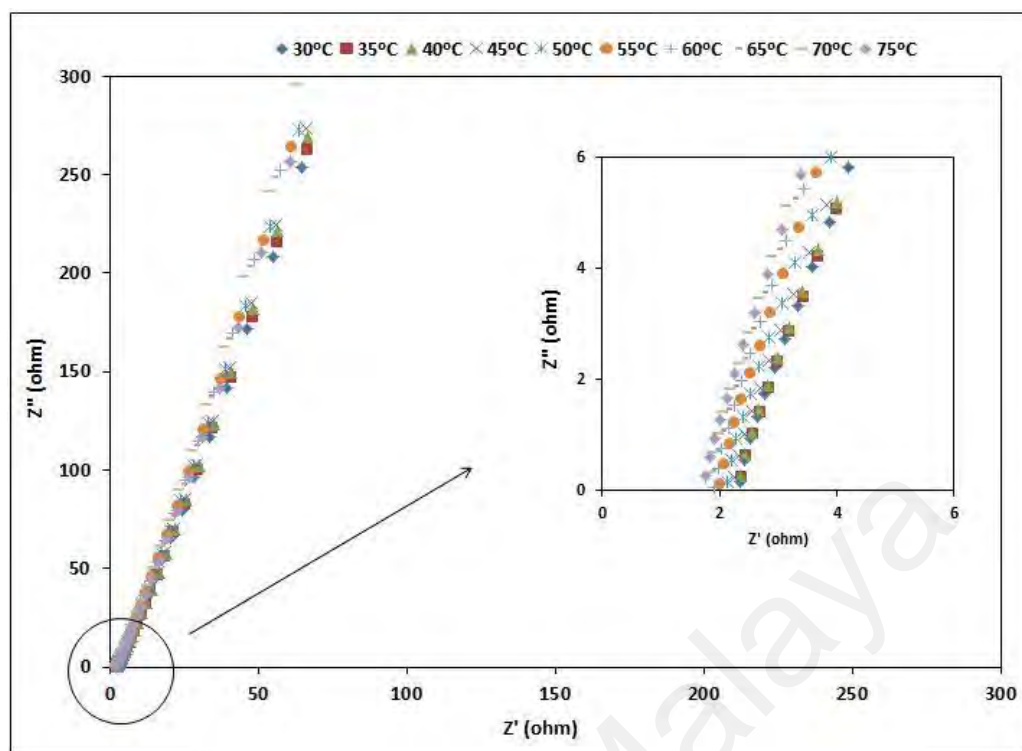
Figure 5.3: Complex impedance spectra for CMC-NaCH₃COO incorporated with 30 wt% [Bmim]Cl film at different temperatures

Presented in Figure 5.4 is the variation of conductivity with ionic liquid content for the CMC-NaCH$_3$COO biopolymer electrolytes. The conductivity increases up to a maximum value at 30 wt% of [Bmim]Cl and dramatically decreases at higher [Bmim]Cl concentration. As shown in the previous chapter, the conductivity of CMC was 7.51×10^{-5} S cm^{-1} while CMC-30 wt% NaCH$_3$COO possessed a conductivity value of 2.83×10^{-3} S cm^{-1}. Addition of 10 wt% of [Bmim]Cl increases the conductivity to 2.92×10^{-3} S cm^{-1}. The conductivity increases further reaching a maximum value of 4.54×10^{-3} S cm^{-1} with 30 wt% loadings of [Bmim]Cl. The main attributor of the increasing trend of conductivity with increase in [Bmim]Cl concentration is most possibility the increase of ion mobility.

This phenomenon is the result of [Bmim]Cl plasticizing effect. This effect weakened the dipole-dipole interactions in the polymer chains thus reduced the solvation of Na$^+$

by polymer matrix. This it promoted ionic decoupling and enhanced the dynamic free volume of the polymer system and thereby enhanced the ionic conductivity (Woo et al., 2011). According to Anuar and co-workers, ionic liquid not only weakens polymer-polymer chain interactions, but also decreases the dipole-ion interactions in the dopant salt. In addition, the plasticizing effect also lowers the T_g, therefore softens the polymer backbone and increases the segmental mobility when electric field is applied across the biopolymer electrolyte, leading to an increase in ionic conductivity (Anuar et al., 2012).
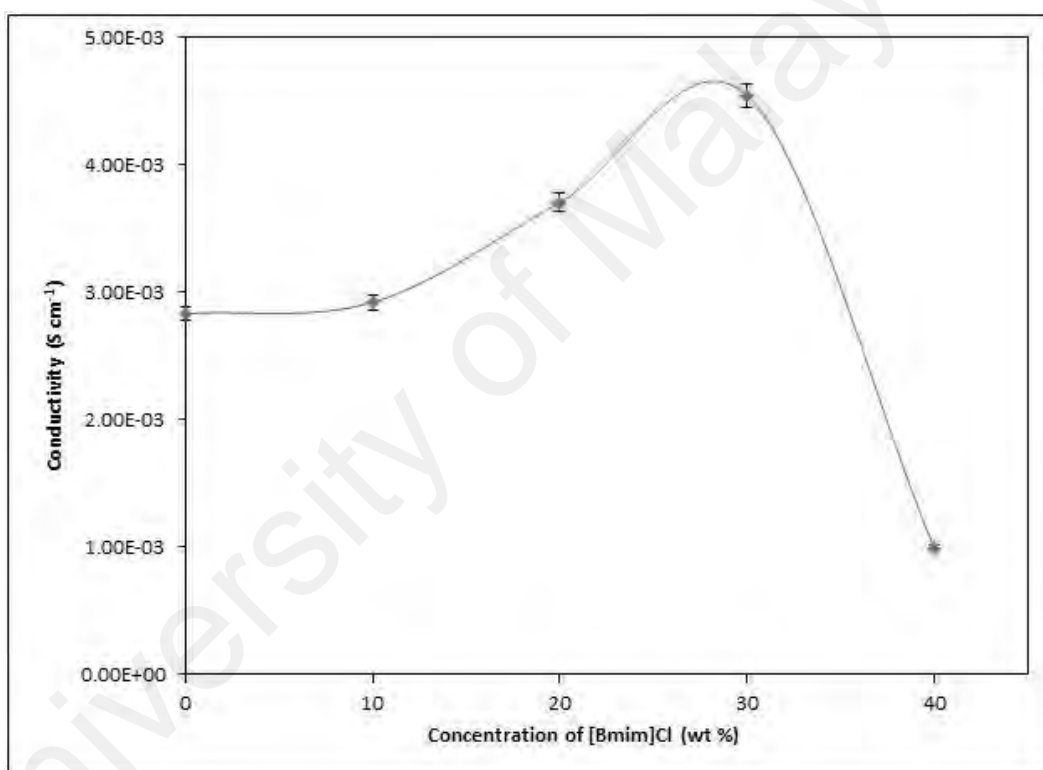
Figure 5.4: Ionic conductivity of CMC-NaCH₃COO-[Bmim]Cl at ambient temperature

Upon addition of more than 30 wt% of [Bmim]Cl, the ionic conductivity is drastically decreased. This drastic decrease phenomenon is possibly due to the formation non-conducting ion-pairs (Woo et al., 2011). The decreased may also cause by the creation of ion aggregates or ion multiples which reduced the number of mobile

ions and limited ion mobility in the biopolymer electrolytes (Woo et al., 2011; Yahya & Arof, 2003).

Temperature dependence of ionic conductivity study was performed to investigate the influence of temperature on green biopolymer electrolytes. Temperature dependence of conductivity for biopolymer electrolyte of different compositions of [Bmim]Cl has been studied in the range temperature of 303-348 K. This measurement can be used to analyse the mechanism of ionic conduction of biopolymer electrolytes (Ramlli et al., 2013). Figure 5.5 illustrates the dependence of ionic conductivity on temperature for the biopolymer electrolyte films.
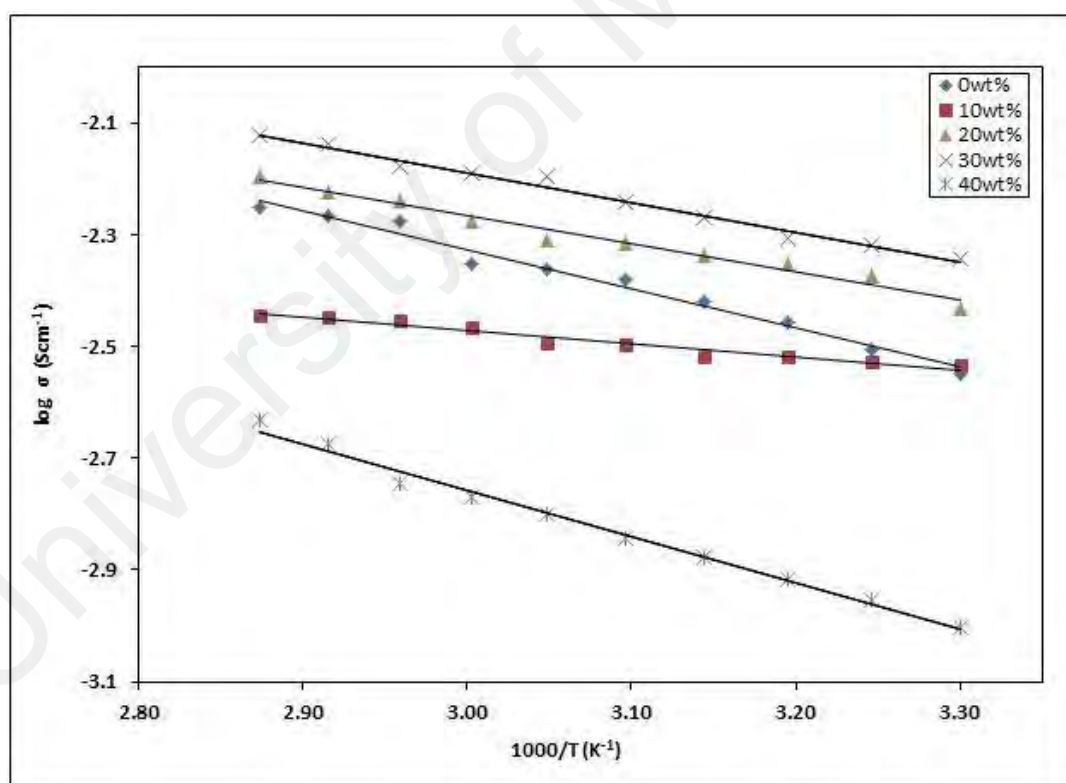
Figure 5.5: Arrhenius plots of CMC-NaCH₃COO containing 0-40 wt% of [Bmim]Cl

The linear variation of log σ vs. 1000/T suggests Arrhenius behaviour or thermally assisted behaviour of ionic conductivity as given by Equation (4.1).

The conductivity does not show any abrupt change with temperature indicating that there was no phase transition in the polymer electrolytes within the selected temperature range. According to (Aziz et al., 2010), this relation shows that the conductivity was thermally assisted meaning that the variation of temperature used affected the conductivity of the samples. It can be assumed that the nature of ion transport, in this case Na^{+}, transport was quite similar to that occurring in ionic crystals, which is the ions jump into the neighbouring vacant sites (Ramesh et al., 2002; Souquet et al., 1994). The activation energy, E_a is the energy required to move an ion, presupposing that the structure remains unchanged, plus the energy required deforming the structure enough to allow the ion to pass. E_a was calculated from Equation (4.1) and the results are depicted in Figure 5.6.
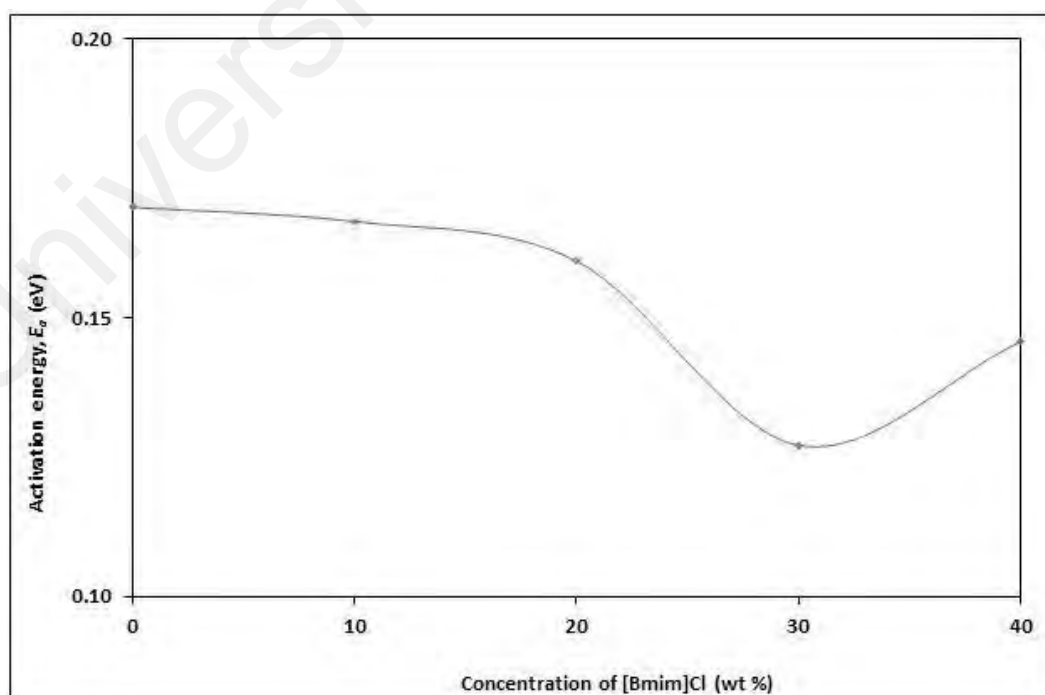
Figure 5.6: Activation energy vs. [Bmim]Cl concentration

Comparing Figure 5.4 and Figure 5.6, it can be seen that E_a for conduction decreases gradually with increase in conductivity, implying that the ions in highly conducting samples required lower energy for migration. The E_a of CMC-NaCH$_3$COO integrated with 30 wt% [Bmim]Cl is 0.13 eV. This E_a is considered low, thus it can be concluded that either Na$^+$ or [Bmim]$^+$ would break and re-bind the coordination bond easily with low energy barrier.

Dielectric relaxation study is a vital tool to elucidate the relaxation of dipoles in polymer electrolytes. In general, polymer shows several kinds of dielectric absorption associated with various kinds of molecular relaxation. Besides, dielectric relaxation study also provides important insights into the polarization effect at the electrode/electrolyte interface which can help in understanding conductivity trend (Howell et al., 1974). According to Hema et al. (2009) and co-workers, the important insights into the ionic transport phenomenon can be gleaned from the dielectric behavior of the system. In this study, a dielectric study was done to gain some insight into ionic transport phenomenon of the CMC-NaCH$_3$COO-Bmim[Cl] biosourced polymer electrolytes. The impedance data measured were used to calculate the real and imaginary parts of the complex permitivity. (iedermann & apc k, 2000) stated that the information about the motion of entities having an electric charge or an electric dipole moment can be obtained from dielectric analysis. For dielectric studies, two important parameters have been studied namely dielectric constant, ε_r; known as storage component, and dielectric loss, ε_i; component used to measure the energy loss for each cycle of the applied electric field (Hema et al., 2008). Both components can be calculated using equations below:

$$\varepsilon_r(\omega) = \frac{Z_i}{\omega C_0 (Z_r{}^2 + Z_i{}^2)} \tag{5.1}$$

$$\varepsilon_i(\omega) = \frac{Z_r}{\omega C_0 (Z_r{}^2 + Z_i{}^2)} \tag{5.2}$$

where $C_o = \varepsilon_o A/t$, $\omega = 2\pi f$ (f is frequency), Z_r is the real part of impedance, Z_i is the imaginary part of impedance, A is electrode-electrolyte contact area and t is the thickness of the electrolyte.

Graphs of dielectric constant and dielectric loss for the sample with the highest ionic conductivity of CMC-NaCH$_3$COO-Bmim[Cl] system are depicted in Figures 5.7 and 5.8, respectively. The incorporation of ionic liquid, Bmim[Cl] which acts as plasticizer, into CMC-NaCH$_3$COO complexes is expected to increase the degree of salt dissociation and enhances the number of free ions. Therefore, the increase in conductivity is due to the association of ions or decrease in mobility of the ions (Rajendran et al., 2004). In Figure 5.7, it can be observed that the variation in ε_r and ε_i with angular frequency could be attributed to the formation of space charge region at the electrode-electrolyte interface. This confirms non-Debye dependence implying that the charge region with respect to the frequency is explained in terms of ion diffusion (Khiar & Arof, 2010; Macdonald, 1987). There were no appreciable relaxation peaks observed in the frequency range employed in this work.

The dielectric plot in Figure 5.7 illustrates higher value of dielectric constant, ε_r in the low frequency region. This phenomenon can be explained by the presence of blocking electrodes as the transfer of mobile ions in the external circuit could not be permitted, resulting in ions accumulation near the electrode and the bulk polarization effect in the materials are produced (Tamilselvi & Hema, 2014). Furthermore, it can be inferred that the enhancement of frequency caused the dipoles unable to keep in pace with the fast changing field. This would lead to drop in ε_r values with increasing

frequency (Devi & Ramachandran, 2011). Meanwhile, the dielectric loss, ε_i becomes very large at lower frequencies as depicted in Figure 5.8, which can be explained by free charge motion that are building up at the interface between the materials and the electrodes. Besides that, the ε_i trend shows the appearance of a dominant dielectric relaxation peak, whose maximum shifts gradually with the increment of frequency with increasing temperature. This high frequency β-relaxation peak may be attributed by the side group dipoles (Tamilselvi & Hema, 2014).

Both the dielectric constant, ε_r and dielectric loss, ε_i increase with temperature and this is due to the migration polarization of the mobile ions (MacCallum & Vincent, 1987). This phenomenon explains that heat or temperature increases the degree of salt dissociation and re-dissociation of ion aggregates resulting in enhancement of conductivity due to higher content of free ions or charge carrier density. On the other hand, the value of ε_r and ε_i decreases with increasing frequency due to the high periodic reversal of the applied field. Therefore, there was no time for charge to build up at the interface. The polarization due to the charge accumulation decreases leading to the drop in the value of ε_r and ε_i (Hamsan et al., 2017; Tripathi & Tripathi, 2017). A further investigation of the dielectric behaviour can be more successfully achieved using modulus study which suppresses the effect of electrode polarization (Shastry & Rao, 1991).
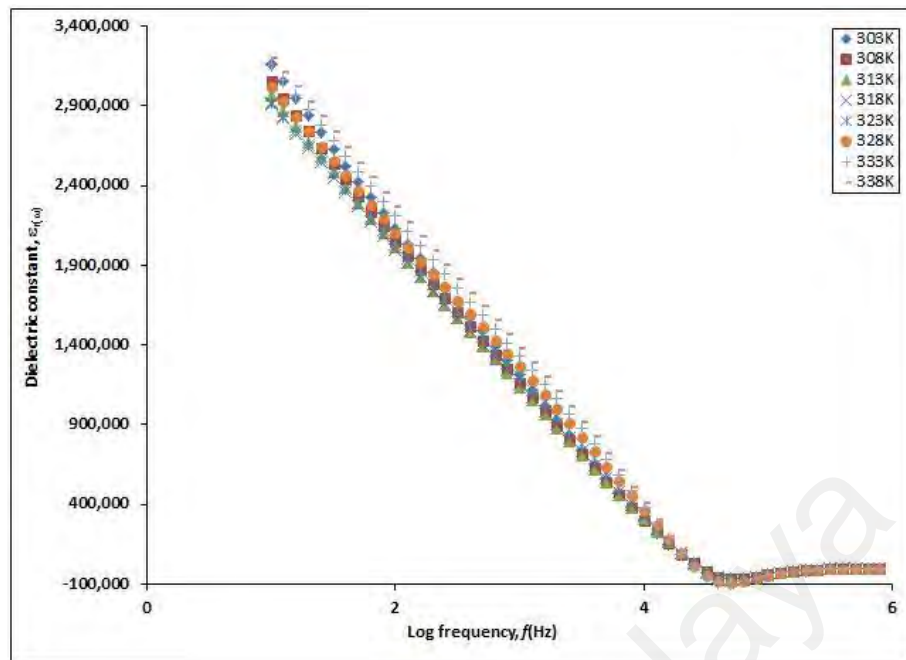
Figure 5.7: Dielectric constant of CMC-NaCH₃COO-30 wt% Bmim[Cl] biosourced polymer electrolyte recorded at different temperatures
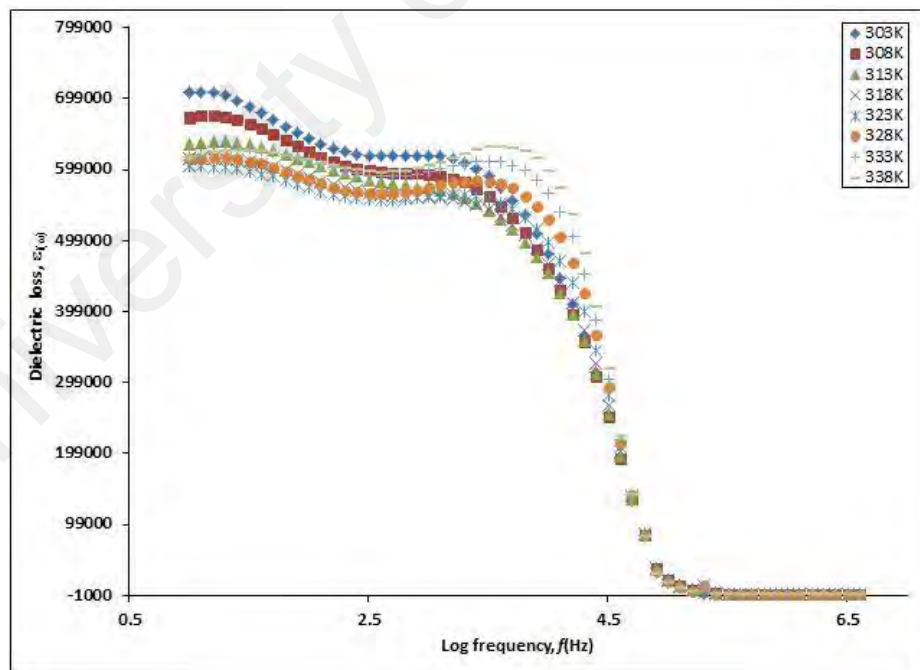
Figure 5.8: Dielectric loss of CMC-NaCH₃COO-30 wt% Bmim[Cl] biosourced polymer electrolytes

5.2.4 Transference Number Measurement

5.2.4.1 Ionic transference number

Figure 5.9 presents the normalized polarization current-time plot for the CMC-NaCH$_3$COOcontaining 30 wt% [Bmim]Cl biopolymer electrolyte. The value of ionic transference number, t_{ion} and electron transference number, t_e may be found using the equation given as follows:

$$t_{ion} = \frac{I_T - I_S}{I_T} \tag{5.5}$$

$$t_e = \frac{I_S}{I_T} \tag{5.6}$$

where the I_t is a total initial current at start (t = 0) (ionic and electronic) and I_s is the current on saturation (electronic current only) which are determined from the plot of normalized polarization current versus time.
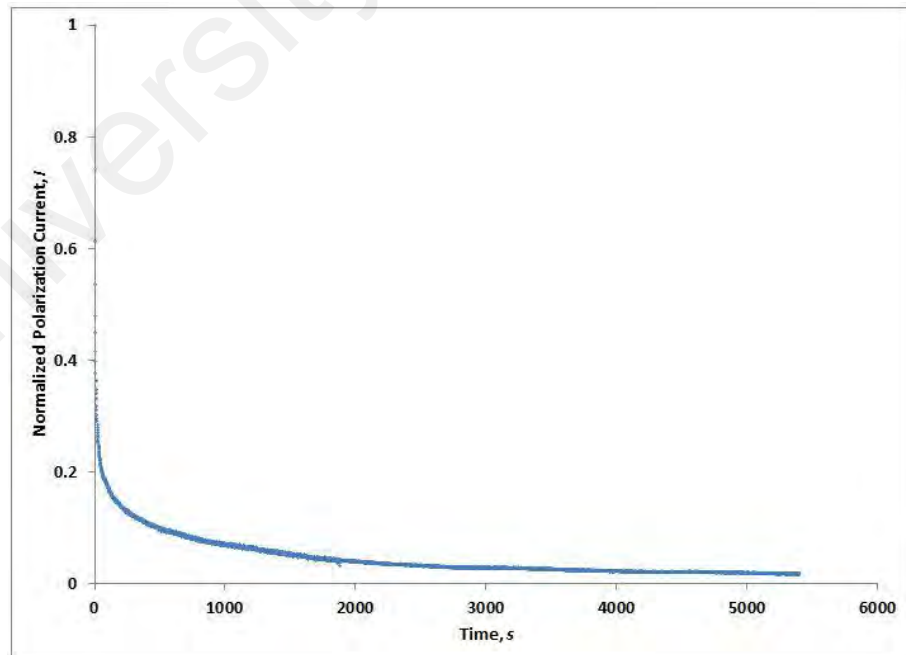
Figure 5.9: Normalized polarization current versus time for the biopolymer electrolyte film of CMC-NaCH$_3$COO-30 wt% [Bmim]Cl

The initial total current decreases with time due to the depletion of the ionic species in the biopolymer electrolyte and became constant in fully depleted situation. Ionic migration occurs until steady state is achieved. At the steady state, the cell is polarized and any residual current flow is due to electron migration across the electrolyte and interfaces. This phenomenon occurs if the biopolymer electrolyte is primarily ionic. The ionic currents through an ion-blocking electrode fall rapidly with time (Ramesh et al., 2002; Samsudin et al., 2011).

Table 5.1 depicts the experimental values of t_i for samples CMC containing 30 wt% NaCH$_3$COO and 30 wt% NaCH$_3$COO with 30 wt% [Bmim]Cl biopolymer electrolytes. t_i for CMC-NaCH$_3$COO is 0.99 showing that it is an almost perfect ionic conductor. This can be explained by the contribution of Na$^+$ ions from NaCH$_3$COO complexed with CMC. The result also suggests that charge transport in CMC-NaCH$_3$COO system was predominantly due to ions and expected to be protons with only a negligible electronic contribution (Linford, 1988).

Table 5.1: The ionic and electronic transport numbers for biopolymer electrolytes at room temperature

Biopolymer electrolyte film	Transport number		
	t_i	t_e	Total t
CMC-NaCH$_3$COO	0.99	0.01	1.00
CMC-NaCH$_3$COO-30 wt% [Bmim]Cl	0.95	0.05	1.00

The integration of [Bmim]Cl into CMC-NaCH$_3$COO biopolymer electrolytes leads to a decrease in t_i. This result is found to be in agreement with that reported by (Ramamohan & Sharma, 2013), which showed a reduction in t_i when plasticizer was added into (PEMA+ PVC + NaIO$_4$) system. The decrease in t_i of the biopolymer electrolyte is due the increment in number ion pairs and neutral ion aggregates that do

not give any contribution in ionic conduction. However, the high t_i implies that majority of charge carriers in the biopolymer electrolytes are expected to be ions.

5.2.4.2 Cationic transference number

Cationic transference number of CMC electrolytes was determined via Bruce and Vincent method, which is expressed as follows:

$$t_+ = \frac{I_{ss}}{I_o}\left[\frac{\Delta V - I_o R_o}{\Delta V - I_{ss} R_{ss}}\right] \tag{5.7}$$

where I_o is initial current ($t = 0$), R_o is electrolyte resistance before polarization, R_{ss} is electrolyte resistance after polarization, I_{ss} is the steady state current and ΔV is applied voltage pulse (1.0 V).
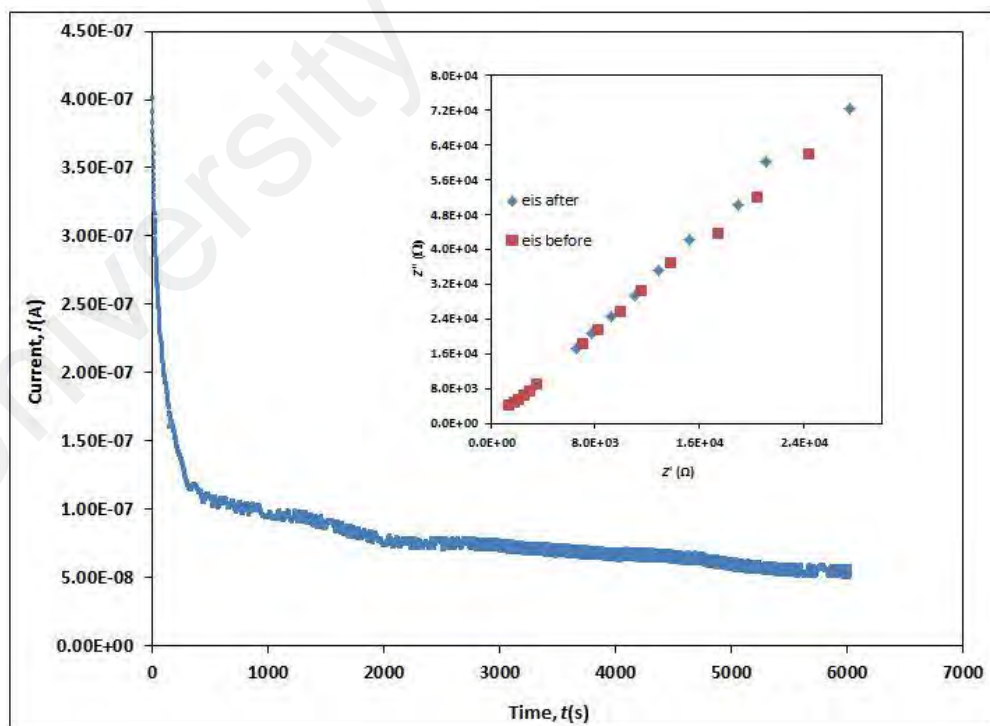
Figure 5.10: Time dependant response of DC polarization for CMC-NaCH₃COO-[Bmim]Cl electrolyte polarized with a potential 1.0 V. AC. The inset graph illustrates the impedance spectra of CMC-NaCH₃COO-[Bmim]Cl electrolyte before and after polarization

Figure 5.10 illustrates the plot of current versus time for the highest conducting CMC-NaCH$_3$COO-[Bmim]Cl for sodium transference number measurements. The calculated cationic transference number shows that CMC-NaCH$_3$COO-[Bmim]Cl has the value of t_{Na+} = 0.129. The small value of cationic transference numbers might be due to oxygen in the polymer chains which trap the cations electrostatically; ionic conduction was mostly contributed by anions (Sequeira & Santos, 2010).

The addition of [Bmim]Cl (Bmim$^+$ and Cl$^-$) may decrease the fraction of Na$^+$ to CH$_3$COO$^-$ ions in the polymer. Na$^+$ ions are surrounded by large number of Cl$^-$ and CH$_3$COO$^-$ anions forming an ionic cluster. Cationic transference number of electrolytes containing ionic liquid conducted by (Zygadło-Monikowska et al., 2014) showed small cationic values in the range of 0.03-0.11. Another work by (Niedzicki et al., 2014) also gives low cationic transference number in the range of 0.02-0.04. The value obtained in this study is comparable with those reported in the literature. Therefore, this result indicates that the majority of ions that contribute to ionic conductivity is not cation (Bmim$^+$ or Na$^+$) but most possibly anions (Cl$^-$ or CH$_3$COO$^-$) (Ali et al., 2006; Bhargav et al., 2009).

5.2.5 Electrochemical Stability Window of CMC-NaCH$_3$COO-[Bmim]Cl Biosourced Polymer Electrolytes

The electrochemical stability study was done on the CMC-NaCH$_3$COO system incorporated with 30 wt% of [Bmim]Cl since it is the highest ionic conducting biopolymer electrolyte. The voltammogram of this biopolymer electrolyte is shown in Figure 5.11. The onset current of the biopolymer electrolyte is detected at about 2.9 V and assumed to be the biopolymer electrolyte's breakdown voltage. This

electrochemical stability window is good enough to allow safe use of this biopolymer electrolyte for fabrication of sodium batteries.
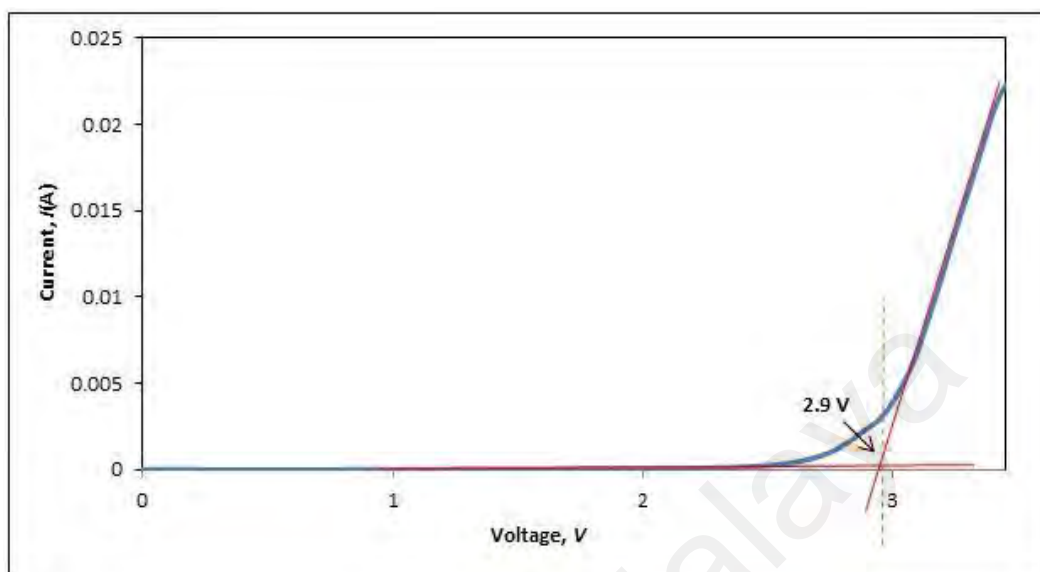
Figure 5.11: Linear sweep voltammogram for the biopolymer electrolyte film of CMC-NaCH₃COO-30 wt% [Bmim]Cl

5.3 Fabrication and Performances of Sodium Battery

A battery consists of three main components; anode, cathode and electrolyte. Oxidation occurs at the anode (negative terminal of the battery in the discharged mode) from where electrons flow to the external circuit. At cathode (positive terminal of the battery in the discharged mode), reduction occurs to which the electrons flow into the external circuit. Practically, the anode must be an efficient oxidizing agent, stable in adhesion with electrolyte, have a useful working voltage and long life time. The cathode must have several characteristics; a good reducing agent, have good conductivity, easy to fabricate and low cost. Generally, metals are mainly used as the anode material. Electrolyte is the medium through which ions are transported between the anode and cathode during charge and discharge in electrochemical devices (Stephan & Nahm, 2006). Usually electrolytes with conductivity range between 10^{-5} to 10^{-2} Scm^{-1} and have

ionic transference number greater than 0.9 are suitable for battery applications (MacCallum & Vincent, 1987).

In previous subsection, it has been shown that the CMC-NaCH$_3$COO-30 wt% [Bmim]Cl system exhibits the highest conductivity. This system was used as the electrolyte to fabricate sodium batteries. Solid-state sodium batteries have been fabricated with configuration of Na/ CMC-NaCH$_3$COO-30 wt% [Bmim]Cl/ I$_2$+ C+ electrolyte. Figure 5.12 shows the schematic architecture of the fabricated coin cells.
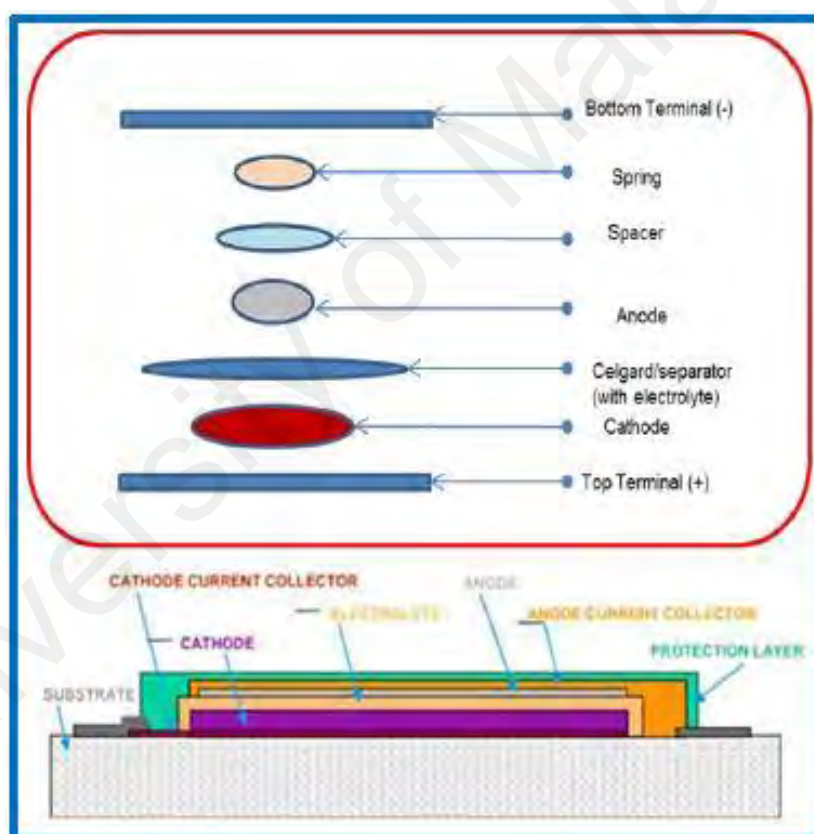
Figure 5.12: Schematic architecture for the fabrication of coin cell (Salehen et al., 2017)

From the configuration, the half-cell reactions can be written as:

At the anode:

$$Na \rightarrow Na^+ + e^-$$

At the cathode:

$$\frac{1}{2}(CH_3COO)_2 + e^- \rightarrow CH_3COO^-$$
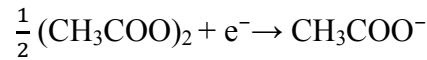
The overall reaction can be written as:

$$Na + \frac{1}{2}(CH_3COO)_2 \rightarrow NaCH_3COO$$
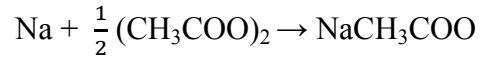
The open circuit voltage (OCV) of the constructed sodium battery was monitored for 24 hours and plotted against time as shown in Figure 5.13. OCV is the difference of electric potential between two terminals of a device when it disconnected from any circuit. There is no external electric current flow between the two terminals. The OCV is determined in order to obtain the maximum voltage and the stability of the battery and it was conducted for 24 hours. The OCV of the cell at ambient temperature shows the initial voltage of 1.68 V, dropping to 1.6 V in the first 6 hours of assembly. This phenomenon could be due to the oxidation of anode (Samsudin et al., 2014). The discharged capacity and other perimeters of the fabricated battery were calculated by the following formula:

$$\text{Power Density} = \frac{\text{Current} \times \text{Voltage (in plateau region)}}{\text{Weight of cell}} \qquad (5.8)$$

$$\text{Energy density} = \text{Power density} \times \text{Discharged time (in plateau region)} \qquad (5.9)$$

$$\text{Internal resistance} = \frac{\text{Open circuit voltage} - \text{voltage}}{\text{Current}} \qquad (5.10)$$

$$\text{Discharged capacity} = \text{Current} \times \text{Discharged time (in plateau region)} \qquad (5.11)$$

The discharge profile of the constructed sodium ion battery is shown in Figure 5.14. The battery was discharged at constant current of 0.1 mA. The load voltage of the

battery drops to 1.13 from 1.54 V in 50 hours of assembly. The initial sharp decrease in voltage of the cell is attributed to the polarization effect and/or formation of a thin layer of sodium salt at the electrode-electrolyte interface (Reddy & Reddy, 2003). The OCV and discharge time for plateau region and other cell parameters for this cell are listed in Table 5.2. From the battery application, it is evident that this battery is suitable for low current density application. However, more work needs to be done to further improve the characteristics of the polymer electrolytes in order to obtain electrochemical cells with better performance.
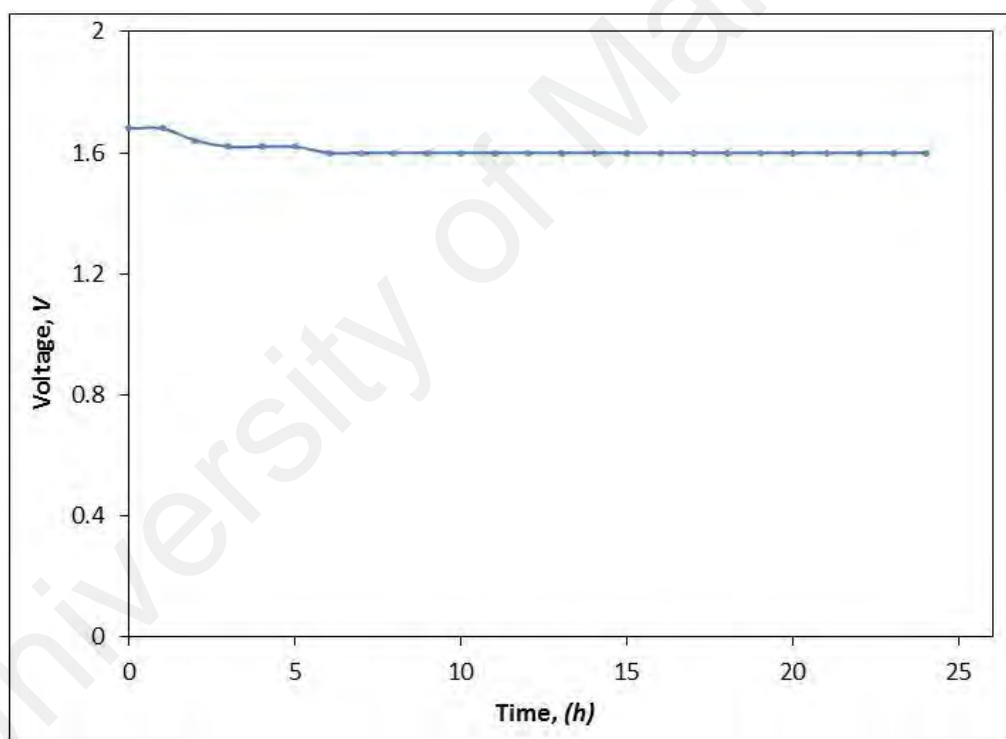
Figure 5.13: OCV as a function of time for CMC-NaCH₃COO-30 wt% [Bmim]Cl
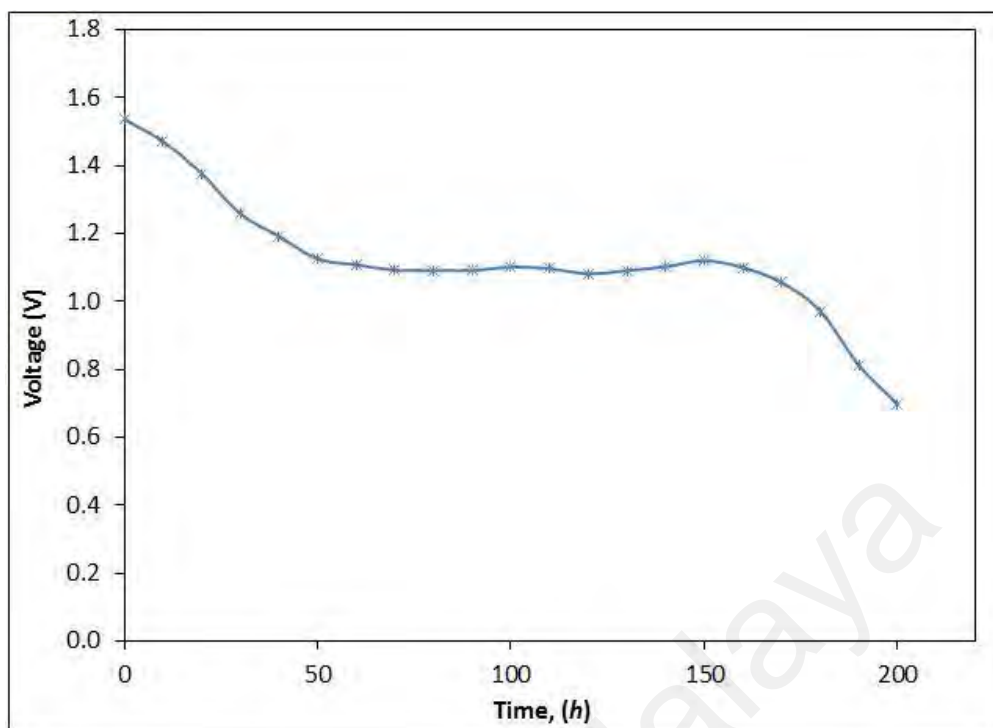
Figure 5.14: Discharged characteristic of CMC-NaCH₃COO-30 wt% [Bmim]Cl

Table 5.2: Cell parameters of Na/ CMC-NaCH₃COO-30 wt% [Bmim]Cl/ I₂+ C+ electrolyte.

Cell parameters	Measured values of discharged 0.1 mA
Cell area (cm^2)	1.33
Cell weight (g)	0.75
Effective cell diameter (cm)	1.3
Cell thickness (cm)	0.1
Open circuit voltage (V)	1.6
Discharged time for plateau region (h)	150
Current density (μAcm^{-2})	32.7
Discharged capacity (mA h)	1.5
Power density ($mWkg^{-1}$)	14.65
Energy density ($Whkg^{-1}$)	2197.5

5.4 Summary

In this chapter, the influences of [Bmim]Cl on the biopolymer electrolytes of kenaf fiber based carboxymethyl cellulose impregnated with NaCH₃COO were discussed.

FTIR analysis confirmed that the interaction between polymer host with sodium salt and ionic liquid. The SEM result showed that imparting of ionic liquid into biopolymer system yielded more amorphous films, as indicated by the decrease of roughness of the CMC-NaCH$_3$COO surface. [Bmim]Cl influenced the ionic conductivity of the biopolymer electrolytes and the best value of 4.54×10^{-3} S cm^{-1} was obtained for the system containing 30 wt% of [Bmim]Cl. Ionic transference number gave indication that conductivity was predominantly due to ions. Linear sweep voltammetry result showed that the electrochemical stability was up to ~2.9 V showing that the biopolymer electrolyte was suitable for practical application in electrochemical devices. Sodium batteries of configurations Na/ NaCH$_3$COO-30 wt% [Bmim]Cl/ I$_2$+ C+ electrolyte have been fabricated. Discharge performance of the electrochemical cell which used the optimized biosourced polymer electrolyte film has succeeded to act as electrolyte and separator in electrochemical cell.

CHAPTER 6: CONCLUSIONS AND SUGGESTIONS FOR FUTURE WORK

6.1   Conclusions

In this study, all objectives have been achieved. Free lignin cellulose was isolated from kenaf bast fiber. The raw fibers were subjected to two step chemical processes; alkali and bleaching treatment. FTIR showed that lignin and hemicellulose were almost entirely removed during the treatment. Chemical modification on free lignin cellulose was carried out to produce carboxymethyl cellulose. The confirmation on the successful chemical modification on cellulose was accomplished by FTIR analysis. The appearance of absorption bands at 1593 cm^{-1} and 1408 cm^{-1} were assigned to asymmetrical COO^- stretching and CH_2 symmetrical bending, respectively confirming the formation of CMC. High degree of substitution of 1.49 was achieved for CMC which was determined by acid-wash technique. The DS value obtained in this work is higher compared to those of the commercial CMCs available in the market, which are around 0.7 to 1.2. The obtained CMCs were then used as polymer host in biopolymer electrolyte systems.

Biopolymer electrolyte systems incorporated with different types of acetate salts; $CMC-CH_3COONH_4$, $CMC-Mg(CH_3COO)_2$, $CMC-NaCH_3COO$ and $CMC-Zn(CH_3COO)_2$ were successfully developed via solution cast technique. Addition of different acetate salts into CMC matrix gave significant effects to the optical, electrical and electrochemical properties. The formation of CMC-acetate salt complexes was indicated by the interactions between the cations from the salts with carboxylic group and hydroxyl group of biopolymer host. This was evidenced by the shifting of carbonyl group (C=O) towards lower wavenumbers of around 1597 to 1569 cm^{-1}. Among the four salted systems prepared, $CMC-NaCH_3COO$ exhibited the best properties; the

highest ionic conductivity and electrochemical stability values. The highest ionic conductivity was exhibited by the system containing 30 wt% of sodium acetate of 2.83×10^{-3} S cm^{-1}. Ionic transference number of this PE was found to be 0.99 showing that the conductivity was predominantly due to ions. LSV result showed that the current that is related to the decomposition of polymer electrolytes increased gradually when the electrode potential are higher than 2.0 V demonstrating that they were suitable for electrochemical device applications.

CMC-NaCH$_3$COO was used to be incorporated with ionic liquid, [Bmim]Cl in order to further enhance its properties. In the plasticized system, the addition of 30 wt% of [Bmim]Cl enhanced the conductivity to 4.54×10^{-3} S cm^{-1}. The presence of [Bmim]Cl into the salted system reduced the crystallinity indicating that the amorphosity nature of the system increased, which facilitated fast ionic motion in the polymer network. Besides that, [Bmim]Cl may have also provided alternative pathways for ionic conduction. Its high dielectric constant value also helps to weaken the Coulombic force between cation and anion, therefore eased the salt dissociation. Ionic transference number gave indication that conductivity was predominantly due to ions. LSV results showed that the electrochemical stability was up to 2.9 V.

In order to explore the potential of BPEs in devices, the electrochemical cell was fabricated using the highest conducting electrolyte system with the configuration of Na/ CMC-NaCH$_3$COO-30 wt% [Bmim]Cl/ I$_2$+ C+ electrolyte. The fabricated cell has relatively stable OCV around 1.6 V. The cell was discharged at 0.1 mA and highest discharged capacity obtained was 1.5 mA h. The biopolymer electrolyte was suitable for practical application in electrochemical devices and the performance of the cell is believed to be improvable by using different cathode in the cell.

6.2   Suggestions for Future Works

For future works, it would be interesting to investigate various approaches that can be carried out in order to enhance the ionic conductivity of biopolymer electrolyte system. The improvement may be achieved by several possible approaches listed below:

i.   The effects of active nanofillers into the electrolytes are also interesting to be investigated. The presence of filler can create favourable pathways for ionic conduction, enhanced the amorphousness and immobilize the anions (Bhattacharya et al., 2017; Kuila et al., 2007).

ii.   Combination of binary/tertiary ionic liquid to be incorporated in CMC based electrolytes system (Bhattacharya et al., 2017; Kuang et al., 2006; Rogers & Seddon, 2003).

iii. Using the combination of filler and plasticizer to be incorporated into the system. The incorporation of filler can improve the mechanical stability while plasticizer can enhance the conductivity (Khanmirzaei & Ramesh, 2014; Zain et al., 2016).

iv.   Using different electrode materials which are more compatible with electrolytes. The use of compatible electrode with electrolytes will improve the battery performance.

REFERENCES

Agrawal, R. C., Hashmi, S. A., & Pandey, G. P. (2007). Electrochemical cell performance studies on all-solid-state battery using nano-composite polymer electrolyte membrane. *Ionics, 13*(5), 295-298.

Agrawal, S. L., Singh, M., Tripathi, M., Dwivedi, M. M., & Pandey, K. (2009). Dielectric relaxation studies on [PEO-SiO$_2$]: NH$_4$SCN nanocomposite polymer electrolyte films. *Journal of Materials Science, 44*(22), 6060-6068.

Ahmad, N. H., & Isa, M. I. N. (2015). Proton conducting solid polymer electrolytes based carboxymethyl cellulose doped ammonium chloride: ionic conductivity and transport studies. *International Journal of Plastics Technology, 19*(1), 47-55.

Ahn, J. H., Wang, G. X., Liu, H. K., & Dou, S. X. (2003). Nanoparticle-dispersed PEO polymer electrolytes for Li batteries. *Journal of Power Sources, 119*, 422-426.

Ali, A. M. M., Subban, R. H. Y., Bahron, H., Winnie, T., Latif, F., & Yahya, M. Z. A. (2008). Grafted natural rubber-based polymer electrolytes: ATR-FTIR and conductivity studies. *Ionics, 14,* 491-500.

Ali, A. M. M., Subban, R. H. Y., Bahron, H., Yahya, M. Z. A., & Kamisan, A. S. (2013). Investigation on modified natural rubber gel polymer electrolytes for lithium polymer battery. *Journal of Power Sources, 244*, 636-640.

Ali, A. M. M., Yahya, M. Z. A., Bahron, H., & Subban, R. H. Y. (2006). Electrochemical studies on polymer electrolytes based on poly (methyl methacrylate)-grafted natural rubber for lithium polymer battery. *Ionics, 12*(4-5), 303-307.

Ambika, C., Hirankumar, G., Thanikaikarasan, S., Lee, K. K., Valenzuela, E., & Sebastian, P. J. (2015). Influence of TiO$_2$ as Filler on the Discharge Characteristics of a Proton Battery. *Journal of New Materials for Electrochemical Systems, 18*(4), 219-213.

Anuar, N. K., Subban, R. H. Y., & Mohamed, N. S. (2012). Properties of PEMA-NH$_4$CF$_3$SO$_3$ added to BMATSFI ionic liquid. *Materials, 5*(12), 2609-2620.

Aravamudhan, A., Ramos, D. M., Nada, A. A., & Kumbar, S. G. (2014). Natural polymers: polysaccharides and their derivatives for biomedical applications. In

Natural and Synthetic Biomedical Polymers (pp. 67-89). Amsterdam, North-Holland: Elsevier.

Armand, M. B., Chabagno, J. M., & Duclot, M. J. (1979). Fast ion transport in solids. In P. Vashishta, J.N. Mundy & G.K. Shenoy (Eds.), *Electrodes and Electrolytes* (pp. 52). Amsterdam, North-Holland: Elsevier.

Azahari, N. A., Othman, N., & Ismail, H. (2011). Biodegradation studies of polyvinyl alcohol/corn starch blend films in solid and solution media. *Journal of Physical Science, 22*(2), 15-31.

Aziz, N. A. N., Idris, N. K., & Isa, M. I. N. (2010). Proton conducting polymer electrolytes of methylcellulose doped ammonium fluoride: Conductivity and ionic transport studies. *International Journal of Physical Sciences, 5*(6), 748-752.

Bandara, T., Aziz, M. F., Fernando, H., Careem, M. A., Arof, A. K., & Mellander, B. E. (2015). Efficiency enhancement in dye-sensitized solar cells with a novel PAN-based gel polymer electrolyte with ternary iodides. *Journal of Solid State Electrochemistry, 19*(8), 2353-2359.

Baranyai, K. J., Deacon, G. B., MacFarlane, D. R., Pringle, J. M., & Scott, J. L. (2004). Thermal degradation of ionic liquids at elevated temperatures. *Australian Journal of Chemistry, 57*(2), 145-147.

Barbucci, R., Magnani, A., & Consumi, M. (2000). Swelling behavior of carboxymethylcellulose hydrogels in relation to cross-linking, pH, and charge density. *Macromolecules, 33*(20), 7475-7480.

Baril, D., Michot, C. L., & Armand, M. (1997). Electrochemistry of liquids vs. solids: Polymer electrolytes. *Solid State Ionics, 94*(1), 35-47.

Basha, S. S., Sundari, G. S., & Kumar, K. V. (2015). Electrical conductivity, Transport and Discharge characteristics of a sodium acetate trihydrate Complexed with polyvinyl alcohol for Electrochemical cell. *International Journal of ChemTech Research, 8*(2), 803-810.

Basha, S. S., Sundari, G. S., & Kumar, K. V. (2016). Optical, Thermal and Electrical studies of PVP based solid Polymer electrolyte For Solid state battery applications. *International Journal of ChemTech Research, 9*(02), 165-175.

Basha, S. K. S., Sundari, G. S., Kumar, K. V., & Rao, M. C. (2017). Optical and dielectric properties of PVP based composite polymer electrolyte films. *Polymer Science, Series A, 59*(4), 554-565.

Baskaran, R., Selvasekarapandian, S., Kuwata, N., Kawamura, J., & Hattori, T. (2006). Conductivity and thermal studies of blend polymer electrolytes based on PVAc–PMMA. *Solid State Ionics, 177*(26-32), 2679-2682.

Bella, F., Mobarak, N. N., Jumaah, F. N., & Ahmad, A. (2015). From seaweeds to biopolymeric electrolytes for third generation solar cells: an intriguing approach. *Electrochimica Acta, 151*, 306-311.

Bender, S. F., Cretzmeyer, J. W., & Reise, T. F. (2002). Zinc/air batteries-button configuration. In D. Linden & T.B. Reddy (Eds.), *Handbook of Batteries* (pp. 13.1-13.21). New York, USA: McGraw-Hill.

Bhargav, P. B., Mohan, V. M., Sharma, A. K., & Rao, V. N. (2007). Structural, electrical and optical characterization of pure and doped poly(vinyl alcohol)(PVA) polymer electrolyte films. *International Journal of Polymeric Materials, 56*(6), 579-591.

Bhargav, P. B., Mohan, V. M., Sharma, A. K., & Rao, V. N. (2009). Investigations on electrical properties of (PVA: NaF) polymer electrolytes for electrochemical cell applications. *Current Applied Physics, 9*(1), 165-171.

Bhattacharya, S., Ubarhande, R. M., Rani, M. U., Babu, R. S., & Arunkumar, R. (2017). TiO_2 as conductivity enhancer in PVdF-HFP polymer electrolyte system. *IOP Conference Series: Materials Science and Engineering, 263*, 022006.

Biswal, D. R., & Singh, R. P. (2004). Characterisation of carboxymethyl cellulose and polyacrylamide graft copolymer. *Carbohydrate Polymers, 57*(4), 379-387.

Blonsky, P. M., Shriver, D. F., Austin, P., & Allcock, H. R. (1986). Complex formation and ionic conductivity of polyphosphazene solid electrolytes. *Solid State Ionics, 18*, 258-264.

Bohnke, O., Frand, G., Rezrazi, M., Rousselot, C., & Truche, C. (1993). Fast ion transport in new lithium electrolytes gelled with PMMA. 1. Influence of polymer concentration. *Solid State Ionics, 66*(1-2), 97-104.

Buraidah, M. H., & Arof, A. K. (2011). Characterization of chitosan/PVA blended electrolyte doped with NH$_4$I. *Journal of Non-crystalline Solids, 357*(16-17), 3261-3266.

Buraidah, M. H., Teo, L. P., Majid, S. R., & Arof, A. K. (2009). Ionic conductivity by correlated barrier hopping in NH$_4$I doped chitosan solid electrolyte. *Physica B: Condensed Matter, 404*(8), 1373-1379.

Chadwick, A. V., Strange, J. H., & Worboys, M. R. (1983). Ionic transport in polyether electrolytes. *Solid State Ionics, 9*, 1155-1160.

Chai, M. N., & Isa, M. I. N. (2011). Carboxyl methylcellulose solid polymer electrolytes: Ionic conductivity and dielectric study. *Journal of Current Engineering Research, 1*(2), 23-27.

Chai, M. N., & Isa, M. I. N. (2016). Novel proton conducting solid bio-polymer electrolytes based on carboxymethyl cellulose doped with oleic acid and plasticized with glycerol. *Scientific Reports, 6*, 27328.

Chandra, A., Srivastava, P. C., & Chandra, S. (1995). Ion transport studies in PEO: NH$_4$I polymer electrolytes with dispersed Al$_2$O$_3$. *Journal of Materials Science, 30*(14), 3633-3638.

Chandra, S. (1981). *Superionic solids: principles and applications.* Amsterdam, North-Holland: Elsevier.

Chandra, S., & Chandra, A. (1994). Solid state ionics: Materials aspect. *Proceedings of National Academy of Sciences India Section* (pp. 141–181). Berlin, Germany: Springer.

Cheung, I. W., Chin, K. B., Greene, E. R., Smart, M. C., Abbrent, S., Greenbaum, S.G., … Surampudi, S. (2003). Electrochemical and solid state NMR characterization of composite PEO-based polymer electrolytes. *Electrochimica Acta, 48*(14-16), 2149-2156.

Cowie, J. M. G., & Martin, A. C. (1987). Ionic conductivity in poly (di-poly (propylene glycol) itaconate)-salt mixtures. *Polymer, 28*(4), 627-632.

Crawford, E. (1996). *Arrhenius: From ionic theory to the greenhouse effect.* Canton, MA: Ed Science History Publications.

Cuba-Chiem, L. T., Huynh, L., Ralston, J., & Beattie, D. A. (2008). In situ particle film ATR-FTIR studies of CMC adsorption on talc: The effect of ionic strength and multivalent metal ions. *Minerals Engineering, 21*(12-14), 1013-1019.

da Silva Neiro, S. M., Dragunski, D. C., Rubira, A. F., & Muniz, E. C. (2000). Miscibility of PVC/PEO blends by viscosimetric, microscopic and thermal analyses. *European Polymer Journal, 36*(3), 583-589.

De Souza, R. F., Padilha, J. C., Gonçalves, R. S., & Dupont, J. (2003). Room temperature dialkylimidazolium ionic liquid-based fuel cells. *Electrochemistry Communications, 5*(8), 728-731.

Dempsey, J. M. (1975). *Fiber crops*. Gainesville, USA: The University Presses of Florida.

Deng, D. (2015). Li-ion batteries: basics, progress, and challenges. *Energy Science & Engineering, 3*(5), 385-418.

Deraman, S. K., Mohamed, N. S., & Subban, R. H. Y. (2013). Conductivity and Electrochemical Studies on Polymer Electrolytes Based on Poly Vinyl (chloride)-Ammonium Triflate-Ionic Liquid for Proton Battery. *International Journal of Electrochemistry Science, 8*(1), 1459-1468.

Devi, P. I., & Ramachandran, K. (2011). Dielectric studies on hybridised PVDF–ZnO nanocomposites. *Journal of Experimental Nanoscience, 6*(3), 281-293.

dos Santos, D. M., de Lacerda Bukzem, A., Ascheri, D. P. R., Signini, R., & de Aquino, G. L. B. (2015). Microwave-assisted carboxymethylation of cellulose extracted from brewer's spent grain. *Carbohydrate Polymers, 131*, 125-133.

Duraikkan, V., Sultan, A. B., Nallaperumal, N., & Shunmuganarayanan, A. (2018). Structural, thermal and electrical properties of polyvinyl alcohol/poly (vinyl pyrrolidone)–sodium nitrate solid polymer blend electrolyte. *Ionics*, *24*(1), 139-151.

Dzulkurnain, N. A., Ahmad, A., & Mohamed, N. S. (2015). P (MMA-EMA) random copolymer electrolytes incorporating sodium iodide for potential application in a dye-sensitized solar cell. *Polymers, 7*(2), 266-280.

Edeerozey, A. M. M., Akil, H. M., Azhar, A. B., & Ariffin, M. I. Z. (2007). Chemical modification of kenaf fibers. *Materials Letters, 61*(10), 2023-2025.

El Seoud, O. A., Nawaz, H., & Arêas, E. P. (2013). Chemistry and applications of polysaccharide solutions in strong electrolytes/dipolar aprotic solvents: An overview. *Molecules, 18*(1), 1270-1313.

Ellis, B. L., & Nazar, L. F. (2012). Sodium and sodium-ion energy storage batteries. *Current Opinion in Solid State and Materials Science, 16*(4), 168-177.

Eyler, R. W., Klug, E. D., & Diephuis, F. (1947). Determination of degree of substitution of sodium carboxymethylcellulose. *Analytical chemistry, 19*(1), 24-27.

Fan, L., Dang, Z., Nan, C. W., & Li, M. (2002). Thermal, electrical and mechanical properties of plasticized polymer electrolytes based on PEO/P(VDF-HFP) blends. *Electrochimica Acta, 48*(2), 205-209.

Fenton, D. E., Parker, J., & Wright, P. (1973). Complexes of alkali metal ions with poly (ethylene oxide). *Polymer, 14*(11), 589.

Frech, R., & Chintapalli, S. (1996). Effect of propylene carbonate as a plasticizer in high molecular weight PEO・ $LiCF_3SO_3$ electrolytes. *Solid State Ionics, 85*(1-4), 61-66.

Fulcher, G. S. (1925). Analysis of recent measurements of the viscosity of glasses. *Journal of the American Ceramic Society, 8*(6), 339-355.

Gang, W., Roos, J., Brinkmann, D., Capuano, F., Croce, F., & Scrosati, B. (1992). Comparison of NMR and conductivity in (PEP) $8LiClO_4$+ γ-$LiAlO_2$. *Solid State Ionics, 53*, 1102-1105.

Geiculescu, O. E., Yang, J., Blau, H., Bailey-Walsh, R., Creager, S. E., Pennington, W. T., & DesMarteau, D. D. (2002). Solid polymer electrolytes from dilithium salts based on new bis[(perfluoroalkyl) sulfonyl] diimide dianions. Preparation and electrical characterization. *Solid State Ionics, 148*(1-2), 173-183.

Genova, F. K. M., Selvasekarapandian, S., Karthikeyan, S., Vijaya, N., Pradeepa, R., & Sivadevi, S. (2015). Study on blend polymer (PVA-PAN) doped with lithium bromide. *Polymer Science Series A, 57*(6), 851-862.

Ghanbarzadeh, B., & Almasi, H. (2013). Biodegradable polymers *Biodegradation-life of Science*, Chap 6, 141-185.

Ghanbarzadeh, B., Almasi, H., & Entezami, A. A. (2011). Improving the barrier and mechanical properties of corn starch-based edible films: Effect of citric acid and carboxymethyl cellulose. *Industrial Crops and Products, 33*(1), 229-235.

Gopalan, A. I., Santhosh, P., Manesh, K. M., Nho, J. H., Kim, S. H., Hwang, C. G., & Lee, K. P. (2008). Development of electrospun PVdF–PAN membrane-based polymer electrolytes for lithium batteries. *Journal of Membrane Science, 325*(2), 683-690.

Hafiza, M. N., & Isa, M. I. N. (2017). Solid polymer electrolyte production from 2-hydroxyethyl cellulose: Effect of ammonium nitrate composition on its structural properties. *Carbohydrate Polymers, 165*, 123-131.

Hamsan, M. H., Shukur, M. F., & Kadir, M. F. Z. (2017). NH_4NO_3 as charge carrier contributor in glycerolized potato starch-methyl cellulose blend-based polymer electrolyte and the application in electrochemical double-layer capacitor. *Ionics*, *23*(12), 3429-3453.

Han, D. G., & Choi, G. M. (1998). Computer simulation of the electrical conductivity of composites: The effect of geometrical arrangement. *Solid State Ionics, 106*, 71-87.

Harris, C. S., Ratner, M. A., & Shriver, D. F. (1987). Ionic conductivity in branched polyethylenimine-sodium trifluoromethanesulfonate complexes: comparisons to analogous complexes made with linear polyethylenimine. *Macromolecules, 20*(8), 1778-1781.

Hema, M., Selvasekarapandian, S., Arunkumar, D., Sakunthala, A., & Nithya, H. (2009). FTIR, XRD and ac impedance spectroscopic study on PVA based polymer electrolyte doped with NH_4X (X= Cl, Br, I). *Journal of Non-Crystalline Solids, 355*(2), 84-90.

Hema, M., Selvasekerapandian, S., Sakunthala, A., Arunkumar, D., & Nithya, H. (2008). Structural, vibrational and electrical characterization of PVA–NH 4 Br polymer electrolyte system. *Physica B: Condensed Matter, 403*(17), 2740-2747.

Hirankumar, G., Selvasekarapandian, S., Kuwata, N., Kawamura, J., & Hattori, T. (2005). Thermal, electrical and optical studies on the poly (vinyl alcohol) based polymer electrolytes. *Journal of Power Sources, 144*(1), 262-267.

Holkar, C. R., Jadhav, A. J., Karekar, S. E., Pandit, A. B., & Pinjari, D. V. (2016). Recent developments in synthesis of nanomaterials utilized in polymer based

composites for food packaging applications. *Journal of Food Bioengineering and Nanoprocessing, 1(1),* 80-105.

Howell, F. S., Bose, R. A., Macedo, P. B., & Moynihan, C. T. (1974). Electrical relaxation in a glass-forming molten salt. *The Journal of Physical Chemistry, 78*(6), 639-648.

Huang, H., He, P., Hu, N., & Zeng, Y. (2003). Electrochemical and electrocatalytic properties of myoglobin and hemoglobin incorporated in carboxymethyl cellulose films. *Bioelectrochemistry, 61*(1), 29-38.

Ibrahim, S., Ali, H., Aishah, S., & Mohamed, N. S. (2010). Characterization of PVDF-HFP-LiCF$_3$SO$_3$-ZrO$_2$ Nanocomposite Polymer Electrolyte Systems. *Advanced Materials Research, 93-94,* 489-492.

Idris, N. K., Aziz, N. A. N., Zambri, M. S. M., Zakaria, N. A., & Isa, M. I. N. (2009). Ionic conductivity studies of chitosan-based polymer electrolytes doped with adipic acid. *Ionics, 15*(5), 643-646.

Imperiyka, M., Ahmad, A., Hanifah, S. A., & Rahman, M. Y. A. (2013). Role of salt concentration lithium perchlorate on ionic conductivity and structural of (glycidyl methacrylate-co-ethyl methacrylate)(70/30) based on a solid polymer electrolyte. *Advanced Materials Research, 626,* 454-458.

Jacob, M. M. E., Prabaharan, S. R. S., & Radhakrishna, S. (1997). Effect of PEO addition on the electrolytic and thermal properties of PVDF-LiClO$_4$ polymer electrolytes. *Solid State Ionics, 104*(3-4), 267-276.

Jacobs, P. W. M., Lorimer, J. W., Russer, A., & Wasiucionek, M. (1989). Phase relations and conductivity in the system poly (ethylene oxide) · LiClO$_4$. *Journal of Power Sources, 26*(3-4), 503-510.

Jafirin, S., Ahmad, I., & Ahmad, A. (2013). Potential use of cellulose from kenaf in polymer electrolytes based on MG49 rubber composites. *BioResources, 8*(4), 5947-5964.

Jayathilaka, P. A. R. D., Dissanayake, M. A. K. L., Albinsson, I., & Mellander, B.-E. (2002). Effect of nano-porous Al$_2$O$_3$ on thermal, dielectric and transport properties of the (PEO)$_9$LiTFSI polymer electrolyte system. *Electrochimica Acta, 47*(20), 3257-3268.

Ji, K. S., Moon, H. S., Kim, J. W., & Park, J.-W. (2003). Role of functional nano-sized inorganic fillers in poly (ethylene) oxide-based polymer electrolytes. *Journal of Power Sources, 117*(1), 124-130.

Jiang, X., Bin, Y., & Matsuo, M. (2005). Electrical and mechanical properties of polyimide–carbon nanotubes composites fabricated by in situ polymerization. *Polymer, 46*(18), 7418-7424.

Jiang, Z., Carroll, B., & Abraham, K. M. (1997). Studies of some poly (vinylidene fluoride) electrolytes. *Electrochimica Acta, 42*(17), 2667-2677.

Johan, M. R., & Fen, L. B. (2010). Combined effect of CuO nanofillers and DBP plasticizer on ionic conductivity enhancement in the solid polymer electrolyte PEO–LiCF$_3$SO$_3$. *Ionics, 16*(4), 335-338.

Jurado, J. F., Trujillo, J. A., Mellander, B. E., & Vargas, R. A. (2003). Effect of AgBr on the electrical conductivity of β-AgI. *Solid State Ionics, 156*(1), 103-112.

Juśkiewicz, J., & Zduńczyk, Z. (2004). Effects of cellulose, carboxymethylcellulose and inulin fed to rats as single supplements or in combinations on their caecal parameters. *Comparative Biochemistry and Physiology Part A: Molecular & Integrative Physiology, 139*(4), 513-519.

Kadir, M. F. Z., Majid, S. R., & Arof, A. K. (2010). Plasticized chitosan–PVA blend polymer electrolyte based proton battery. *Electrochimica Acta, 55*(4), 1475-1482.

Kamarudin, K. H., & Isa, M. I. N. (2013). Structural and DC Ionic conductivity studies of carboxy methylcellulose doped with ammonium nitrate as solid polymer electrolytes. *International Journal of Physical Science, 8*(31), 1581-1587.

Kargarzadeh, H., Ahmad, I., Abdullah, I., Dufresne, A., Zainudin, S. Y., & Sheltami, R. M. (2012). Effects of hydrolysis conditions on the morphology, crystallinity, and thermal stability of cellulose nanocrystals extracted from kenaf bast fibers. *Cellulose, 19*(3), 855-866.

Karnani, R., Krishnan, M., & Narayan, R. (1997). Biofiber-reinforced polypropylene composites. *Polymer Engineering & Science, 37*(2), 476-483.

Ketabi, S., Decker, B., & Lian, K. (2014). Effect of Cation on Proton Conductivity of a Non-fluorinated Ionic Liquid. *ECS Meeting Abstracts 24*, 1055.

Khanmirzaei, M. H., & Ramesh, S. (2014). Nanocomposite polymer electrolyte based on rice starch/ionic liquid/TiO₂ nanoparticles for solar cell application. *Measurement, 58*, 68-72.

Khanmirzaei, M. H., Ramesh, S., & Ramesh, K. (2015). Polymer electrolyte based dye-sensitized solar cell with rice starch and 1-methyl-3-propylimidazolium iodide ionic liquid. *Materials & Design, 85*, 833-837.

Khiar, A. S. A., & Arof, A. K. (2010). Conductivity studies of starch-based polymer electrolytes. *Ionics, 16*(2), 123-129.

Kim, H. S., Idris, R., & Moon, S. I. (2004). Synthesis and electrochemical performances of epoxidised natural rubber for lithium-ion polymer batteries. *Bulletin of Electrochemistry, 20*(10), 465-469.

Kim, K. J., & Shahinpoor, M. (2003). Ionic polymer–metal composites: II. Manufacturing techniques. *Smart materials and structures, 12*(1), 65.

Klemm, D., Heublein, B., Fink, H. P., & Bohn, A. (2005). Cellulose: fascinating biopolymer and sustainable raw material. *Angewandte Chemie International Edition, 44*(22), 3358-3393.

Koksbang, R., Olsen, I. I., & Shackle, D. (1994). Review of hybrid polymer electrolytes and rechargeable lithium batteries. *Solid State Ionics, 69*(3), 320-335.

Kontturi, K., Mafé, S., Manzanares, J. A., Pellicer, J., & Vuoristo, M. (1994). A new method for determining transport numbers of charged membranes from convective diffusion experiments. *Journal of Electroanalytical Chemistry, 378*(1-2), 111-116.

Köster, T. K. J., & van Wüllen, L. (2010). Cation–anion coordination, ion mobility and the effect of Al₂O₃ addition in PEO based polymer electrolytes. *Solid State Ionics, 181*(11), 489-495.

Kuang, D., Ito, S., Wenger, B., Klein, C., Moser, J. E., Humphry-Baker, R., . . . Grätzel, M. (2006). High molar extinction coefficient heteroleptic ruthenium complexes for thin film dye-sensitized solar cells. *Journal of the American Chemical Society, 128*(12), 4146-4154.

Kucińska- ipka, J., Gubańska, I., & Janik, H. (2014). Polyurethanes modified with natural polymers for medical application. Part II. Polyurethane/gelatin, polyurethane/starch, polyurethane/cellulose. *Polimery, 59*(3).

Kuila, T., Acharya, H., Srivastava, S. K., Samantaray, B. K., & Kureti, S. (2007). Enhancing the ionic conductivity of PEO based plasticized composite polymer electrolyte by LaMnO$_3$ nanofiller. *Materials Science and Engineering: B, 137*(1), 217-224.

Kumar, A., & Deka, M. (2010). *Nanofiber Reinforced Composite Polymer Electrolyte Membranes.* Crotia: Intech.

Kumar, B., Scanlon, L., Marsh, R., Mason, R., Higgins, R., & Baldwin, R. (2001). Structural evolution and conductivity of PEO: LiBF$_4$–MgO composite electrolytes. *Electrochimica Acta, 46*(10-11), 1515-1521.

Kumar, K. S. S., Nair, C. R., & Ninan, K. N. (2006). Rheokinetic investigations on the thermal polymerization of benzoxazine monomer. *Thermochimica acta, 441*(2), 150-155.

Kurita, K. (2001). Controlled functionalization of the polysaccharide chitin. *Progress in Polymer Science, 26*(9), 1921-1971.

Lam, E., Leung, A. C. W., Liu, Y., Majid, E., Hrapovic, S., Male, K. B., & Luong, J. H. (2012). Green strategy guided by Raman spectroscopy for the synthesis of ammonium carboxylated nanocrystalline cellulose and the recovery of byproducts. *ACS Sustainable Chemistry & Engineering, 1*(2), 278-283.

ewandowski, A., Zajder, M., Frąckowiak, E., & Beguin, F. (2001). Supercapacitor based on activated carbon and polyethylene oxide–KOH–H$_2$O polymer electrolyte. *Electrochimica Acta, 46*(18), 2777-2780.

Li, Q., Chen, J., Fan, L., Kong, X., & Lu, Y. (2016). Progress in electrolytes for rechargeable Li-based batteries and beyond. *Green Energy & Environment, 1*(1), 18-42.

Li, Q., Sun, H. Y., Takeda, Y., Imanishi, N., Yang, J., & Yamamoto, O. (2001). Interface properties between a lithium metal electrode and a poly (ethylene oxide) based composite polymer electrolyte. *Journal of Power Sources, 94*(2), 201-205.

Li, Z., Su, G., Wang, X., & Gao, D. (2005). Micro-porous P (VDF-HFP)-based polymer electrolyte filled with Al$_2$O$_3$ nanoparticles. *Solid State Ionics, 176*(23-24), 1903-1908.

iedermann, K., & apc k Jr, L. (2000). Dielectric relaxation in hydroxyethyl cellulose. *Carbohydrate Polymers, 42*(4), 369-374.

Liew, C. W., Ramesh, S., & Arof, A. K. (2014). A novel approach on ionic liquid-based poly (vinyl alcohol) proton conductive polymer electrolytes for fuel cell applications. *International Journal of Hydrogen Energy, 39*(6), 2917-2928.

Lii, C. Y., Tomasik, P., Zaleska, H., Liaw, S. C., & Lai, V. M. F. (2002). Carboxymethyl cellulose–gelatin complexes. *Carbohydrate Polymers, 50*(1), 19-26.

Lim, C. S., Teoh, K. H., Ng, H. M., Liew, C. W., & Ramesh, S. (2017). Ionic conductivity enhancement studies of composite polymer electrolyte based on poly (vinyl alcohol)-lithium perchlorate-titanium oxide. *Advanced Materials Letter, 4,* 465-471.

Linford, R. (1988). Experimental techniques for studying polymer electrolytes. In B.V.R. Chowdari, S. Radhakrishna (Eds.). *Solid state ionics devices* (pp. 551-571). Singapore: World Scientific

Long, L., Wang, S., Xiao, M., & Meng, Y. (2016). Polymer electrolytes for lithium polymer batteries. *Journal of Materials Chemistry A, 4*(26), 10038-10069.

Lu, D. R., Xiao, C. M., & Xu, S. J. (2009). Starch-based completely biodegradable polymer materials. *Express Polymer Letters, 3*(6), 366-375.

Ma, X., Yu, J., He, K., & Wang, N. (2007). The effects of different plasticizers on the properties of thermoplastic starch as solid polymer electrolytes. *Macromolecular Materials and Engineering, 292*(4), 503-510.

MacCallum, J. R., & Vincent, C. A. (1987). Ion-molecule and ion-ion interactions. *Polymer Electrolyte Reviews, 1*, 23-37.

Macdonald, J. R. (1987). *Impedance spectroscopy- emphasizing solid materials and systems.* New York, USA: Wiley.

Majid, S. R., & Arof, A. K. (2005). Proton-conducting polymer electrolyte films based on chitosan acetate complexed with NH_4NO_3 salt. *Physica B: Condensed Matter, 355*(1), 78-82.

Manjuladevi, R., Thamilselvan, M., Selvasekarapandian, S., Mangalam, R., Premalatha, M., & Monisha, S. (2017a). Mg-ion conducting blend polymer electrolyte based on poly (vinyl alcohol)-poly (acrylonitrile) with magnesium perchlorate. *Solid State Ionics, 308*, 90-100.

Manjuladevi, R., Thamilselvan, M., Selvasekarapandian, S., Selvin, P. C., Mangalam, R., & Monisha, S. (2017b). Preparation and characterization of blend polymer electrolyte film based on poly (vinyl alcohol)-poly (acrylonitrile)/MgCl$_2$ for energy storage devices. *Ionics, 24*(4), 1083-1095.

Marcì, G., Mele, G., Palmisano, L., Pulito, P., & Sannino, A. (2006). Environmentally sustainable production of cellulose-based superabsorbent hydrogels. *Green Chemistry, 8*(5), 439-444.

Mobarak, N. N., Ahmad, A., Abdullah, M. P., Ramli, N., & Rahman, M. Y. A. (2013). Conductivity enhancement via chemical modification of chitosan based green polymer electrolyte. *Electrochimica Acta, 92*, 161-167.

Mobarak, N. N., Jumaah, F. N., Ghani, M. A., Abdullah, M. P., & Ahmad, A. (2015). Carboxymethyl carrageenan based biopolymer electrolytes. *Electrochimica Acta, 175*, 224-231.

Mohamed, N. S., Subban, R. H. Y., & Arof, A. K. (1995). Polymer batteries fabricated from lithium complexed acetylated chitosan. *Journal of Power Sources, 56*(2), 153-156.

Mohamed, N. S., Zakaria, M. Z., Ali, A. M. M., & Arof, A. K. (1997). Characteristics of poly (ethylene oxide)-NaI polymer electrolyte and electrochemical cell performances. *Journal of Power Sources, 66*(1), 169-172.

Muda, N., Ibrahim, S., Kamarulzaman, N., & Mohamed, N. S. (2011). PVDF-HFP-NH$_4$CF$_3$SO$_3$-SiO$_2$ Nanocomposite Polymer Electrolytes for Protonic Electrochemical Cell. *Key Engineering Materials, 471*, 373-378.

Nava, R., Halachev, T., Rodr guez, R., & Castano, V. M. (2002). Synthesis, characterization and catalytic behavior of a zinc acetate complex immobilized on silica-gel. *Applied Catalysis A: General, 231*(1-2), 131-149.

Ng, L. S., & Mohamad, A. A. (2008). Effect of temperature on the performance of proton batteries based on chitosan–NH$_4$NO$_3$–EC membrane. *Journal of Membrane Science, 325*(2), 653-657.

Niaounakis, M. (2013). *Biopolymers: Reuse, Recycling, and Disposal*. Amsterdam, North-Holland: Elsevier.

Niedzicki, L., Karpierz, E., Bitner, A., Kasprzyk, M., Zukowska, G. Z., Marcinek, M., & Wieczorek, W. (2014). Optimization of the lithium-ion cell electrolyte composition through the use of the LiTDI salt. *Electrochimica Acta, 117*, 224-229.

Nieschlag, H. J. (1960). A search for new fibre crops. *Tappi, 43*(3), 193-201.

Noda, A., & Watanabe, M. (2000). Highly conductive polymer electrolytes prepared by in situ polymerization of vinyl monomers in room temperature molten salts. *Electrochimica Acta, 45*(8-9), 1265-1270.

Noor, I. S., Majid, S. R., & Arof, A. K. (2013). Poly (vinyl alcohol)–LiBOB complexes for lithium–air cells. *Electrochimica Acta, 102*, 149-160.

Noor, M. M., Buraidah, M. H., Careem, M. A., Majid, S. R., & Arof, A. K. (2014). An optimized poly (vinylidene fluoride-hexafluoropropylene)–NaI gel polymer electrolyte and its application in natural dye sensitized solar cells. *Electrochimica Acta, 121*, 159-167.

Noor, S. A. M., Ahmad, A., Talib, I. A., & Rahman, M. Y. A. (2010). Morphology, chemical interaction, and conductivity of PEO-ENR50 based on solid polymer electrolyte. *Ionics, 16*(2), 161-170.

Osman, Z. Ahmad, A., & Isa, K. M. (2011). Conductivity and structural studies of plasticized polyacrylonitrile (PAN)-lithium triflate polymer electrolyte films. *Sains Malaysiana, 40*(7), 691-694.

Pandey, G. P., & Hashmi, S. A. (2009). Experimental investigations of an ionic-liquid-based, magnesium ion conducting, polymer gel electrolyte. *Journal of Power Sources, 187*(2), 627-634.

Park, J. T., Koh, J. H., Roh, D. K., Shul, Y. G., & Kim, J. H. (2011). Proton-conducting nanocomposite membranes based on P (VDF-co-CTFE)-g-PSSA graft copolymer and TiO_2–PSSA nanoparticles. *International Journal of Hydrogen Energy, 36*(2), 1820-1827.

Pas, S. J., Ingram, M. D., Funke, K., & Hill, A. J. (2005). Free volume and conductivity in polymer electrolytes. *Electrochimica Acta, 50*(19), 3955-3962.

123

Peerce, P. J., & Bard, A. J. (1980). Polymer films on electrodes: Part III. Digital simulation model for cyclic voltammetry of electroactive polymer film and electrochemistry of poly(vinylferrocene) on platinum. *Journal of Electroanalytical Chemistry and Interfacial Electrochemistry, 114*(1), 89-115.

Pitawala, H., Dissanayake, M., Seneviratne, V., Mellander, B. E., & Albinson, I. (2008). Effect of plasticizers (EC or PC) on the ionic conductivity and thermal properties of the (PEO) 9LiTf: Al_2O_3 nanocomposite polymer electrolyte system. *Journal of Solid State Electrochemistry, 12*(7-8), 783-789.

Polu, A. R., & Kumar, R. (2011). AC impedance and dielectric spectroscopic studies of Mg^{2+} ion conducting PVA–PEG blended polymer electrolytes. *Bulletin of Materials Science, 34*(5), 1063-1067.

Polu, A. R., & Kumar, R. (2013). Ionic conductivity and discharge characteristic studies of PVA-Mg(CH_3COO) 2 solid polymer electrolytes. *International Journal of Polymeric Materials, 62*(2), 76-80.

Polu, A. R., Kumar, R., & Joshi, G. M. (2014). Effect of zinc salt on transport, structural, and thermal properties of PEG-based polymer electrolytes for battery application. *Ionics, 20*(5), 675-679.

Polu, A. R., & Rhee, H. W. (2015). Nanocomposite solid polymer electrolytes based on poly (ethylene oxide)/POSS-PEG (n= 13.3) hybrid nanoparticles for lithium ion batteries. *Journal of Industrial and Engineering Chemistry, 31*, 323-329.

Polu, A. R., & Rhee, H. W. (2017). Ionic liquid doped PEO-based solid polymer electrolytes for lithium-ion polymer batteries. *International Journal of Hydrogen Energy, 42*(10), 7212-7219.

Porcarelli, L., Gerbaldi, C., Bella, F., & Nair, J. R. (2016). Super soft all-ethylene oxide polymer electrolyte for safe all-solid lithium batteries. *Scientific Reports, 6*, 19892.

Pratap, R., Singh, B., & Chandra, S. (2006). Polymeric rechargeable solid-state proton battery. *Journal of Power Sources, 161*(1), 702-706.

Premalatha, M., Mathavan, T., Selvasekarapandian, S., Selvalakshmi, S., & Monisha, S. (2017). Incorporation of NH4Br in tamarind seed polysaccharide biopolymer and its potential use in electrochemical energy storage devices. *Organic Electronics, 50*, 418-425.

Pushpamalar, V., Langford, S. J., Ahmad, M., & Lim, Y. Y. (2006). Optimization of reaction conditions for preparing carboxymethyl cellulose from sago waste. *Carbohydrate Polymers, 64*(2), 312-318.

Qiao, J., Fu, J., Lin, R., Ma, J., & Liu, J. (2010). Alkaline solid polymer electrolyte membranes based on structurally modified PVA/PVP with improved alkali stability. *Polymer, 51*(21), 4850-4859.

Rahman, M., & Brazel, C. S. (2006). Ionic liquids: New generation stable plasticizers for poly (vinyl chloride). *Polymer Degradation and Stability, 91*(12), 3371-3382.

Rajendran, S., Sivakumar, M., & Subadevi, R. (2004). Investigations on the effect of various plasticizers in PVA–PMMA solid polymer blend electrolytes. *Materials Letters, 58*(5), 641-649.

Rajendran, S., & Uma, T. (2000a). Effect of ceramic oxide on PMMA based polymer electrolyte systems. *Materials Letters, 45*(3), 191-196.

Rajendran, S., & Uma, T. (2000b). Effect of ZrO_2 on conductivity of PVC-PMMA-$LiBF_4$-DBP polymer electrolytes. *Bulletin of Materials Science, 23*(1), 31-34.

Ramalingaiah, S., Reddy, D. S., Reddy, M. J., Laxminarsaiah, E., & Rao, U. S. (1996). Conductivity and discharge characteristic studies of novel polymer electrolyte based on PEO complexed with $Mg(NO_3)_2$ salt. *Materials Letters, 29*(4-6), 285-289.

Ramamohan, K., & Sharma, A. K. (2013). Effect of plasticizer on (PVC+ PEMA+ $NaIO_4$) solid polymer blend electrolyte system for battery characterization studies. *Advance in Polymer Science Technology, 3*, 49-53.

Ramesh, S., Leen, K. H., Kumutha, K., & Arof, A. K. (2007). FTIR studies of PVC/PMMA blend based polymer electrolytes. *Spectrochimica Acta Part A: Molecular and Biomolecular Spectroscopy, 66*(4), 1237-1242.

Ramesh, S., Liew, C. W., Morris, E., & Durairaj, R. (2010). Effect of PVC on ionic conductivity, crystallographic structural, morphological and thermal characterizations in PMMA–PVC blend-based polymer electrolytes. *Thermochimica Acta, 511*(1), 140-146.

Ramesh, S., Liew, C. W., & Ramesh, K. (2011). Evaluation and investigation on the effect of ionic liquid onto PMMA-PVC gel polymer blend electrolytes. *Journal of Non-crystalline Solids, 357*(10), 2132-2138.

Ramesh, S., Yahaya, A. H., & Arof, A. K. (2002). Dielectric behaviour of PVC-based polymer electrolytes. *Solid State Ionics, 152*, 291-294.

Ramlli, M. A., Chai, M. N., & Isa, M. I. N. (2013). Influence of propylene carbonate as a plasticizer in CMC-OA based biopolymer electrolytes: Conductivity and electrical study. *Advanced Materials Research, 802*, 184-188.

Ramya, C. S., Selvasekarapandian, S., Savitha, T., Hirankumar, G., & Angelo, P. C. (2007). Vibrational and impedance spectroscopic study on PVP–NH$_4$SCN based polymer electrolytes. *Physica B: Condensed Matter, 393*(1), 11-17.

Rao, S. S., Reddy, M. J., Narsaiah, E. L., & Rao, U. S. (1995). Development of electrochemical cells based on (PEO+NaYF$_4$) and (PEO+KYF$_4$) polymer electrolytes. *Materials Science and Engineering: B, 33*(2-3), 173-177.

Ratner, M. A. (1987). Aspects of the theoretical treatment of polymer solid electrolytes: transport theory and models. *Polymer Electrolyte Reviews, 1*, 173-236.

Reddy, C. V. S., Sharma, A., & Rao, V. N. (2006). Electrical and optical properties of a polyblend electrolyte. *Polymer, 47*(4), 1318-1323.

Reddy, M. J., & Chu, P. P. (2002). Optical microscopy and conductivity of poly (ethylene oxide) complexed with KI salt. *Electrochimica Acta, 47*(8), 1189-1196.

Reddy, M. J., Rao, S. S., Laxminarsaiah, E., & Rao, U. S. (1995). Study of a thin film electrochemical cell based on (PVP+AgNO$_3$) electrolyte. *Solid State Ionics, 80*(1-2), 93-98.

Reddy, R. N., & Reddy, R. G. (2003). Sol–gel MnO$_2$ as an electrode material for electrochemical capacitors. *Journal of Power Sources, 124*(1), 330-337.

Risacher, F., & Fritz, B. (2009). Origin of salts and brine evolution of Bolivian and Chilean salars. *Aquatic Geochemistry, 15*(1-2), 123-157.

Rogers, R. D., & Seddon, K. R. (2003). Ionic liquids-solvents of the future? *Science, 302*(5646), 792-793.

Rozali, M. L. H., Samsudin, A. S., & Isa, M. I. N. (2012). Ion conducting mechanism of carboxy methylcellulose doped with ionic dopant salicylic acid based solid polymer electrolytes. *International Journal of Applied Sciences, 2*(4), 113-121.

Rudhziah, S., Ahmad, A., Ahmad, I., & Mohamed, N. S. (2015). Biopolymer electrolytes based on blend of kappa-carrageenan and cellulose derivatives for potential application in dye sensitized solar cell. *Electrochimica Acta, 175*, 162-168.

Rudhziah, S., Ibrahim, S., & Mohamed, N. S. (2011). Polymer Electrolyte of PVDF-HFP/PEMA-NH$_4$CF$_3$SO$_3$-TiO$_2$ and its Application in Proton Batteries. *Advanced Materials Research*, *287,* 285-288.

Rudziah, S., Muda, N., Ibrahim, S., Rahman, A. A., & Mohamed, N. S. (2011). Proton conducting polymer electrolytes based on PVDF-HFP and PVDF-HFP/PEMA blend. *Sains Malaysiana, 40*(7), 707-712.

Saikia, D., & Kumar, A. (2004). Ionic conduction in P (VDF-HFP)/PVDF–(PC+ DEC)–LiClO$_4$ polymer gel electrolytes. *Electrochimica Acta, 49*(16), 2581-2589.

Sain, M., & Panthapulakkal, S. (2006). Bioprocess preparation of wheat straw fibers and their characterization. *Industrial Crops and Products, 23*(1), 1-8.

Salehen, P. M. W., Razali, H., Sopian, K., Lee, T. K., & Su'ait, M. S. (2017). Evaluation of Charge-Discharge Characteristic of Lithium Cobalt Nickel Manganese Oxide for High–Energy Density Lithium-Ion Batteries. *Journal of the Society of Automotive Engineers Malaysia, 1*(3), 183-190.

Samsudin, A. S., Kuan, E. C. H., & Isa, M. I. N. (2011). Investigation of the potential of proton-conducting biopolymer electrolytes based methyl cellulose-glycolic acid. *International Journal of Polymer Analysis and Characterization, 16*(7), 477-485.

Samsudin, A. S., Lai, H. M., & Isa, M. I. N. (2014). Biopolymer materials based carboxymethyl cellulose as a proton conducting biopolymer electrolyte for application in rechargeable proton battery. *Electrochimica Acta, 129*, 1-13.

Sasikala, U., Kumar, P. N., Rao, V. V. R. N., & Sharma, A. K. (2012). Structural, electrical and parametric studies of a PEO based polymer electrolyte for battery applications. *International Journal of Engineering Science Advanced Technology, 2*(3), 722-730.

Selvasekarapandian, S., Hirankumar, G., Kawamura, J., Kuwata, N., & Hattori, T. (2005). 1H solid state NMR studies on the proton conducting polymer electrolytes. *Materials Letters, 59*(22), 2741-2745.

Sequeira, C., & Santos, D. (2010). *Polymer electrolytes- Fundamentals and Applications*. Amsterdam, North-Holland: Elsevier.

Shamsudin, I. J., Ahmad, A., Hassan, N. H., & Kaddami, H. (2016). Biopolymer electrolytes based on carboxymethyl к-carrageenan and imidazolium ionic liquid. *Ionics, 22*(6), 841-851.

Shastry, M. C. R., & Rao, K. J. (1991). Ac conductivity and dielectric relaxation studies in AgI-based fast ion conducting glasses. *Solid State Ionics, 44*(3-4), 187-198.

Sheha, E. M., Nasr, M. M., & El-Mansy, M. K. (2015). The role of $MgBr_2$ to enhance the ionic conductivity of PVA/PEDOT: PSS polymer composite. *Journal of Advanced Research, 6*(4), 563-569.

Shin, J. H., Henderson, W. A., Scaccia, S., Prosini, P. P., & Passerini, S. (2006). Solid-state $Li/LiFePO_4$ polymer electrolyte batteries incorporating an ionic liquid cycled at 40 C. *Journal of Power Sources, 156*(2), 560-566.

Shukur, M. F., Ithnin, R., & Kadir, M. F. Z. (2014). Electrical characterization of corn starch-LiOAc electrolytes and application in electrochemical double layer capacitor. *Electrochimica Acta, 136*, 204-216.

Shukur, M. F., & Kadir, M. F. Z. (2015). Hydrogen ion conducting starch-chitosan blend based electrolyte for application in electrochemical devices. *Electrochimica Acta, 158*, 152-165.

Singh, B., & Sekhon, S. (2005a). Ion conducting behaviour of polymer electrolytes containing ionic liquids. *Chemical Physics Letters, 414*(1), 34-39.

Singh, B., & Sekhon, S. (2005b). Polymer electrolytes based on room temperature ionic liquid: 2, 3-dimethyl-1-octylimidazolium triflate. *The Journal of Physical Chemistry B, 109*(34), 16539-16543.

Singh, P. K., Nagarale, R. K., Pandey, S. P., Rhee, H. W., & Bhattacharya, B. (2011). Present scenario of solid state photoelectrochemical solar cell and dye sensitized solar cell using PEO-based polymer electrolytes. *Advances in Natural Sciences: Nanoscience and Nanotechnology, 2*(2), 023002–0203015.

Singh, R., Shukla, A., Tiwari, S., & Srivastava, M. (2014). A review on delignification of lignocellulosic biomass for enhancement of ethanol production potential. *Renewable and Sustainable Energy Reviews, 32*, 713-728.

Sivakumar, M., Subadevi, R., Rajendran, S., Wu, H. C., & Wu, N. L. (2007). Compositional effect of PVdF–PEMA blend gel polymer electrolytes for lithium polymer batteries. *European Polymer Journal, 43*(10), 4466-4473.

Souquet, J. L., Levy, M., & Duclot, M. (1994). A single microscopic approach for ionic transport in glassy and polymer electrolytes. *Solid State Ionics, 70*, 337-345.

Stephan, A. M., & Nahm, K. S. (2006). Review on composite polymer electrolytes for lithium batteries. *Polymer, 47*(16), 5952-5964.

Stephan, A. M., Saito, Y., Muniyandi, N., Renganathan, N. G., Kalyanasundaram, S., & Elizabeth, R. N. (2002). Preparation and characterization of PVC/PMMA blend polymer electrolytes complexed with $LiN(CF_3SO_2)_2$. *Solid State Ionics, 148*(3-4), 467-473.

Stygar, J., Żukowska, G., & Wieczorek, W. (2005). Study of association in alkali metal perchlorate–poly (ethylene glycol) monomethyl ether solutions by FT-IR spectroscopy and conductivity measurements. *Solid State Ionics, 176*(35-36), 2645-2652.

Su'ait, M. S., Ahmad, A., Hamzah, H., & Rahman, M. Y. A. (2011). Effect of lithium salt concentrations on blended 49% poly (methyl methacrylate) grafted natural rubber and poly (methyl methacrylate) based solid polymer electrolyte. *Electrochimica Acta, 57*, 123-131.

Taleb, M. F. A., El-Mohdy, H. A., & El-Rehim, H. A. (2009). Radiation preparation of PVA/CMC copolymers and their application in removal of dyes. *Journal of Hazardous Materials, 168*(1), 68-75.

Tamilselvi, P., & Hema, M. (2014). Conductivity studies of $LiCF_3SO_3$ doped PVA: PVdF blend polymer electrolyte. *Physica B: Condensed Matter, 437*, 53-57.

Tamman, G., & Hesse, W. (1926). Dynamic crossover in polymers. Role of molecular weight. *Journal of Inorganic and General Chemistry, 156*, 245-257.

Thakur, V. K., Ding, G., Ma, J., Lee, P. S., & Lu, X. (2012). Hybrid materials and polymer electrolytes for electrochromic device applications. *Advanced Materials, 24*(30), 4071-4096.

Tiwari, A. K., Sowmiya, M., & Saha, S. K. (2012). Micellization behavior of gemini surfactants with hydroxyl substituted spacers in water and water-organic solvent mixed media: the spacer effect. *Journal of Molecular Liquids, 167*, 18-27.

Tripathi, M., & Tripathi, S. K. (2017). Electrical studies on ionic liquid-based gel polymer electrolyte for its application in EDLCs. *Ionics, 23*(10), 2735-2746.

Tripathi, S. K., Gupta, A., Jain, A., & Kumari, M. (2013). Electrochemical studies on nanocomposite polymer electrolytes. *Indian Journal of Pure & Applied Physics, 51,* 358-361.

Uma, T., Mahalingam, T., & Stimming, U. (2005). Conductivity studies on poly (methyl methacrylate)–Li_2SO_4 polymer electrolyte systems. *Materials Chemistry and Physics, 90*(2-3), 245-249.

Velazquez-Morales, P., Le Nest, J. F., & Gandini, A. (1998). Polymer electrolytes derived from chitosan/polyether networks. *Electrochimica Acta, 43*(10), 1275-1279.

Verma, M. L., & Sahu, H. D. (2015). Ionic conductivity and dielectric behavior of PEO-based silver ion conducting nanocomposite polymer electrolytes. *Ionics, 21*(12), 3223-3231.

Vogel, H. (1921). The law of the relation between the viscosity of liquids and the temperature. *Phys. Z, 22*, 645-646.

Wang, H., Jusys, Z., & Behm, R. J. (2006). Ethanol electro-oxidation on carbon-supported Pt, PtRu and Pt 3 Sn catalysts: a quantitative DEMS study. *Journal of Power Sources, 154*(2), 351-359.

Wang, P., Zakeeruddin, S. M., Exnar, I., & Grätzel, M. (2002). High efficiency dye-sensitized nanocrystalline solar cells based on ionic liquid polymer gel electrolyte. *Chemical Communications*, *24,* 2972-2973.

Webber III, C. L., & Bledsoe, R. E. (1993). *Kenaf: Production, harvesting, processing, and products.* New York, USA: Wiley.

Webber III, C. L., & Bledsoe, V. K. (2002). *Kenaf yield components and plant composition.* Alexandria, Egypt: ASHS Press.

Welton, T. (1999). Room-temperature ionic liquids. Solvents for synthesis and catalysis. *Chemical Reviews, 99*(8), 2071-2084.

Weston, J. E., & Steele, B. C. H. (1982). Effects of inert fillers on the mechanical and electrochemical properties of lithium salt-poly (ethylene oxide) polymer electrolytes. *Solid State Ionics, 7*(1), 75-79.

White, G. A., Cummings, D. G., Whiteley, E. J., Fike, W. T., Grieg, F. K., Martin, F. A., … Clark, T. F. (1970). *Cultural and harvesting methods for kenaf: an annual crop source of pulp in the Southeast.* Washington, USA: USDA Production Research Report.

Wieczorek, W., Stevens, J. R., & Florjańczyk, Z. (1996). Composite polyether based solid electrolytes. The Lewis acid-base approach. *Solid State Ionics, 85*(1-4), 67-72.

Woo, H. J., Majid, S. R., & Arof, A. K. (2011). Conduction and thermal properties of a proton conducting polymer electrolyte based on poly (ε-caprolactone). *Solid State Ionics, 199*, 14-20.

Wright, P. V. (1975). Electrical conductivity in ionic complexes of poly(ethylene oxide). *British Polymer Journal, 7*(5), 319-327.

Xia, L., Yu, L., Hu, D., & Chen, G. Z. (2017). Electrolytes for electrochemical energy storage. *Materials Chemistry Frontiers, 1*(4), 584-618.

Yahya, M. Z. A., & Arof, A. K. (2003). Effect of oleic acid plasticizer on chitosan–lithium acetate solid polymer electrolytes. *European Polymer Journal, 39*(5), 897-902.

Yahya, M. Z. A., Harun, M. K., Ali, A. M. M., Mohammat, M. F., Hanafiah, M. A. K. M., Ibrahim, S. C., . . . Latif, F. (2006). XRD and surface morphology studies on chitosan-based film electrolytes. *Journal of Applied Sciences, 6*(15), 3150-3154.

Yaksic, A., & Tilton, J. E. (2009). Using the cumulative availability curve to assess the threat of mineral depletion: The case of lithium. *Resources Policy, 34*(4), 185-194.

Yang, C. C., Lin, S. J., & Wu, G. M. (2005). Study of ionic transport properties of alkaline poly (vinyl) alcohol-based polymer electrolytes. *Materials Chemistry and Physics, 92*(1), 251-255.

Yang, M., & Hou, J. (2012). Membranes in lithium ion batteries. *Membranes, 2*(3), 367-383.

Yang, Y., Hu, H., Zhou, C. H., Xu, S., Sebo, B., & Zhao, X. Z. (2011). Novel agarose polymer electrolyte for quasi-solid state dye-sensitized solar cell. *Journal of Power Sources, 196*(4), 2410-2415.

Ye, Y. S., Rick, J., & Hwang, B. J. (2013). Ionic liquid polymer electrolytes. *Journal of Materials Chemistry A, 1*(8), 2719-2743.

Yilmaz, S., Turkoglu, O., Ari, M., & Belenli, I. (2011). Electrical conductivity of the ionic conductor tetragonal (Bi_2O_3) 1-x (Eu_2O_3) x. *Cerâmica, 57*(342), 185-192.

Zain, N. F., Zainal, N., & Mohamed, N. S. (2016). The effects of MgO nanofiller to the physicochemical and ionic liquid retention properties of PEMA-MgTf$_2$-EMITFSI nanocomposite polymer electrolytes. *Polymer Composites*, 39(5), 1500-1506.

Zentner, G. M., Rathi, R., Shih, C., McRea, J. C., Seo, M. H., Oh, H., … Weitman, S. (2001). Biodegradable block copolymers for delivery of proteins and water-insoluble drugs. *Journal of Controlled Release, 72*(1), 203-215.

Zhou, S., & Fang, S. (2007). High ionic conductivity of all-solid polymer electrolytes based on polyorganophosphazenes. *European Polymer Journal, 43*(8), 3695-3700.

Zygadło-Monikowska, E., Florjańczyk, Z., Kubisa, P., Biedroń, T., Sadurski, W., Puczyłowska, A., . . . Ostrowska, J. (2014). ithium electrolytes based on modified imidazolium ionic liquids. *International Journal of Hydrogen Energy, 39*(6), 2943-2952.

LIST OF PUBLICATIONS AND PAPERS PRESENTED

List of Publications:

1) **Rani, M. S. A.**, Rudhziah, S., Ahmad, A., & Mohamed, N. S. (2014). Biopolymer electrolyte based on derivatives of cellulose from kenaf bast fiber. *Polymers*, 6(9), 2371-2385.

2) **Rani, M. S. A.**, Dzulkurnain, N. A., Ahmad, A., & Mohamed, N. S. (2015). Conductivity and dielectric behavior studies of carboxymethyl cellulose from kenaf bast fiber incorporated with ammonium acetate-BMATFSI biopolymer electrolytes. *International Journal of Polymer Analysis and Characterization*, 20(3), 250-260.

3) **Rani, M. S. A.**, Hassan, N. H., Ahmad, A., Kaddami, H., & Mohamed, N. S. (2016). Investigation of biosourced carboxymethyl cellulose-ionic liquid polymer electrolytes for potential application in electrochemical devices. *Ionics*, 22(10), 1855-1864.

4) Rudhziah, S., **Rani, M. S. A.**, Ahmad, A., Mohamed, N. S., & Kaddami, H. (2015). Potential of blend of kappa-carrageenan and cellulose derivatives for green polymer electrolyte application. *Industrial Crops and Products*, 72, 133-141.

5) **Rani, M. S. A.**, Ahmad, A., & Mohamed, N. S. (2018). A Comprehensive Investigation on electrical characterization and ionic transport properties of cellulose derivatives from kenaf fiber based biopolymer electrolytes. *Polymer Bulletin (Accepted).*

6) **Rani, M. S. A.**, Ahmad, A., & Mohamed, N. S. (2017). Influence of nanosized fumed silica on physicochemical and electrochemical properties of cellulose derivatives-ionic liquid biopolymer electrolytes. *Ionics.(Accepted)*

7) **Rani, M. S. A.**, Ahmad, A., & Mohamed, N. S. (2018). Effect of different cations on physicochemical behaviour of carboxymethyl cellulose based biosourced polymer electrolytes. *(Manuscript in preparation)*

8) **Rani, M. S. A.**, Ahmad, A., & Mohamed, N. S. (2018). A novel approach on ionic liquid-based carboxymethyl cellulose biosourced polymer electrolytes towards safer sodium-ion batteries. *(Manuscript in preparation)*

List of Papers Presented at Regional/International Conferences:

1) **Rani, M. S. A.**, Hassan, N. H., Ahmad, A., Kaddami, H., & Mohamed, N. S., Characterization of Green Biopolymer Electrolytes based on Carboxymethyl Cellulose from Kenaf Integrated with Butyl-trimethyl Ammonium Bis(trifluoromethylsulfonyl)imide paper presented at XIV International Symposium on Polymer Electrolytes (ISPE-14), Australia, 24-29 August 2014.

2) **Rani, M. S. A.**, Dzulkurnain, N. A., Ahmad, A., & Mohamed, N. S., Conductivity and dielectric behavior studies of carboxymethyl cellulose from kenaf bast fiber incorporated with ammonium acetate-BMATFSI biopolymer electrolytes. Paper presented at 28th Regional Conference on Solid State Science and Technology (RCSSST 2014), Cameron Highlands, 25-27 November 2014.

3) **Rani, M. S. A.**, Ahmad, A. & Mohamed, N. S., Investigation of biosourced carboxymethyl cellulose-ionic liquid polymer electrolytes for potential application in electrochemical devices. Paper presented at 2nd Edition Smart Materials & Surfaces (SMS Korea 2016), Incheon, Korea, 23-25 March 2016.

4) **Rani, M. S. A.**, Ahmad, A., & Mohamed, N. S., Bio-Based Cellulose Derivatives from Hibiscus Cannabinus Based Biopolymer Electrolytes: A Comprehensive Investigation on Morphology, Conductivity and Ionic Transport Properties. Paper presented at Innovation of Polymer Science and Technology 2016 (IPST 2016), Medan, Indonesia, 7-10 November 2016.

List of award:

1) Gold Award in IIDEX 2015 (Altilium: Biopolymer Electrolytes From Kenaf Bast Fiber For Future Green Battery Technology).

2) Bronze Award in IIDEX 2015 (The Invention of High Performance Green BioPEs Based Photoelectrochemical Cell).